Modeling and Assessment of Produced Water Discharges Emitted from Offshore Petroleum Platforms in the East Coast of Canada

Lin Zhao

A Thesis

in

The Department

of

Building, Civil and Environmental Engineering

Presented in Partial Fulfillment of the Requirements for the Degree of Master of Applied Science (Civil Engineering) at

Concordia University

Montreal, Quebec, Canada

June 2007

Your file Votre référence
ISBN: 978-0-494-34727-0
Our file Notre référence
ISBN: 978-0-494-34727-0

ABSTRACT

Modeling and Assessment of Produced Water Discharges Emitted from Offshore Petroleum Platforms in the East Coast of Canada

Lin Zhao

The discharge of produced water accounts for the largest volume of waste associated with offshore oil and gas production operations. With the development and expansion of Canada's offshore oil and gas reserves, there is concern over the potential long-term impacts of produced water discharges in the ocean. Furthermore, recent evidence from other offshore oil fields in the world has suggested that production water discharges may impact the biota at greater distances from operational platforms than originally envisaged. To deal with this emerging issue, the present study focused on the development of tool for the assessment of environmental risks associated with produced water discharges based on the integration of ocean hydrodynamic and pollutant dispersion models.. .

Specifically, a numerical approach, POM-RW, is developed based on an integration of the Princeton Ocean Model (POM) and a Random Walk (RW) simulation for pollutant transport. The POM is employed to simulate the ambient oceanographic conditions. It provides three-dimensional (3D) hydrodynamic input to a Random Walk model focused on the dispersion of toxic components within the produced water effluent stream at a regional spatial scale. Furthermore, a Monte Carlo approach, with the use of water quality standards, has been incorporated into the POM-RW to reflect uncertainties and to quantify the environmental risks associated with produced water discharges. Development and field validation of the predicted current field and pollutant concentrations were conducted in conjunction with a water quality and ecological monitoring program for an offshore facility located on the Grand Banks of Canada. Results demonstrated the utility of this model to support the effective management of produced water discharges in the future.

ACKNOWLEDGEMENTS

My grateful thanks to my professor Dr. Zhi Chen for his patience, guidance and support throughout my M.A.Sc studies and for providing me the opportunity to go on a field cruise to the Hibernia site for the present research. His constant inspiration has encouraged me to furnish my best effort, leading to the successful completion of the present study and the submission of the thesis in the present form.

My deepest gratitude to my co-supervisor, senior research scientist at the COOGER research centre at the DFO, Dr. Kenneth Lee, who contributed to the present research and supported me extensively including the field cruise to the Hibernia site for model validation. It was a great opportunity to work with specialists with a vast knowledge of research and with enormous practical and real site experiences, which improved my scientific knowledge tremendously.

I am also indebted to Dr. J.Y. Qu, Dr. C.G. Hannah, Dr. S.B. Sadr Ghayeni, and other members in the Environmental Modeling and Assessment group at Concordia University.

This study was funded by the 2005-2006 PetroCanada Young Innovator Program, Natural Science and Engineering Research Council Canada Discovery Program, Fisheries and Oceans Canada, and the Program of Energy Research and Development (PERD).

TABLE OF CONTENTS

List of Figures

List of Tables

List of Symbols

x, y, z	Conventional Cartesian coordinates
σ	Sigma vertical coordinate
H	Bottom depth (m)
η	Surface elevation (m)
U, V	Horizontal velocities (m s^{-1})
W (ω)	Sigma coordinate vertical velocity (m s^{-1})
D	$\equiv H + \eta$ is the total elevation of the surface water (m)
t	Time (s)
K_M	Vertical kinematic viscosity (m^2 s^{-1})
T	Temperature (°C)
S	Salinity (ug L^{-1})
f	Coriolis parameter (s^{-1})
g	Gravitational acceleration (m s^{-2})
ρ'	$= \rho - \rho_{mean}$ before the integration is carried out
ρ_{mean}	Generally the initial density field which is area averaged on *z*-levels and then transferred to sigma coordinates in the exact same way as the initial density field
F_x, F_y	Horizontal diffusion terms (m^2 s^{-2})
K_H	Vertical diffusivity (m^2 s^{-1})
q^2	Twice the turbulence kinetic energy (m^2 s^{-2})
ℓ	Turbulence length scale (m)
wu(0), wv(0)	Surface turbulence momentum flux (m^2 s^{-2})

el	Surface elevation
ua and va	Vertically integrated velocities
ϕ	Represents U, V, η.
c	Phase speed value (m s^{-1})
C_d	Drag coefficient (dimentionless)
K	=4 is the von Karman's constant
z_0	Roughness parameter (m)
X_{new}, Y_{new}, Z_{new}	Position of a particle at the start of a model timestep
X_{old}, Y_{old}, Z_{old}	Position of a particle at the end of a model timestep
Dt	Timestep length
f_x, f_y, f_z	Diffusion coefficients (m)
α, β, γ	Random numbers from a standard normal distribution (-1, 1)
K_h, K_z	Horizontal and vertical mixing coefficients (m^2s^{-1})
C	Average concentration in a cell (ug L^{-1})
m	Mass of a particle (i.e. total mass of the system divided by the number of particles) (mg)
P	Number of particles in the cell
A	Area of the cell (m^2)
$\bar{h}$	Average depth of the cell (m)
E	The percent error with respect to the mean (%).
$z_{\alpha/2}$	The critical value, the positive z value that is at the vertical boundary for the area of α/2 in the right tail of the standard normal distribution

σ_{stv}	The population standard deviation
n	The sample size
$N(\sigma_x, \mu_x)$	Represents a normal distribution function of σ_x and μ_x
σ_x	Standard deviation of x
μ_x	Mean value of x
$f_L(L)$	Associated probability density function
$P(L>C_0)$	Probability of concentration L larger than C_0
R	Risk level

List of Acronyms

BASIN	Offshore Eastern Canada hydrocarbon database
BBLT	Benthic Boundary Layer Transport model
BIO	Bedford Institute of Oceanography
BMT	British Maritime Technology
CCALMR	Center for Coastal and Land-Margin Research
CCGS	Canadian Coast Guard Services
CFL	Courant-Friedrich-Lewy stability condition
CHARM	Chemical Hazard Assessment and Risk Management
C-NLOPB	Labrador Offshore Petroleum Board
COOGER	Centre for Offshore Oil and Gas Environmental Research
DFO	Department of Fisheries and Oceans Canada
DREAM	Dose Related Risk and Effect Assessment Model
EIF	Environmental Impact Factor
ELCIR	Eulerian-Lagrangian Circulation
EM	Eulerian-based Methods
GBS	Gravity Base Structure
HQ	Hazard Quotient
IOS	Institute of Ocean Sciences
KEC	Known Environmental Criteria
LM	Lagrangian-based Methods
MC	Monte Carlo method
MI-POM	Meteorological Institute's POM

MMS	Minerals Management Service
MUDMAP	Combined Drilling Muds and Produced Water Model
NOAA	National Oceanic & Atmospheric Administration
OBCs	Open Boundary Conditions
ONR	Office of Naval Research
OOC	Offshore Operators Committee
PEC	Predicted Environmental Concentration
PERD	Program of Energy Research and Development
PNEC	Predicted No Effect Concentration
POM	Princeton Ocean Model
POM-RW	POM – Random Walk model
PROFS	Princeton Regional Ocean Forecast System
PROTEUS	Pollution Risk Offshore Technical EvalUation System
ROMS	Regional Ocean Model System
RPC	Research & Productivity Council
RQ	Risk Quotient
SCRUM	S-coordinate Rutgers University Model
SELFE	Semi-implicit Eulerian-Lagrangian Finit Element
TAF	Trace Analysis Facility
WAD	Wetting and Drying

Chapter 1

Introduction

1.1 Background

Produced water represents the largest volume waste generated from offshore oil and gas production operations. Many regions of the world, including eastern Canada, are currently experiencing a rapid increase in the exploration and development of oil and gas reserves on their continental shelves; consequently, the impact of produced water discharges into the ocean has become an emerging environmental concern (Gordon et al., 2000). Although produced water discharges are associated with rapid dilution and trace to low level of pollutants, significant concern remains over its long-term cumulative effect (Lee et al., 2005).

The environmental impact potentially caused by produced water is related to the fate and transport of its individual components including inorganic chemicals (eg., heavy metals, nutrients and natural radionuclides), organic compounds (petroleum hydrocarbons,), and treatment process chemicals (Hodgins, 1993). Among these chemicals, the greatest environmental concern for produced water destined for ocean disposal, because of the potential for bioaccumulation and toxicity, are the metals and hydrocarbons, particularly those dissolved in the water phase (Neff, 2002; Neff et al., 2006). It is noted that hydrocarbons and heavy metals show different transport and fate mechanisms due to their differences in physiochemical properties. Low-level hydrocarbons in a large quantity of produced water discharges can be rapidly diluted by tidal currents and decay over time due to aerobic degradation. Thus, the effects of hydrocarbons associated with produced water discharges are primarily linked to localized areas and unlikely to cause large-scale environmental impacts (National Research Council, 1985). Heavy metals in produced water include barium, cadmium, chromium, copper, lead, mercury, nickel, silver, strontium, and zinc. While they are with trace to low concentrations, these heavy metals are stable, environmentally persistent, and highly toxic. Furthermore, they can be accumulated by marine life in concentrations several thousand times higher than those in the surrounding seawater (Foster, 1976; Bryan and Langston, 1982).

Both experimental and modeling studies have been conducted since the early 1990s to assess the environmental risks associated with produced water. For example, Schobben and Scholten (1993) reviewed two methods of ecotoxicological risk assessment based on characterization of the "no-effect concentration characterization", HAZARD -

to define the probability of a random species being influenced; and REFEREE – to quantify the risks on selected species within a given target area. HAZARD has been widely used for monitoring produced water discharges in the North Sea (Karman and Reerink, 1998; Thatcher et al., 1999; Reed et al., 1996). A method similar to the REFEREE was applied by Meinhold et al. (1996a-c) to assess ecological risks associated with produced water discharges from the Gulf of Mexico. Karman (1996) successfully used the Chemical Hazard Assessment and Risk Management (CHARM) model to calculate the concentration of specific chemicals in the water around an offshore platform for comparison with known toxicity thresholds for biota. Reed et al. (2001) developed the Dose Related Risk and Effect Assessment Model (DREAM) which calculates an environmental impact factor (EIF) that considers the volume of seawater which contains a concentration of produced water chemicals that exceeds a pre-determined risk criterion. To be environmentally relevant, it is obvious that any risk assessment model for produced water discharges must take into account the fate and transport of its constituents within the water column following its release.

Numerous models have been developed for the prediction of the dispersion and transport of produced water discharge in the coastal environment. For example, Rye et al. (1996) have proposed a dispersion-dilution model to study the transport and dilution of produced water and the resulting uptake and biomagnifications in marine biota. Smith et al. (2004) used field data to verify the Mud and Produced Water Discharge Model of the Offshore Operators Committee (OOC). Gillibrand et al. (1995) have simulated the dispersion of produced water in the northern North Sea (East Shetland area) using a random walk model. Riddle et al. (2001) have also developed a random walk model to compute the concentration distribution of dispersed oil in the North Sea resulting from produced water discharges. In their study, a statistical analysis has been adopted to interpolate the uncertainties from a small number of model runs by means of a regression approach.

Most previous studies have focused on petroleum exploration activities around the North Sea in Europe and the Gulf of Mexico in North America (Ray and Engelhardt, 1992; Reed and Johnsen, 1996). Few studies have addressed the long term risk and impact on the regional marine environment on the East Coast of Canada. The offshore oil and gas production in Atlantic Canada is currently in its early stages of development. However, the unique physical setting in each marine environment leads to different characteristics of the fate and transport of contaminants. For instance, the North Sea is a semi-enclosed water body that for the most part is relatively shallow whereas the Canadian East Coast is in a very nearly opposite situation, the currently producing facilities being located on offshore banks that are nearly unbounded (CAPP, 2001). In addition, the composition and concentration of produced water constituents varies between geological formations. Table 1-1 indicates the range of lead concentrations in produced water in the Gulf of Mexico, the North Sea, and a Canadian offshore field.

Table 1-1 Comparisons of Lead Concentration in Produced Water*

	Lead Concentration in Produced Waters (ug/L)
Copan	8-45
Gulf of Mexico Oil Platforms	<0.08-5700
North Sea Oil Platforms	<1-400
North Sea Gas Platforms	<1-18000

* Adapted from CAPP (2001)

Typically the volume of produced water discharge significantly increases as the well's oil reserves approach depletion. With anticipated increases in the age of existing wells and the development of new offshore platforms, the discharge of produced water has been identified to be an issue of concern by both regulators and environment groups. While both monitoring and preliminary modeling efforts have been reported over past decades, additional knowledge is required, especially with regard to the possible long-term adverse effects of produced water discharge into localized marine environments. It is also necessary to develop and validate new modeling tools to support effective management of our ocean environment and its living resources. Of the existing dispersion models in use, only a few have considered the influence of ocean hydrodynamics that govern the physical motion of discharged produced water components which would directly influence the scale of environmental impacts.

The present study developed a new modeling approach, POM-RW, which integrates the hydrodynamic ocean current model and dispersion model to simulate the fate and transport of contaminants associated with produced water discharges in the ocean. The simulation of currents and dispersion of the model were validated with field data collected at the site of an offshore production platform located on the Grand Banks of Newfoundland, to evaluate the long-term environmental impacts associated with the produced water discharges. To improve our accuracy on the prediction of long-term environmental impacts associated with the produced water discharges, an integrated risk management approach was formulated by linking the POM-RW model with the Monte Carlo method.

1.2 Objectives of the Study

The objectives of the research entering into the present thesis are as follows:

1. To develop a new modeling approach, POM-RW model, coupling the pollutant dispersion model with the 3D ocean current modeling component. This includes the development of a random walk pollutant dispersion model, a POM 3D ocean current model for the study area, and their integration;

2. To validate the new modeling approach with field observation data collected at the site of an offshore production platform located on the Grand Banks of Newfoundland for both current modeling results and pollutant dispersion simulation results;

3. To visualize the 3D dispersion of Pb in the dissolved phase resulting from produced water discharges at an offshore platform on the Grand Banks of Canada;

4. To develop an integrated risk assessment method to conduct long term risk assessment for produced water discharges over the lifetime of an oil platform; and

5. To characterize the risk level by combining produced water modeling and risk models to provide decision makers with a clear view of the risks of produced water discharges.

1.3 Organization of the Thesis

The following chapters of the present thesis are organized as follows.

Chapter 2 provides a literature review of existing ocean current models and marine pollutant dispersion models, of previous studies of Princeton Ocean Model and Random Walk Model, and of risk assessment studies of produced water discharges in coastal area.

Chapter 3 describes the methodology developed in the present research, including the coupled Random Walk model and POM approach (POM-RW), integrated risk assessment method and the numerical algorithms such as governing equations, boundary considerations, and structure of the computations for both the ocean current model and the dispersion model.

Chapter 4 introduces the study area, the field sampling approach and sample analysis results.

Chapter 5 presents the ocean current modeling results in the study area. In this chapter, the considerations of the boundary conditions in the study area, the validation of the ocean current with field data, and 3D simulation results for the study area are presented.

Chapter 6 presents the predicted produced water pollutants dispersion and risk assessment results for the study area. Detailed model settings, validation for the developed POM-RW model, 3D simulation results of produced water dispersion, and uncertainty and risk analysis are presented in this chapter.

Chapter 7 discusses the factors affecting the ocean current modeling, pollutant dispersion prediction and risk assessment results.

Chapter 8 presents the conclusions and recommendations for future work.

Chapter 2

Literature Review

In this chapter, an extensive literature review of previous studies on produced water discharges is undertaken. This literature survey establishes the need for the development of new approaches to implement risk assessment and management of large volumes of produced water discharges.

2.1 Princeton Ocean Model and Other Ocean Circulation Models

The Princeton Ocean Model (POM) is a sigma-coordinate, free-surface, ocean model, which includes a turbulence sub-model for surface and bottom mixed layer dynamics. It was developed and first introduced by Blumberg and Mellor (1987), with subsequent contributions from other researchers. The model has been used for the modeling of estuaries, coastal regions, and basin and global oceans (Hakkinen and Mellor, 1992; Ezer and Mellor, 1994; Ezer et al., 1995; Mellor and Ezer, 1995; Ezer, 1999, 2001; Oey et al., 2005). Support has been provided by ONR, NOAA, MMS, and other agencies. The POM is an open source code, which is available on the Princeton Ocean Model Website (Web 1).

The Princeton Ocean Model (POM) is well-tested and widely-used. As of March 2005, POM has 2184 registered users from 71 countries (Foreman et al., 2005). One of the applications of POM is found in the coastal ocean forecasting system. The Princeton Regional Ocean Forecast System (PROFS) is a hindcast, nowcast and forecast ocean model based on POM (Oey et al., 2005). PROFS has been in active development over the past decade. The quality of the model is monitored and reassessed by comparing the results with observations. Zhang et al. (2002) have developed an optimal adjoint variational data assimilation technique to assimilate subtidal water levels sampled along the US East Coast into the two-dimensional Princeton Ocean Model (POM). This technique has been used in the Experimental East Coast Water Level Data Assimilation Nowcast/Forecast Model System. The simulated results from POM are in good agreement with the observed subtidal water levels at coastal water level gauge stations. Yao et al. (2000) have coupled a multi-category sea-ice model and POM to implement ice-ocean forecasts for the Labrador Sea and the surrounding continental shelves on the East Coast of Canada. Sea-ice behavior is coupled to the POM using the coupling scheme devised by Mellor and Kantha (1989). This model has also been used by the Canadian Ice Service to provide daily digital ice maps (DFO-OES, 2007). Other systems and models based on or coupled with POM in the worldwide area can be found at the Princeton Ocean Model website (Web 1).

Other previous studies have made efforts to improve the present version of POM and to enhance the application. For example, Oey (2005, 2006) has proposed and applied a wetting and drying (WAD) scheme to POM in its most general three-dimensional setting with stratification, bathymetry, and forcing. Ezer and Mellor (2004) have compared the behavior of bottom boundary layers when either terrain-following (sigma or combined sigma and z-level) or a z-level vertical grid is used when most of the other numerical aspects remain unchanged. The results show that terrain-following ocean models provide reasonable climatology and water masses. Ezer and Mellor (1994), Ezer et al. (1995), Ezer (1999) and (2001) have used the same sigma coordinate coastal ocean model (POM) as a tool to study the processes involved in the adjustment of the ocean to extreme climatic changes at high latitudes. The Norwegian Meteorological Institute developed a numerical model called the Meteorological Institute's POM (MI-POM). Besides the production of daily forecasts on a routine basis, MI-POM has been applied in several studies and assignments, e.g., for the public administration and the oil companies engaged in offshore activity in Norwegian waters, and for climate change studies (Meteorological Institute, 2007).

One limitation of the method (in fact, this is a limitation of all finite difference methods) concerns the coarse staircase-like approximation that arises when trying to represent the complex network of islands, channels, and fiords. In order to capture these features, a very high resolution or nested grid that places more demands on computational resources is required. Another limitation is the lack of a wetting-and-drying capability in

POM (Foreman et al., 2005; Oey, 2005). These limitations should not be main factors on the East Coast of Canada since the offshore area is nearly unbounded and there are no significant mudflats. Moreover, because of the model features and the fact that the model solves for the sea-level directly, POM can represent ocean physics as realistically as possible. It particularly suits coastal ocean simulation (Oey, 2005).

For the purpose of comparison, some other ocean models are presented as follows:

- ROMS (The Regional Ocean Model System) is a free-surface, hydrostatic, primitive equation ocean model that uses stretched, terrain-following coordinates in the vertical and orthogonal curvilinear coordinates in the horizontal. It was based on the S-coordinate Rutgers University Model (SCRUM) described by Song and Haidvogel (1994). ROMS was completely rewritten to improve both its numerics and efficiency in single and multi-threaded computer architectures. Currently ROMS does not designate a single model, but a variety of versions developed in an open mode by different institutions (e.g. Rutgers University, Center for Earth Systems Research, USGS, etc.). Ezer (2001) and Ezer et al. (2002) have evaluated the different numerical aspects by using a comparison of POM and ROMS. Robertson et al. (2001) have also simulated internal tides using both ROMS and a modified version of POM for two different cases of stratification and topography. They have compared the results from POM and ROMS. Though the numerical algorithms, model configuration, and code size between POM and ROMS are very different, both models are good at simulating the estuaries and coastal ocean current. POM is a sigma coordinate ocean current model whereas ROMS uses an s (stretched vertical) coordinate system. After transforming from Cartesian coordinates, the dynamic equations from an s coordinate system become somewhat more complicated. In addition, ROMS has more extra options (e.g. the mixing options in a computational scheme of horizontal and vertical viscosity and diffusion, horizontal free-slip or no-slip boundaries, etc.) and is more sophisticated and, consequently, more difficult to use;

- ELCIR (Eulerian-Lagrangian Circulation) model is developed by the Center for Coastal and Land-Margin Research (CCALMR) of the OGI School of Science & Engineering at the Oregon Health & Science University. ELCIRC is an unstructured-grid model designed for the effective simulation of 3D baroclinic circulation across river-to-ocean scales. It uses a finite-volume/finite-difference Eulerian-Langrangian algorithm to solve the shallow water equations, written to realistically address a wide range of physical processes and of atmospheric, ocean and river forcings (Zhang et al., 2004; Baptista et al., 2005). In the vertical direction, ELCIRC employs level surfaces. Unlike ROMS and POM, ELCIRC can simulate the wetting and drying of tide flats. The triangular grid allows a variable resolution and better fitting of complicated coastlines and high resolution in regions with sharp gradients.

- SELFE (Semi-implicit Eulerian-Lagrangian Finite Element) is a prognostic finite element method that has more recently been developed by the CORIE (a pilot environmental observation and forecasting system for the Columbia River) team (Zhang and Baptista, 2004). Like ELCIRC, its use of an Eulerian-Lagrangian method for the material derivative terms and semi-implicit time stepping for many of the other terms means that it can employ large time steps without compromising accuracy. The major differences between SELFE and ELCIRC are in their horizontal and vertical discretizations. While predominantly constant shape functions consistent with a finite volume formulation are used in the ELCIRC horizontal approximations, linear shape functions in the context of a finite element approach are used in SELFE. In the vertical, ELCIRC employs level surfaces whereas SELFE uses terrain-following sigma or S-coordinate surfaces (Song and Haidvogel, 1994). However, according to the test implemented by the Institute of Ocean Sciences (IOS) in Fisheries and Oceans Canada (DFO), the results from both ELCIRC and SELFE are not as accurate as POM and ROMS in preserving sharp features like fronts, and in generating nonlinear features like eddies (Foreman et al., 2005).

- Delft3D model was developed by WL/Delft Hydraulics. This model is a three-dimensional morphological model to simulate three-dimensional flow, surface waves, water quality, ecology, sediment transport and bottom morphology (Delft3D-FLOW User Manual, 2006). Delft 3D-Flow provides realistic flow simulation results in in-land rivers, lakes, reservoirs, or coastal areas and estuaries, where it is better to have measurement data or a tidal table along each boundary. It might not provide a good solution without known field data for a model area that has four lateral open boundaries. Delft3D is a modeling system that consists of a number of integrated modules such as current, waves, water quality, chemical transport, and biochemical and biological processes.

2.2 Numerical Dispersion Models

Numerical dispersion models can be classified into two categories: Lagrangian-based methods (LM) and Eulerian-based methods (EM). Concentration models based on EM or ELM are still widely applied to the study of coastal areas where the flows are dominated by advection. However, these methods are known to give erroneous results near source points (Manson and Wallis, 1998; Suh, 2006). Lagrangian-based approaches (LM), however, compared to EM, give fewer numerical errors and better maintain the physics in the tracking and identification of particle locations (Suh, 2006). Another limitation of concentration models is that the computational effort is spread evenly across the domain. By contrast, the computational effort of LM is concentrated in the regions containing the most particles (Dimou, 1989).

In response to the problem occurring in concentration models, the Random Walk model based on the particle tracking method was developed to avoid the numerical errors produced by fixed grid numerical methods in diverse areas such as groundwater transport (Zheng et al., 2000), coastal biophysical problems related to zooplankton or fish larvae (Batchelder, 2002), sediment plume behavior and its effects on phytoplankton growth due to light attenuation (Xie and Yapa, 2002), coastal oceanic fronts of river discharge (Korotenko, 2000), coral reef modeling (Spagnol et al., 2002), and chemical exposure assessment in marine environment (Sabeur et al., 2002).

The random walk method has been proved to be a good tool for modeling the dispersion of pollutants in areas such as estuaries and coastal zones (Riddle, 1997). In such cases the method can give details of plume dilution near outfalls on a sub-grid scale. The method has also been used for predicting the movement, spread, and loss of oil from disasters such as the Braer wreck (Proctor et al., 1994) and the dispersion of produced water discharges from oil installations (Rye et al., 1996; Murray-Smith et al., 1997). Suh (2006) has presented a hybrid approach to predict the dispersion of contaminants in coastal areas, where a neutral random walk particle tracking method was adopted in the near field while Eulerian-Lagrangian concentration models were used in the far field. Rye et al. (1998) have developed a PARTRACK model for the calculation of the spreading and deposition on the bottom of drilling mud and cuttings as well as the spreading of chemicals in free water masses based on the particle tracking approach.

In comparison, for other models of the dispersion and dilution of waste water related to offshore oil and gas development, the descriptions are as follows:

- Benthic Boundary Layer Transport (BBLT) model has been developed by DFO, Marintimes region, to predict the transport and dispersion of suspended particulate drill waste on the continental shelf (Hannah et al., 1995, 1996, 1998; Boudreau et al., 1999; Gordon et al., 2000). The model includes important shear dispersion processes. This model is mainly used to simulate the dispersion of flocculated drill mud fines, which can have settling velocities that allow them to be concentrated near the seafloor. Model predictions in conjunction with results of biological/chemical studies have been used to assess the risk of environmental impacts resulting from offshore oil/gas developments.

- OOC model was developed by the Offshore Operators Committee (OOC) and Exxon Production Research Company to predict the initial fate of drilling mud and cuttings in a marine environment (Brandsma and Sauer, 1983a, 1983b; O'Reilly et al., 1988; Brandsma and Smith, 1992). The model has been modified to allow the prediction of the initial dynamics and passive diffusion of produced water. Industry and regulatory agencies have used the OOC Model to estimate the behavior and fate of produced water and drilling discharges (Smith et al., 2004).

- CORMIX model was developed by Doneker and Jirka (1990). This model may be used for the prediction of aqueous toxic or conventional pollutant discharges to surface water bodies. It mainly emphasizes the prediction of plume geometry and dilution within an initial mixing zone. The model can also be used to predict plume behavior at greater distances (Bouchard et al., 1995). The limitation is that the model limits the discharge height to the range of one third of local water depth.

- MUDMAP (Combined Drilling Muds and Produced Water Model), developed by Applied Science Associates (ASA), is a personal computer-based model that predicts the transport, dispersion, and seabed deposition of drilling muds and produced water derived from drill cuttings (Kolluru et al., 1993). In MUDMAP's near field model, the governing equations are the same as in the case of the OOC model, whereas the far field transport and fate of the discharge are calculated by a particle-based model using a random walk method.

- PROVANN model is a three-dimensional model that is able to simulate the spreading of particles in three dimensions (Reed et al., 1996). This model requires a steady state input or the inputs of time varying wind and current data The particles are spread due to vertical and horizontal diffusion and advected away due to the currents. The concentrations of the release are estimated from the calculated particle density of the release at various distances from the source. This model has been imbedded into DREAM, which has been described in Section 2.3.

Based on the overview of the dispersion models, most existing models require the ocean current as inputs, but very few of them couple the ocean circulation model to make an integrated approach.

2.3 Risk and Risk Assessment Associated with Produced Water Discharges

Produced water is defined as the water extracted from the subsurface with oil and gas. More than 90% of the inputs into the marine environment from extraction activities are from produced water discharges, which release low but continuous amounts of dissolved components and dispersed crude oil (Utvik, 1999). Most of the contaminants discharged in produced water occur naturally in the geologic reservoir along with the oil and gas. Many of the contaminants are toxic to marine organisms at high concentrations. Produced water also contains added biocides or other treatment chemicals that aid in the separation of the oil and gas or that prevent some adverse effect such as corrosion or scale formation. In shallow coastal environments, contaminants have been detected in water, sediment, and organisms several hundred meters from the discharge. The effects on benthic organisms in shallow coastal settings and on organisms in the biofouling mat close to discharge points have been documented (Boesh and Rabalais, 1989; Gallaway et al., 1981).

Early environmental decision-making was based on qualitative descriptions of the effects of pollutant discharges on organisms and the environment, with some reliance on the assumption that the protection of human health would also ensure an adequate protection of the environment. Current information and environmental regulations suggest a need for a more quantitative risk-based approach to decision-making for environmental protection. A consultative risk assessment approach is necessary to evaluate the scale of potential hazardous environmental impacts on the ecology and human health. The benefit of risk assessment is to assist the decision making and planning framework for management of a given region.

Risk assessment models related to produced water discharges have been developed. Here we present some current models:

- CHARM (Chemical Hazard Assessment and Risk Management) model is a tool that supports the environmental evaluation of the use of production chemicals on the basis of available data about these production chemicals and platform-related conditions. CHARM does not assess any potential harm caused during the production and transport of chemicals or the handling of unused remainders. It only produces information on the potential harm that occurs in the marine environment.

The CHARM model comprises a set of rules that calculate the internationally accepted Hazard Quotient (HQ), which represents the ratio of the Predicted Environmental Concentration (PEC) to the Predicted No Effect Concentration (PNEC). The user has to define the criteria for using CHARM and has also to define the basis for decisions to be made on the results of CHARM, as it is a decision support tool and not a decision imposing method. All the rules are described in the CHARM User Guide (Thatcher et al., 1999, 2001).

- DREAM (Dose-related Risk and Effect Assessment Model) has been developed by a group of Norwegian companies to assess acute and chronic risks associated with long term, low-level releases to the marine environment. It is derived from PROVANN (Reed et al., 1996b) and CHARM (Thatcher et al., 1999, 2001). The major components of DREAM include the time-space variations of discharge concentration fields, the exposure of organisms with different behaviour patterns, the assessment of mixtures of chemicals, and the assessment of sub-lethal chronic effects.

DREAM links these processes together within a unified model system, including databases (Crawford et al., 2002).

- PROTEUS (Pollution Risk Offshore Technical EvalUation System), developed by BMT (British Maritime Technology) Cordah Ltd., predicts the physical dispersion, the chemical interactions and the ecotoxicological risks for discharges during all phases of petroleum projects. PROTEUS has been developed over a five year period, during which time academic research into water plume and particulate mixing behaviour, as well as into offshore chemical behaviour and marine ecotoxicology, has focused on developing the models required to predict the overall impact of discharges. PROTEUS is widely used within the European oil industry. Sabeur et al. (2003) describe the numerical development, experimental validation and application of the production discharges module within the PROTEUS system.

The estimation of risks to the natural environment requires explicit description of uncertainties in assumptions, models, and parameters and the incorporation of these uncertainties into the final expression of risk. The most widely used approach to characterize uncertainty in risk assessment studies is the Monte Carlo (MC) simulation (USEPA, 1996). In a Monte Carlo analysis, a sample from the distribution of an input parameter is placed into a simulation run to interact in a model with samples from other input parameters. A number of previous studies on the risk assessment of produced water using the Monte Carlo method to conduct probabilistic analysis have been carried out. For example, Mukhtasor et al. (2004) present an approach to evaluate the toxicity risk resulting from produced water in an offshore platform using the Monte Carlo simulation method correlated with the CHARM model. Moreover, Riddle et al. (2001) have conducted a study on modeling the uncertainty in predicting produced water concentrations using a modified Monte Carlo (MC) approach. They considered that, owing partly to the CPU requirement and the size of the database, it was not possible to estimate uncertainties using traditional Monte Carlo (MC) simulations. Meinhold et al. (1996a) have employed Monte Carlo simulations to assess the human health risks of radium and lead in produced water. Chowdhury et al. (2004) have used Monte Carlo simulations to predict the human health risks from radioactive materials in produced water. Though MC simulation has its limitations, for example, that the insufficient or imprecisely informative data can hardly be analyzed by MC (Lee, 1996), Mukhtasor et al. (2002) have suggested that MC simulation is still the best choice for environmental-failure analysis (exceedance probability on concentration) of ocean outfalls.

2.4 Summary

Reviewing the literatures above, it is found that previous risk assessment based on produced water dispersion modeling has not included a full consideration of the hydrodynamic effects of ocean current. This inadequacy may lead to an incorrect assessment of the risk to the water areas possibly affected by massive produced water discharges. Therefore, there is a need and necessity to develop a new model approach containing both the current and pollutant dispersion components as an integrated tool for the risk assessment of produced water discharges from offshore oil/gas productions.

Based on the review of ocean circulation models, POM and ROMS are more suitable for coastal circulation modeling. When the features of POM and ROMS are compared, it is seen that they have similar advantages and disadvantages. However, POM is less sophisticated and is easier to read, and it can be modified to deal with problems in the present thesis study. Particularly, many applications of POM have been implemented internationally, especially in the Atlantic Ocean from estuaries, coastal regions to global ocean. Other models have also been successfully coupled with POM. Moreover, POM is an open-source platform system that can be modified and extended, whereas some other models and software are unmodifiable or very expensive.

There are some numerical dispersion models that have been used in the produced water simulations in the literatures. Among them, the Random Walk model produces fewer numerical errors and more satisfactory simulations in high concentration areas than traditional concentration models do. This feature is useful for the simulation of produced water in the marine environment since the contaminants can be rapidly diluted following discharges. The more concerned area for risk assessment are the areas with relatively high concentrations.

Based on the literature review for risk assessment associated with produced water, few studies were found for quantifying system uncertainties and predicting the risks of produced water. Therefore, in the present thesis study, the Monte Carlo method is used for uncertain analysis involved in the risk assessment. A probabilistic risk evaluation and a RQ factor derived from the CHARM model is incorporated to quantify the possible risk levels. The detailed solution is described in Chapter 3.

Chapter 3

Methodology of the Study

The modeling of pollutant transport in a complex marine environment requires the integration of a hydrodynamic ocean current model and a dispersion model. A new integrated modeling approach (POM-RW) based on the ocean circulation model (POM) and a pollutant dispersion model (Random Walk model) is developed in the present chapter. Furthermore, the Monte Carlo method is further incorporated with POM-RW to quantify the risks associated with produced water discharges into the ocean.

3.1 Introduction

The ocean current is the most important factor determining the direction and rate at which produced water disperses. The complex thermodynamics of coastal waters require the application of a high-resolution circulation model in both the horizontal and vertical directions for the model to produce adequate simulations (Korotenko et al., 2000). In the present study, POM, as a sigma-coordinate, free-surface coastal ocean model, is implemented to simulate the velocity field of the coastal area under study.

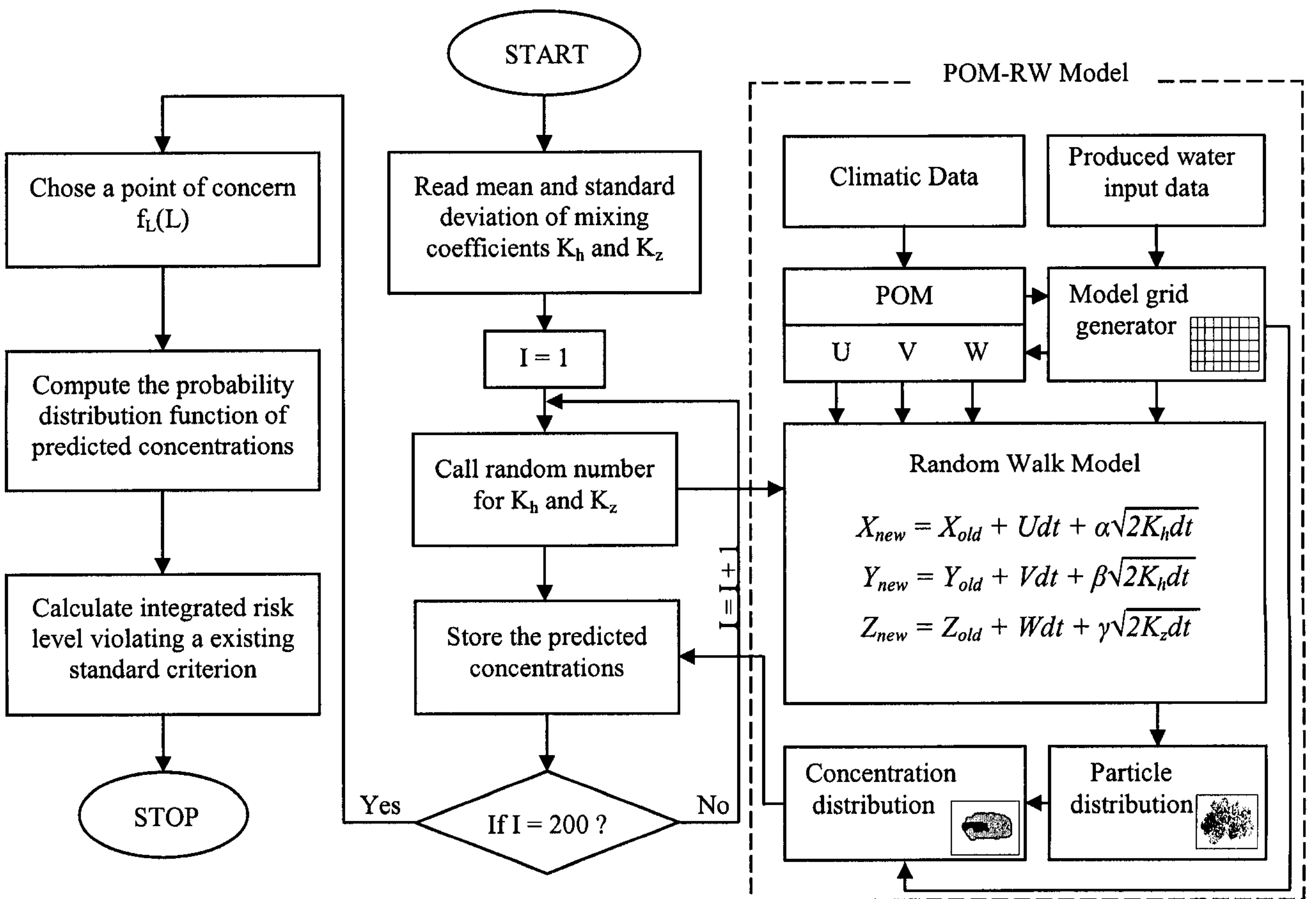

Figure 3-1 The integrated risk assessment approach based on POM-RW and Monte Carlo simulation

A new pollutant dispersion modeling approach coupled with the pollutant dispersion model (Random Walk model) with the 3D ocean current modeling component from POM has been developed. It is hereafter called the POM-RW approach. The POM-RW method includes three major components: data collection and input processing, flow field simulation, and 3D pollutant dispersion modeling. The framework of the developed POM-RW approach is presented in Figure 3-1.

An integrated risk assessment approach based on the POM-RW model and the Monte Carlo method is developed to quantify system uncertainties and to evaluate the environmental risks associated with the produced water discharges. Figure 3-1 shows the computational process of the integrated risk-assessment method. Details of the numerical algorithm are described in the following sections.

3.2 Three Dimensional Ocean Circulation Model – POM

POM has been chosen to simulate the ocean current field in the present study. The core code of POM has remained the same as that provided on the POM website (Web 1). The program is transformed into a Windows version in the present study. The initial conditions, the lateral and surface boundary conditions, and the output code have been rewritten to deal with specific problems in the Canadian context. POM is coupled with the dispersion model in conjunction with a grid generator submodel in POM. The original grid code is written with a curvilinear horizontal grid. Cartesian coordinate horizontal grids are utilized in the present study since they are appropriate for a regional study. The vertical sigma coordinate grid is kept as in POM. The interpolations of topography, temperature, and salinity data to model grid cells are all completed with the use of the grid generator. The grid generator also provides the grid arrangement for both the current model and the dispersion model.

3.2.1 Model Description

POM, the Princeton Ocean Model, is a three-dimensional, primitive equation, time-dependent, sigma coordinate, free surface, estuarine and coastal ocean circulation model. Its apparently unique feature is the imbedded turbulent closure submodel, which yields realistic, Ekman surface and bottom layers (Blumberg and Mellor, 1987). The model represents ocean physics as realistically as possible and addresses large scale and long term phenomena, depending on the basin size and grid resolution. The principal attributes of the model are as follows (adapted from Mellor, 2004):

- An imbedded second moment turbulence closure sub-model is included to provide vertical mixing dynamics between layers.
- It employs a sigma coordinate or a terrain-following transformation in the vertical to provide a continuous representation of changing bathymetry.
- The horizontal grid uses curvilinear orthogonal or Cartesian coordinates and an "Arakawa C" differencing scheme. In the following applications of this study, only Cartesian coordinate grids are utilized as they are simple and appropriate for limited area domains.
- The horizontal time differencing is explicit whereas the vertical differencing is implicit. The latter eliminates time constraints for the vertical coordinate and permits the use of fine vertical resolution in the surface and bottom boundary layers.
- The model has a free surface and a split time step. The external mode portion of the model is two-dimensional and uses a short time step. The internal mode is three-dimensional and uses a long time step.
- Complete thermodynamics have been implemented

3.2.2 Governing Equations

Sigma coordinate transformation

Figure 3-2 illustrates the sigma coordinate system. The sigma coordinate equations are based on the following transformation (Blumberg and Mellor, 1978, 1987; Mellor, 2004):

$$x^* = x \ , y^* = y \ , \sigma = \frac{z-\eta}{H+\eta}, t^* = t \tag{3.1}$$

where x, y, z are the conventional Cartesian coordinates; H (x, y) is the bottom topography and η (x, y, t) is the surface elevation.

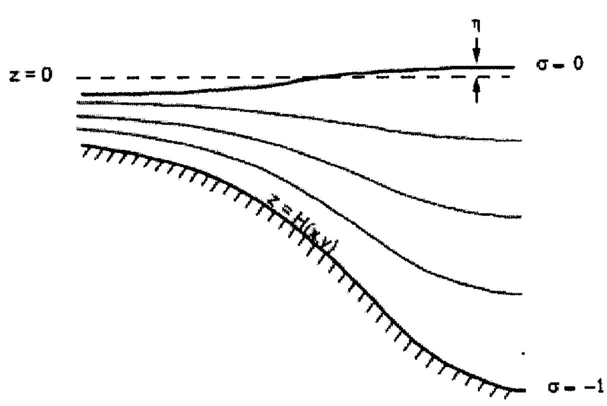

Figure 3-2 The sigma coordinate system (Mellor, 2004)

The continuity equation

$$\frac{\partial DU}{\partial x} + \frac{\partial DV}{\partial y} + \frac{\partial \omega}{\partial \sigma} + \frac{\partial \eta}{\partial t} = 0 \tag{3.2}$$

The momentum equations

$$\frac{\partial UD}{\partial t} + \frac{\partial U^2 D}{\partial x} + \frac{\partial UVD}{\partial y} + \frac{\partial U\omega}{\partial \sigma} - fVD + gD\frac{\partial \eta}{\partial x} + \frac{gD^2}{\rho_0}\int_\sigma^0 \left[\frac{\partial \rho'}{\partial x} - \frac{\sigma'}{D}\frac{\partial D \partial \rho'}{\partial x \partial \sigma'}\right] d\sigma' = \frac{\partial}{\partial \sigma}\left[\frac{K_m}{D}\frac{\partial U}{\partial \sigma}\right] + F_x \tag{3.3}$$

$$\frac{\partial VD}{\partial t} + \frac{\partial UVD}{\partial x} + \frac{\partial V^2 D}{\partial y} + \frac{\partial V\omega}{\partial \sigma} + fUD + gD\frac{\partial \eta}{\partial y} + \frac{gD^2}{\rho_0}\int_\sigma^0 \left[\frac{\partial \rho'}{\partial y} - \frac{\sigma'}{D}\frac{\partial D \partial \rho'}{\partial y \partial \sigma'}\right] d\sigma' = \frac{\partial}{\partial \sigma}\left[\frac{K_m}{D}\frac{\partial V}{\partial \sigma}\right] + F_y \tag{3.4}$$

The turbulence closure equations

$$\frac{\partial q^2 D}{\partial t}+\frac{\partial U q^2 D}{\partial x}+\frac{\partial V q^2 D}{\partial y}+\frac{\partial \omega q^2}{\partial \sigma}=\frac{\partial}{\partial \sigma}\left[\frac{K_q}{D}\frac{\partial q^2}{\partial \sigma}\right]+\frac{2K_M}{D}\left[\left(\frac{\partial U}{\partial \sigma}\right)^2+\left(\frac{\partial V}{\partial \sigma}\right)^2\right]+\frac{2g}{\rho_0}K_H\frac{\partial \tilde{\rho}}{\partial \sigma}-\frac{2Dq^3}{B_1 l}+F_q \quad (3.5)$$

$$\frac{\partial q^2 lD}{\partial t}+\frac{\partial U q^2 lD}{\partial x}+\frac{\partial V q^2 lD}{\partial y}+\frac{\partial \omega q^2 l}{\partial \sigma}=\frac{\partial}{\partial \sigma}\left[\frac{K_q}{D}\frac{\partial q^2 l}{\partial \sigma}\right]+E_1 l\left(\frac{K_M}{D}\left[\left(\frac{\partial U}{\partial \sigma}\right)^2+\left(\frac{\partial V}{\partial \sigma}\right)^2\right]+\frac{E_3 g}{\rho_0}K_H\frac{\partial \tilde{\rho}}{\partial \sigma}\right)-\frac{Dq^3}{B_1}\tilde{W}+F_l \quad (3.6)$$

The temperature equation:

$$\frac{\partial TD}{\partial t}+\frac{\partial TUD}{\partial x}+\frac{\partial TVD}{\partial y}+\frac{\partial T\omega}{\partial \sigma}=\frac{\partial}{\partial \sigma}\left[\frac{K_H}{D}\frac{\partial T}{\partial \sigma}\right]+F_T-\frac{\partial R}{\partial \sigma} \quad (3.7)$$

The salinity equation:

$$\frac{\partial SD}{\partial t}+\frac{\partial SUD}{\partial x}+\frac{\partial SVD}{\partial y}+\frac{\partial S\omega}{\partial \sigma}=\frac{\partial}{\partial \sigma}\left[\frac{K_H}{D}\frac{\partial S}{\partial \sigma}\right]+F_S \quad (3.8)$$

where U, V are the horizontal velocities (m s^{-1}); ω is the velocity component normal to sigma surfaces (m s^{-1}); T is the temperature (ºC); S is the salinity (ug L^{-1}); η is the surface elevation (m); D ≡ H + η is the total elevation of the surface water (m); x, y are the horizontal Cartesian coordinates (m); σ is the sigma vertical coordinate (m); t is time (s); *f* is the Coriolis parameter (s^{-1}); g is the gravitational acceleration; ρ' = ρ - ρ_{mean} before the integration is carried out; ρ_{mean} is generally the initial density field which is area averaged on *z*-levels and then transferred to sigma coordinates in the exact same way as the initial density field (Mellor et al., 1994; Mellor et al., 1998); K_M is the vertical kinematic viscosity (m^2 s^{-1}); F_x, F_y are the horizontal diffusion terms (m^2 s^{-2}); K_H is the vertical diffusivity (m^2 s^{-1}); q^2 is twice the turbulence kinetic energy (m^2 s^{-2}); ℓ is the turbulence length scale (m).

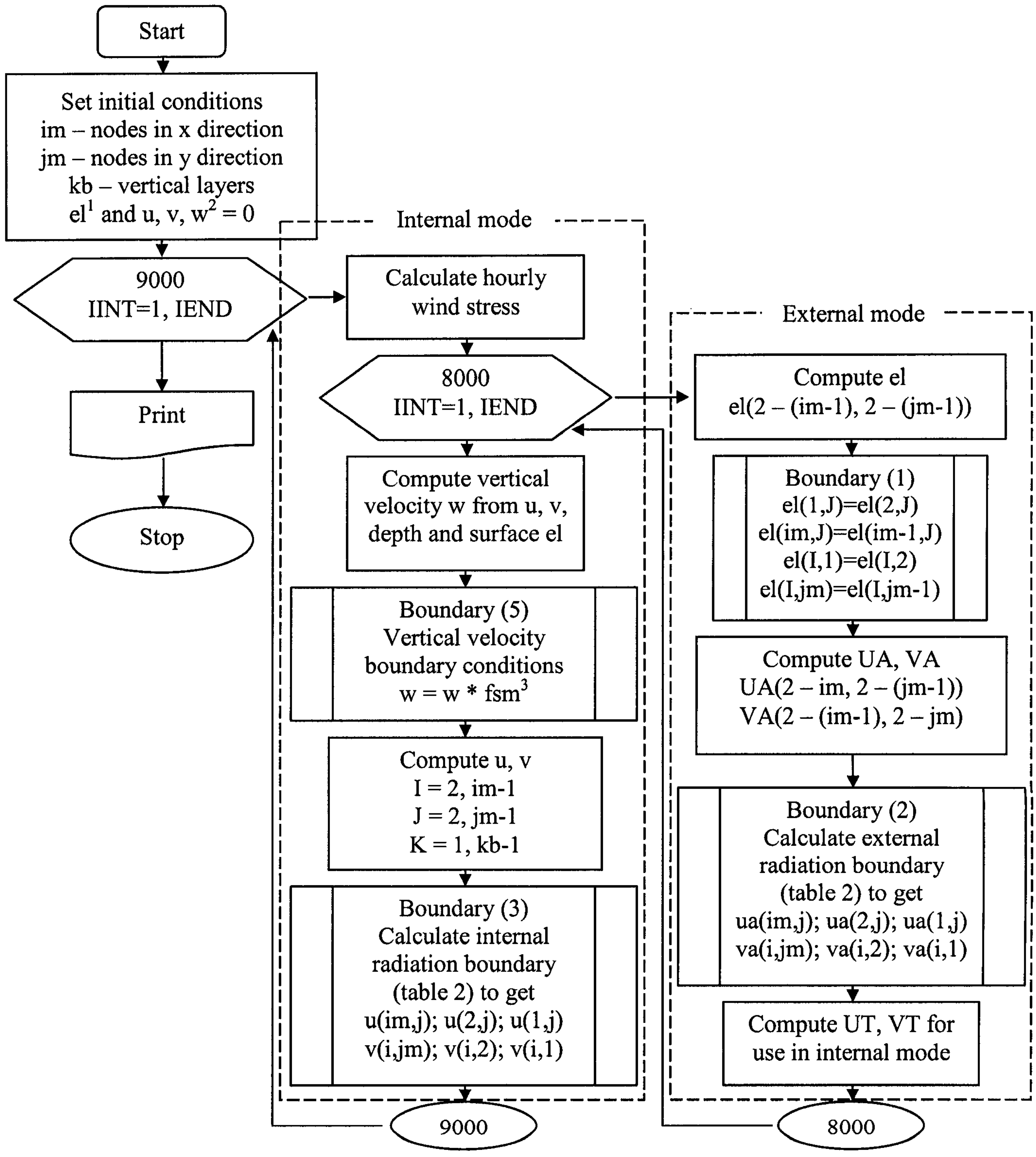

Figure 3-3 Process of computing velocities for internal and external mode (modified from Mellor (2004))

1 el is surface elevation
2 u, v, w are the three components of velocity
3 fsm is mask for scalar variables: = 0 over land: =1 over water

3.2.3 Structure of the Computation

The governing equations that present the dynamics of coastal circulation contain fast moving external gravity waves and slow moving internal gravity waves. The understanding and use of POM for a regional coastal area involves the configuration of the computation process. POM separates the vertically integrated equations (external mode) from the vertical structure equations (internal mode). This technique, known as mode splitting (Simons, 1974; Madala and Piacsek, 1977), permits the calculation of the free surface elevation with little sacrifice in computational time by solving the velocity transport separately from the three-dimensional calculation of the velocity and the thermodynamic properties.

The calculation of the three-dimensional variables in internal mode is separated into two steps: an advection plus horizontal diffusion time step and a vertical diffusion time step. The former is explicit whereas the latter is implicit, thereby accommodating small vertical spacing near the surface. To illustrate, consider Equation (3.3), which can be rewritten as follows:

$$\frac{\partial DU}{\partial t} + Adv(U) - Dif(U) = \frac{1}{D}\frac{\partial}{\partial \sigma}\left(K_H \frac{\partial U}{\partial \sigma}\right) - \frac{\partial R}{\partial \sigma} \tag{3.9}$$

where *Adv(U)* and *Dif(U)* represent the advection and horizontal diffusion terms. Thus, the advection and horizontal diffusion parts are differenced according to

$$\frac{DU - D^{n-1}U^{n-1}}{2\Delta t} = -Adv(U^n) + Dif(U^{n-1}) \tag{3.10}$$

The vertical diffusion part is differenced according to

$$\frac{D^{n+1}U^{n+1} - DU}{2\Delta t} = \frac{1}{D^{n+1}}\frac{\partial}{\partial\sigma}\left(K_H \frac{\partial U^{n+1}}{\partial\sigma}\right) - \frac{\partial R}{\partial\sigma} \tag{3.11}$$

Note that DU can be any three dimensional variable since it will be canceled when Equations (3.10) and (3.11) are added on both sides.

The calculation method of velocities in external mode is obtained by integrating the internal mode equations over the depth, thereby eliminating all vertical structure. Equation (3.12) denotes the integrated velocities in the calculations of the external mode.

$$\overline{U} \equiv \int_{-1}^{0} U d\sigma \tag{3.12}$$

Figure 3-3 shows the calculation process for the internal mode and the external mode. The internal mode calculation results in updates for u, v, t, s and for the turbulence quantities. The external mode calculation results in updates for surface elevation, *el*, and the vertically integrated velocities, *ua* and *va*, which govern the dynamics of coastal circulation.

3.2.4 Boundary Conditions

Horizontal boundary conditions

Ocean current modeling often involves open boundary conditions (OBCs), which play a crucial role in achieving the validity of the modeling outputs. Ideally, the numerical analysis of OBCs should allow fluid motions to be generated in the computational domain without affecting the interior solution. That is, waves can cross these boundaries unhampered without reflections (Tang et al., 1996). The OBCs could be divided into passive OBCs and active OBCs. Passive OBCs are particularly useful when the circulation data at the boundaries are unknown, a situation which is often the case for ocean current modeling (Palma et al., 1998). In the present study, on the basis of the physical characteristics of the study area, which has open boundaries in four laterals, passive OBCs are applied to simulate the flow field in the study area where the field boundary information is not available. Namely, the interior circulation determines the dynamics of the flow at the open boundary.

Mellor (2004) included possible open boundary conditions for POM characterized by external and internal modes. The most popular one is the so-called radiation boundary condition based on the assumption that many problems in geophysical fluid dynamics are hyperbolic by nature. One of the difficulties arises in the determination of the phase speed value (c). In the context of the shallow water equations the traditional choice is $c = \sqrt{gH}$, where H is the local water depth, which corresponds to the assumption that the waves approaching the boundary are surface gravity waves.

Palma et al. (1998) have also studied different types of boundaries, and compared the modeling solutions with the numerical experiments that were conducted in a zonal channel that includes different forms of bottom topography. The comparison results indicated that gravity-wave and flather radiation conditions gave a good agreement with both theoretical analysis and a benchmark experiment in flows dominated by wind stress and gravity waves.

In the present study, the radiation boundary conditions are chosen for the flow simulations for the coastal area. The governing equations for the radiation conditions stem from the one-dimensional Sommerfeld's equation (Orlanski, 1976; Chapman, 1985):

$$\frac{\partial \phi}{\partial t} \pm C \frac{\partial \phi}{\partial x} = 0 \tag{3.13}$$

where ϕ can represent U, V, η. C is the phase speed of incoming waves, and x is the coordinate normal to the open boundary.

Table 3-1 Open boundary conditions for the current model (modified from Mellor (2004))

Formula	Boundary	Calculations
External Mode Radiation Boundary $HU \pm c_e \eta = 0$	**East**	u(im,j) = sqrt(grav/h(imm1,j))* el(imm1,j) v(im,j) = v(im-1,j)
	West	u(2,j) = - sqrt(grav/ h(2,j))* el(2,j) v(1,j) = v(2,j)
	North	v(i,jm) = sqrt(grav/ h(i,jmm1))* el(i,jmm1) u(i,jm) = u(i,jm-1)
	South	v(i,2) = - sqrt(grav/ h(i,2))* el(i,2) u(i,1) = u(i,2)
Internal Mode Radiation Boundary $\frac{\partial U}{\partial t} \pm c_i \frac{\partial U}{\partial x} = 0$	**East**	gai = sqrt(h(im,j)/hmax) u(im,j,k) = gai*u(imm1,j,k) + (1.-gai)*u(im,j,k) v(im,j,k) = v(im-1,j,k)
	West	gai = sqrt(h(2,j)/hmax) u(2,j,k) = gai*u(3,j,k) + (1.-gai)*u(2,j,k) v(1,j,k) = v(2,j,k)
	North	gai = sqrt(h(i,jm)/hmax) v(i,jm,k) = gai*v(i,jmm1,k) + (1.-gai)*v(i,jm,k) u(i,jm,k) = u(i,jm-1,k)
	South	gai = sqrt(h(i,2)/hmax) v(i,2,k) = gai*v(i,3,k) + (1.-gai)*v(i,2,k) u(i,1,k) = u(i,2,k)

Table 3-1 shows the detailed solutions of the external and internal mode boundary conditions for the present study. In the external mode, the phase speed uses the equation $c_e = \sqrt{gH}$. In the internal mode, the speed c_i satisfies the Courant-Friedrich-Lewy stability condition (Tang and Grimshaw, 1995).

$$0 < \gamma \equiv c_i \Delta t_i / \Delta x < 1 \qquad (3.14)$$

The finite difference expression can be written (Mellor, 2004) as follows:

$$U_{im}^{n+1} = \gamma U_{im-1}^{n} + (1-\gamma)U_{im}^{n} \quad where \quad \gamma = \sqrt{\frac{H}{H_{max}}} \tag{3.15}$$

The boundary conditions determined are with a radiation condition on the u component in the east and in the west, and a v component in the north and in the south. The tangential velocities are set to the adjacent velocities on both boundaries.

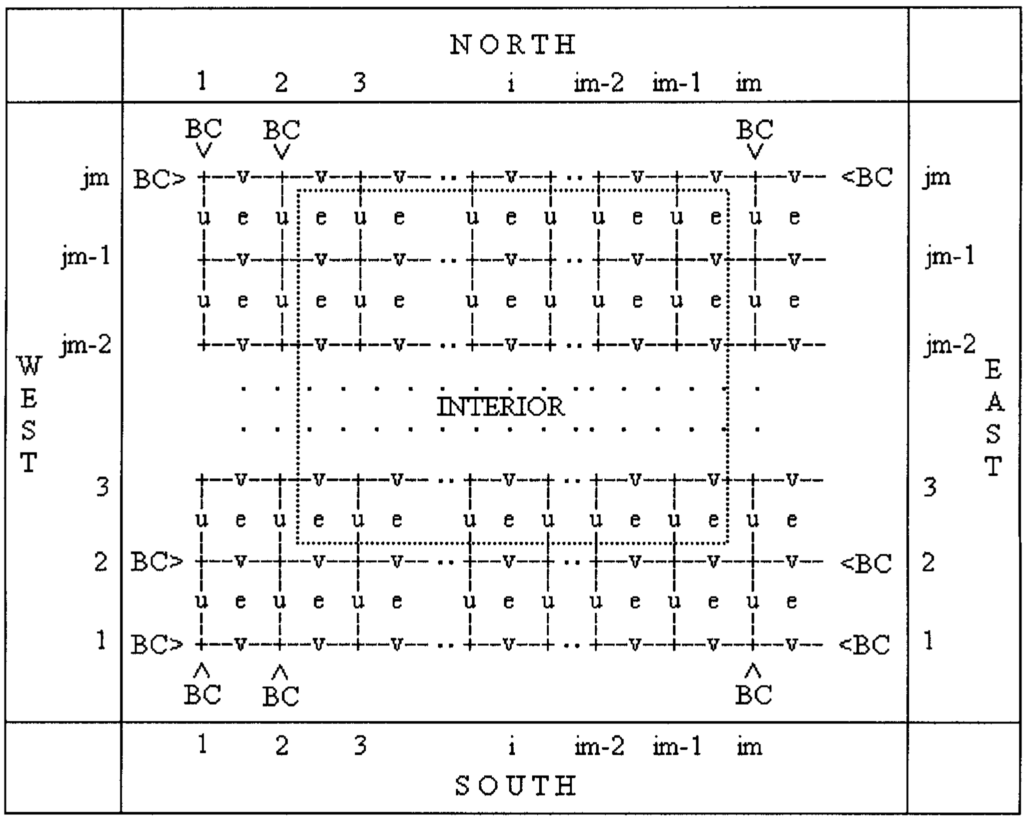

Figure 3-4 Grid points specified by open boundary conditions
(modified from Mellor (2004))

Figure 3-4 shows the grid points calculated based on the open boundary conditions. The dotted line bounds the interior (non-boundary) grid points. "BC" indicates a line of points where the boundary conditions should be specified. Closed boundary conditions are automatically enabled through a specification of the masks, *dum*, *dvm* and *fsm*, in which the open conditions will be overwritten during computation.

Vertical boundary conditions

The surface boundary conditions for Equation (3.2) are as follows:

$$\omega(0) = \omega(-1) = 0 \tag{3.16}$$

The surface boundary conditions for Equations (3.3) and (3.4) are (Mellor, 2004) as follows:

$$\frac{K_M}{D}\left(\frac{\partial U}{\partial \sigma}, \frac{\partial V}{\partial \sigma}\right) = -(< wu(0) >, < wv(0) >), \sigma \to 0 \tag{3.17}$$

where the right hand side wu(0), wv(0) is the input values of the surface turbulence momentum flux ($m^2\ s^{-2}$).

In the present case study, ocean surface forcing mainly results from the climatological wind stress fields, which are determined by surface-layer variables and the bulk aerodynamic formula (Hasse el al., 1996) as follows:

$$\tau = \rho C_d U^2 \tag{3.18}$$

where the drag coefficient C_d represents the influence of the turbulence on the relation between wind and stress. Calculating it is based on the stability and the wind speed and/or the sea state, which can be expressed (Wu, 1980) as follows:

$$C_d = \begin{cases} 1.2875 \times 10^{-3} & \textit{for} \quad U < 7.5 ms^{-1} \\ (0.8 + 0.065U) \times 10^{-3} & \textit{for} \quad U \geq 7.5 ms^{-1} \end{cases} \tag{3.19}$$

The bottom boundary conditions are as follows:

$$\frac{K_M}{D}\left(\frac{\partial U}{\partial \sigma}, \frac{\partial V}{\partial \sigma}\right) = C_z \left[U^2 + V^2\right]^{1/2} (U, V), \sigma \to -1 \tag{3.20}$$

where $C_z = \max[k^2/(\ln(z/z_0)), 0.0025]$, k=0.4 is the von Karman's constant and z_0 is the roughness parameter.

3.3 Dispersion Model – Random Walk Model

A Random Walk model is developed in the present research as the dispersion model coupled with the ocean circulation model (POM) and grid generator as described above. The basic solution of the Random Walk model comes from the literature. The program code is written in FORTRAN 9.0 language.

3.3.1 Model Description

The random walk model is based on a particle tracking approach in which the substance is modeled by an assemblage of discrete particles, which are subject to advection and diffusion. Based on this method, the advection is simulated by a translation of the individual particles in the local fluid velocity field. The turbulent diffusion is simulated by a random walk technique that displaces each particle a certain distance, which is derived from the variance of a given distribution function (Røe et al., 1996).

This method offers some advantages over the concentration models (EM or ELM), since the advection can be computed with a simpler and more accurate formulation and since it produces fewer numerical errors and better maintains the physics in the tracking and identification of particle locations (Røe et al., 1996; Suh, 2006). The particle tracking method does not include numerical dispersion in the classical sense, making it better suited to resolve sharp gradients. The main disadvantage of the method is the random fluctuation of computed concentrations. The relative size of the statistical fluctuations can be reduced by increasing the number of particles used, but thereby in turn increasing the computational burden (Røe et al., 1996).

3.3.2 Governing Equations

In the process of simulating the dispersion of pollutants in the produced water, the particles are represented as real entities spread across the computational domain rather than as concentrations. The effluent discharge is represented by placing, at the outfall position at each timestep (Riddle, 1998), a fixed number of "particles" converted from the discharge rate and concentration. The Princeton Ocean Model is implemented to seamlessly provide the velocity components at each coordinate. These particles are moved during each subsequent timestep (Riddle et al., 2001):

$$\begin{aligned} X_{new} &= X_{old} + Udt + f_x\alpha \\ Y_{new} &= Y_{old} + Vdt + f_y\beta \\ Z_{new} &= Z_{old} + Wdt + f_z\gamma \end{aligned} \tag{3.21}$$

where X, Y and Z represent the position of a particle and the subscripts "old" and "new" represent the positions at the start and end of a model timestep; dt is the timestep length and U, V and W are the horizontal and vertical velocity components at time t from the POM model and the effect of wind, respectively. The functions f_x, f_y and f_z define the mixing process, and α, β and γ are random numbers from a standard normal distribution.

Each particle represents a fixed mass of effluent. It is assumed that no degradation takes place.

A constant diffusion coefficient based on Fickian equation is used to characterize the horizontal and vertical diffusion as follows:

$$f_x = f_y = \sqrt{2K_h dt}$$
$$f_z = \sqrt{2K_z dt} \tag{3.22}$$

where K_h and K_z are the horizontal and vertical mixing coefficients (m^2 s^{-1}), which are uncertain parameters and can be quantified based on Equation (3.26).

3.3.3 Conversion to Concentration

Conversion of particle numbers and locations into concentrations is straightforward. The concentration distribution of a pollutant in the water is quantified using a counting cell. The number of particles in a grid cell over a depth interval from the water surface down to a specified depth is counted, giving the mass of the pollutant in a known volume, and therefore the concentration is computed. We can write the following expression for the concentration calculation under the assumption that each particle has the same mass (Suh, 2006):

$$\boldsymbol{C} = \boldsymbol{m}\frac{\boldsymbol{P}}{\boldsymbol{A}\boldsymbol{h}} \tag{3.23}$$

where C is the average concentration in a cell (ug L^{-1}); m is the mass of a particle in mg (i.e. total mass of the system divided by the number of particles); P is the number of particles in the cell; A is the area of the cell (m^2) and $\bar{h}$ is the average depth of the cell (m).

3.4 Integrated Risk Assessment

Lowrance (1976) defines risk as a measure of the probability and severity of adverse effects. In order to quantify risks, it is necessary to specify the spatial and temporal distribution of contaminants in the environment, the uncertainties in the system, and the method of risk evaluation. In the present study, POM-RW model predictions that examine the contaminant transport affected by produced water dispersion, in conjunction with the environmental guidelines for protection of aquatic life, will be used to quantify the risk of environmental impacts resulting from offshore oil/gas developments and productions. The Monte Carlo method will be used to analyze the system uncertainties. What follows will introduce the integrated risk assessment approach developed in the present research.

3.4.1 Description of the Integrated Risk Assessment Approach

Figure 3-1 illustrates the detailed computational process for the integrated simulation and risk assessment model proposed, comprised of the POM-RW model linked to a risk assessment module. The following steps are used to quantify the level of environmental risks for a produced water species released into marine water based on the application of known regulatory toxic threshold limits:

1. Generate a random field based on site-investigation data (i.e., call the random number subroutine to generate probabilistic distributions of horizontal and vertical mixing coefficients);

2. Implement POM-Random Walk Model to simulate pollutant transport for each set of coefficients generated from Step 1;

3. The outputs generating from Step 2 for each set of data will be stored until the chosen sample size of simulations is finished;

4. Choose a point of concern and generate statistics of simulation outputs and conduct an uncertainty analysis;

5. Identify chemical standards to calculate the risk level; and

6. Obtain a complete set of risk-level predictions using risk characterization methods.

3.4.2 Sample Size Determination

One of the first problems encountered when applying the Monte Carlo simulation is to decide on the number of samples. Determining sample size is a very important issue because samples that are too large may waste time and resources, whereas samples that are too small may lead to inaccurate results. The sample size of Monte Carlo simulations is derived by Equation (3.24) (Mendenhall, 1994) as follows:

$$E = z_{\alpha/2} \bullet \frac{\sigma_{stv}}{\sqrt{n}} \tag{3.24}$$

where E is the percent error with respect to the mean; $z_{\alpha/2}$ is known as the critical value, the positive z value that is at the vertical boundary for the area of $\alpha/2$ in the right tail of the standard normal distribution; σ_{stv} is the population standard deviation; n is the sample size. Rearranging this formula, the sample size can be solved to produce results accurate to a specified confidence and percent error with respect to the mean as follows:

$$n = \left[\frac{z_{\alpha/2} \sigma_{stv}}{E} \right]^2 \tag{3.25}$$

3.4.3 Monte Carlo Method for Quantifying System Uncertainty

Recent emphasis in the risk analysis has focused on uncertainty in the risk assessment process (Schuhmacher et al., 2001). To perform risk assessment, model uncertainty and data uncertainty should be taken into account. "Uncertainty" can be described as a lack of knowledge regarding the true value of a parameter. Since a lack of knowledge does not imply total ignorance, it is possible to characterize the relative likelihood of different values for a parameter. Monte Carlo simulation is used for quantifying system uncertainties, with the modeling outputs serving as bases for risk quantification.

Considering the uncertain parameters in the POM-RW model, the horizontal mixing coefficient K_h and the vertical mixing coefficient K_z are the key input variables in the simulations. It has been reported that the mixing coefficient resulted in generally normal distributions (Riddle et al., 2001). Using the Monte Carlo approach, the values of those parameters are generated from a uniform distribution. The normal generators can be simply expressed as follows:

$$x = N(\sigma_x, \mu_x) \tag{3.26}$$

where x = the horizontal mixing coefficient K_h or the vertical mixing coefficient K_z; $N(\sigma_x, \mu_x)$ represents a normal distribution function of σ_x and μ_x ; σ_x = standard deviation of x; and μ_x = the mean value of x.

It should be noted that the results of the uncertainty analysis depend directly on the distributions assumed for each of the parameters. Hence, good representative data are required to obtain reliable estimates of uncertainty.

After generating certain sets of random samples for each parameter, the distribution of predicted concentrations for each grid square can be calculated by the POM-RW model. The distribution results can then be used to define a 5^{th} and 95^{th} percentile concentration, and an uncertainty factor is calculated as the ratio of the 95 and 5 percentile concentrations.

3.4.4 Risk Characterization

Levels of risks or adverse effects associated with produced water discharges are studied using two methods in the present thesis: probabilistic risks and the Risk Quotient (RQ) factor derived from the CHARM model (Thatcher et al., 1999, 2001).

Probabilistic risk assessment

Probabilistic risk assessment often refers to the generation of distributions of exposure or risk representing uncertainty or variability or both. This approach attempts to account for information from a range of sources and for the quality and relevance of that information (McDaniels et al., 2004). The integrated risk simulation calculates numerous scenarios of a model by repeatedly picking values from a probability distribution for the uncertain variables and using those values for the model. These probabilities are propagated through the model, and an output distribution describing the probability of various outcomes is generated (Figure 3-5).

More specifically, environmental risk associated with the discharging of produced water could be expressed as the probability of a pollutant's concentration (denoted as random number L) exceeding local environmental guidelines (denoted as C_0), i.e., R = $P(L>C_0)$, R denotes risk. Thus, the risk can be quantified as follows (Chen et al., 1998):

$$R = P(L > C_0) = \int_{C_0}^{\infty} f_L(L)dL \tag{3.27}$$

where R = risk level quantified as the probability of system failure; f_L = associated probability density function.

Therefore, the POM-RW can be logically used with a probabilistic risk model to provide in-depth and systematic risk quantification.

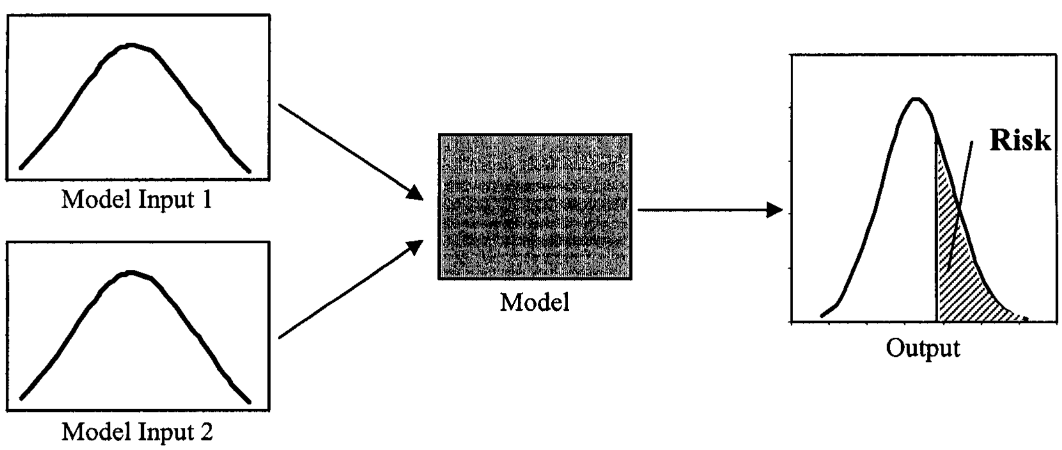

Figure 3-5 Probabilistic Risk

Risk Quotient (RQ) evaluation

This characterization of risks is carried out based on the comparison of the predicted environmental concentration (PEC) to the known environmental criteria (KEC) for protection of aquatic life in the marine environment.

The risk quotient (RQ) factor is calculated as follows:

$$RQ = \frac{PEC}{KEC} \tag{3.28}$$

This method is derived from the CHARM (Chemical Hazard Assessment and Risk Management) model. CHARM is a primary tool to support the environmental evaluation of the use of production chemicals on the basis of available data about these production chemicals and platform related conditions (Thatcher et al., 1999, 2001). The CHARM model comprises a set of rules to calculate the internationally accepted Hazard Quotient (HQ), which originally represents the ratio of the Predicted Environmental Concentration (PEC) to the Predicted No Effect Concentration (PNEC). In the present research, the PEC represents the modeling results, whereas the PNEC values are referred to the local environmental guideline for a species.

The risk quotient (RQ) can be viewed as the "severity measures" of risks. When an RQ is greater than 1, adverse environmental effects, e.g. fish growth or mortality, may be expected. The higher the value of RQ above 1, the greater the possibility of environmental risks. To evaluate the probability of RQ as more than 1, the probabilistic distribution for each concern point resulting from the Monte Carlo method (see output in Figure 3-5) is taken into account for the quantification of the quotient risks. For the case study described in the following chapters, the RQ distribution under 95^{th} percentile concentrations, which present the "worst case" scenario, will be performed to map the severity risk levels.

3.5 Summary

The methodology used in the present study can be summarized as follows:

1. A new modeling approach (POM-RW), which coupled the dispersion model (Random Walk model) with the ocean current model (POM), has been developed to simulate the three-dimensional dispersion of contaminants of the produced water;

2. POM, as a three-dimensional, sigma coordinate, free surface, estuarine and coastal ocean circulation model, provides realistic ocean current components to the dispersion model. Its governing equations and computational scheme with a full consideration of boundary conditions are presented in this chapter;

3. With the detailed description of the velocity field from POM, the Random Walk model based on the particle tracking method may provide the exact dispersion and advection of pollutants of produced water discharges through the integration with the ocean current model.

4. Considering the uncertainty parameters in the POM-RW model system, a Monte Carlo method has been integrated to quantify system uncertainties and to provide the probability distribution of predicted concentrations for each grid square. The results from the Monte Carlo approach will serve as the bases for the environmental risk assessment.

5. Two methods for quantifying risks have been presented and incorporated with POM-RW in this chapter: a probabilistic risk assessment and the Risk Quotient (RQ) factor. Mapping of the possible risk severities based on these two methods is demonstrated in the following chapters.

Chapter 4

Study Case and Field Investigation – Hibernia Platform

After presenting the methodology of the numerical approach for the present research, an oil platform at the Hibernia site has been chosen to be a case study. This particular platform was chosen for the study because it will be by far the largest future produced water discharge on the Canadian East Coast (CAPP, 2001). In this chapter, are presented the detailed information of the study site, the field sampling and sample analysis conducted in the present thesis study on a research cruise, and all the initial data collected for modeling in the study area.

4.1 Overview of the Study Site

Data from the Hibernia offshore oil platform on the Grand Banks of Newfoundland (46°45' N, 48°46' W) was chosen for analysis within the current study (see Figure 4-1). The production platform, a Gravity Base Structure (GBS), located on this site at 80 m of water accounts for the largest volume of produced water currently discharged into the waters of Atlantic Canada (CAPP, 2001).

Figure 4-1 illustrates the location of Hibernia GBS and the geographical limits of the area used in the ocean current simulation analysis for data input into the model. This scale was chosen to minimize the influence of open boundaries on the study area, a 50 km × 50 km grid around the Hibernia GBS. A detailed consideration of the model setting is discussed in Chapter 5.

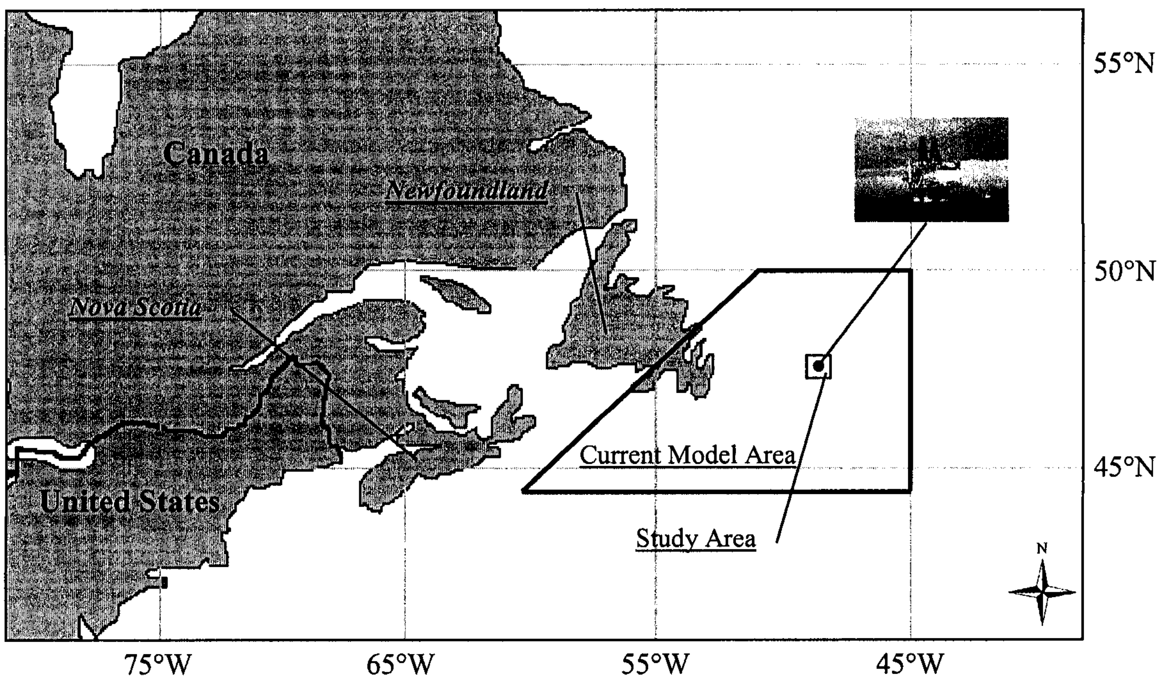

Figure 4-1 Study site and modeling area

Temperatures at the Hibernia site range from -8 °C to 7 °C in the winter and can go as high as 20 °C in the summer. The ocean surface temperature varies from -3 °C in the winter to greater than 15 °C in the summer. The average wind speed is 37 km per hour in the winter and 22 km per hour in the summer. The Guinness World Book of Records calls the Grand Banks the foggiest place on Earth. During winter, there is 40% coverage with fog and up to 84% during June and July.

The Hibernia oil field was discovered in 1979. The completed platform was towed to the Hibernia oil field and positioned on the ocean floor in June of 1997. The first production from the massive Hibernia platform began in November 1997. The Hibernia platform has a design capacity of approximately 230,000 barrels (40,000 m^3) of crude oil production per day (bpd) – the maximum annual production rate for the platform under Labrador Offshore Petroleum Board (C-NLOPB) regulations is 220,000 bpd (35,000 m^3/day). In June 2006, Canada-Newfoundland and C-NLOPB increased its reserve estimates for the Hibernia field. Total reserves are now estimated at 1,244 million barrels (200 million m^3), representing an estimated increase of 379 million barrels over the previous estimate (Oil and Gas, 2006). Cumulative production at Hibernia from the first oil in November 1997 up to the end of 2006 was 520 million barrels (80 million m^3) – leaving approximately 740 million barrels (120 million m^3) of reserves yet to be extracted. Also, Petro-Canada estimates that the Hibernia field still has a remaining production life of 20 to 25 years (Petro-Canada, 2005). This estimation is based on an updated assessment of the full field.

4.2 Structure of Hibernia Platform

Hibernia consists of two separate components: the Gravity Base Structure (GBS) and the Top sides. The Hibernia platform is uniquely designed to resist the impact of sea ice and icebergs. It can withstand the impact of a one-million ton iceberg with no damage.

- **Gravity Base Structure (GBS):** The GBS houses the ballast control system that maintains platform buoyancy. When moored to the ocean floor, the GBS is almost completely submerged. The ice wall of Hibernia GBS consists of 16 concrete teeth designed to absorb the impact of icebergs. Each tooth of the 1.4 meter-thick ice wall is designed to distribute the impact of an oncoming iceberg evenly throughout the entire structure.

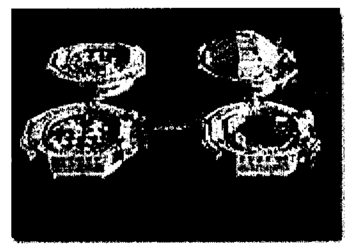

Gravity Base Structure
(Web 1)

- **Topsides:** The Topsides, which house the main oil derricks, the helicopter pads and other critical operations, remain above the ocean surface. The topsides facilities on the Hibernia platform accommodate all drilling, producing, and utility equipment, as well as the living quarters for workers. The topsides consist of five super-modules and seven smaller topside mounted structures.

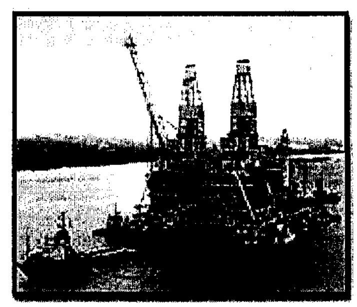

Topsides
(Web 1)

4.3 Discharge Volume of Produced Water

The volume of produced water usually increases with the age of a well (Henderson et al., 1999). In nearly depleted fields, production may be 98% produced water and 2% fossil fuel (Stephenson, 1992; Shaw et al., 1999). BASIN (2007) (Offshore Eastern Canada hydrocarbon database) provide monthly production information for oil/gas platforms in the East Coast of Canada. Table 4-1 and Figure 4-2 show Hibernia Platform oil/gas production and produced water volume since 1997. As just mentioned, the produced water discharges increase rapidly with the oil/gas production after 2002. At present the production of oil is higher than that of produced water. In 2005 and 2006, 62% of the production was oil and 38% of the production was produced water. The oil production was almost 1.6 times that of produced water. In total, the amount of oil production is 4 times larger than that of the produced water.

The produced water of the Hibernia platform is discharged through a horizontally oriented port, which is 30.48 cm in diameter. This port is located 40 m above the seafloor.

Table 4-1 Hibernia Platform oil/gas production (BASIN (2007))

Year	Oil Production (10^3 cubic meter)	Produced Water (10^3 cubic meter)	Gas Production (10^6 cubic meter)
1997	202	0.73	45
1998	3784	0.60	909
1999	5786	15	1435
2000	8394	198	2393
2001	8631	599	2596
2002	10472	448	2445
2003	11785	2447	2686
2004	11854	4885	2742
2005	11541	7076	2808
2006	10350	6559	2495
Total	82799	22228.3	20554

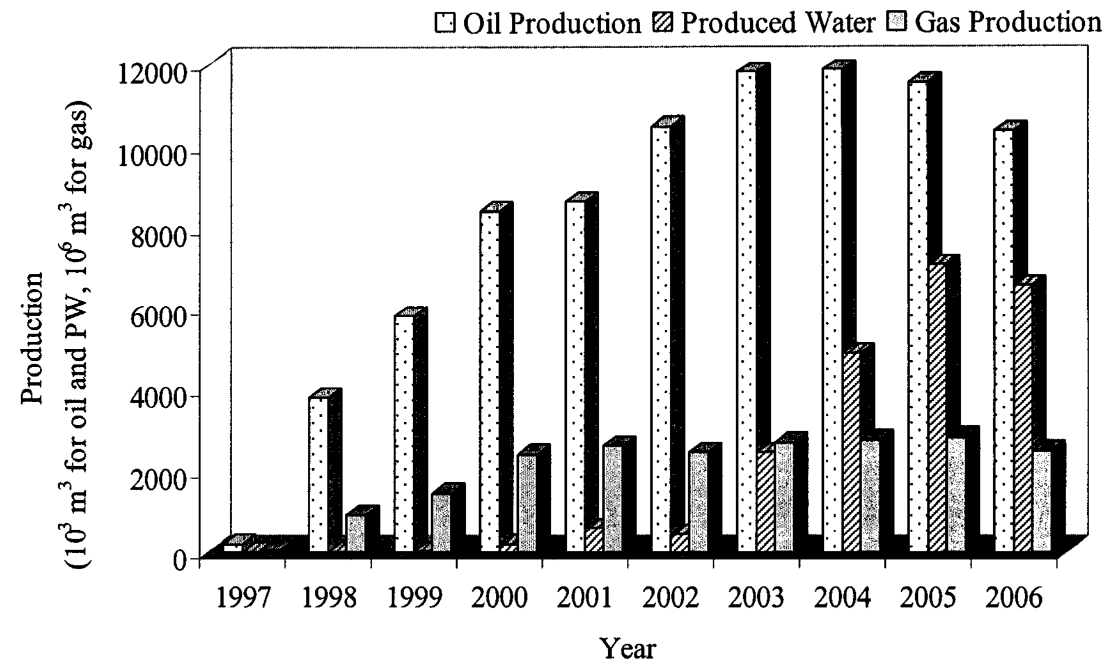

Figure 4-2 Hibernia Platform oil/gas production (adapted from BASIN (2007))

4.4 Field Investigation and Sampling

In response to the great concern that the produced water discharges may impact the marine environment at greater distances from operational platforms due to the anticipated growth of offshore oil and gas industry in Canada. Both regulators and habitat/resource managers are required to identify the acceptable disposal limits that would support changes to the regulatory waste treatment guidelines in order to protect the quality of the ocean's environment in Canada. To carry out the research that was necessary, two major oceanographic expeditions to the Hibernia platform were conducted with the CCGS Hudson in 2005 and 2006 under the PERD (Program of Energy Research and Development) research program (Ecological Risk of Produced Water Discharges from

East Coast Oil and Gas Operations) by BIO (Bedford Institute of Oceanography) and COOGER (Centre for Offshore Oil and Gas Environmental Research) scientific team.

In order to conduct the field sampling and the site investigation for the present thesis study and also to acquire the experience that comes from working in a real world classroom, I joined DFO staff and the crew of the Hudson on the mission to Hibernia in June of 2006. After a brief Search and Rescue mission in winds reportedly in excess of 70 kts and waves as high as 40 ft, the retrieval of water samples for various types of analysis was carried out. This mission to monitor the environmental effects of produced water provided concrete examples of how difficult it is to work at sea and how the interdisciplinary interactions are necessary to provide useful data for modeling. By the time the present research report was prepared, the sample analysis results of 2005 were ready. These data will be used to conduct the simulation, validation and risk assessment presented in the following chapters. Here we present the detailed sampling information.

4.4.1 Sampling Equipment

Based on the observations made during my research cruise trip, all the sampling equipment had been pre-installed on the Hudson research ship. A temporal lab was established for sub-sample and to preserve samples collected from the field. The sampling equipment is described as follows:

- **CTD/ROSETTE**: CTD instruments measure three important parameters directly – conductivity, temperature and pressure. This instrument has been installed and connected to the ROSETTE system. The ROSETTE system is for sampling water from different depths. Each Niskin bottle can be closed at a different depth, thus sampling water from many different depths at one time. This 21 × 10-L bottles ROSETTE has two component systems: 1) a computer-directed surface control interface/power supply and 2) a logic-controlled submersible sampler mounting array that selects and remotely closes water sampling bottles. In 2005, the samples were collected from the depths of 2 m, 10 m, 25 m, 50 m, and 5 m off the bottom, respectively.

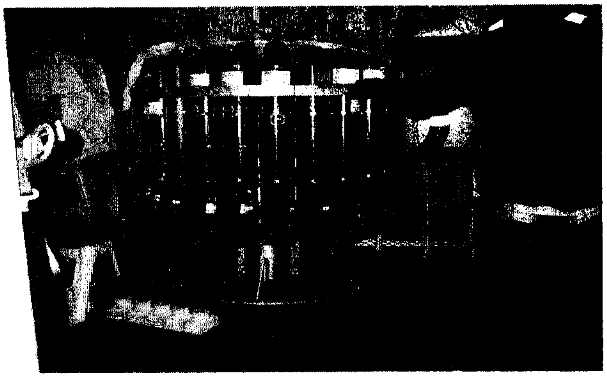

CTD + ROSETTE (taken by Lin Zhao)

- **BOB**: BOB is the latest version of a mechanically operated device for sampling water and suspended particulate material at several heights within 0.5 m of the seabed, in the benthic boundary layer (BBL). BOB is capable of collecting larger water samples than is the BOSS (Benthic Organic Seston Sampler), but fewer samples are collected per deployment. In 2005, on the Hudson expeditions, samples from 5 cm, 15 cm, 25 cm, 35 cm and 45 cm were collected, respectively.

BOB (taken by Lin Zhao)

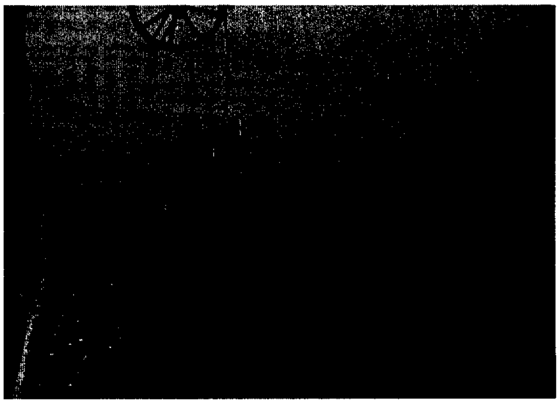

CAMPOD (taken by Lin Zhao)

- **CAMPOD**: is a light-weight, three-legged platform equipped with a video system similar to that installed on the Video

Grab. It is used for very high resolution colour imagery of the sea floor. It is designed primarily for making images of the benthic environment.

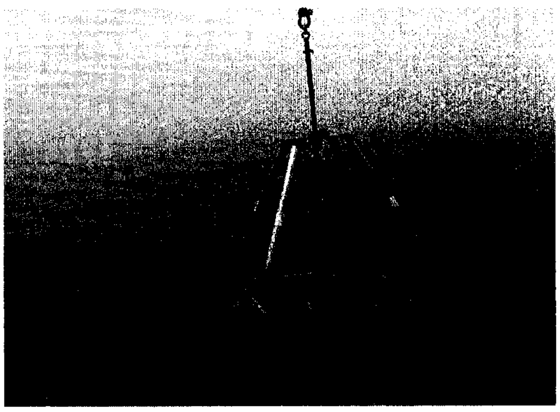

SLO-CORER (taken by Lin Zhao)

- **SLO – CORER**: is a hydraulically dampened gravity corer used to take sediment cores (with an undisturbed sediment-water interface) from the ocean floor.

- **Niskin Bottle Casts**: Inorganic samples (metal analysis) were collected using Lever-Action Niskin bottles (General Oceanics) attached to a ¼" stainless-steel wire cable with a 25Kg stainless-steel weight at it's end. To reduce the possibility of metals contamination, these bottles for metals analysis are specially designed with all operating mechanisms on the outside of the bottle, and the inside is coated with Teflon. The messenger weight to trip the bottles closed at the desired depth was fabricated from Teflon. Water samples for inorganic analyses were collected at 10m, 35 m and 60 m depths.

4.4.2 Sampling Locations

The sample locations (called stations) include West, North, South, South-West, South-East, North-West, and North-East. In 2005, samples from almost 30 stations were collected. The nearest station is 500 meters away from the Hibernia platform; the farthest station is called R100, which is 100 km away from the Hibernia site. Figure 4-3 shows the 2005 stations that have been used in the present study for purpose of validation. W, S, and N represent West, North, and South.

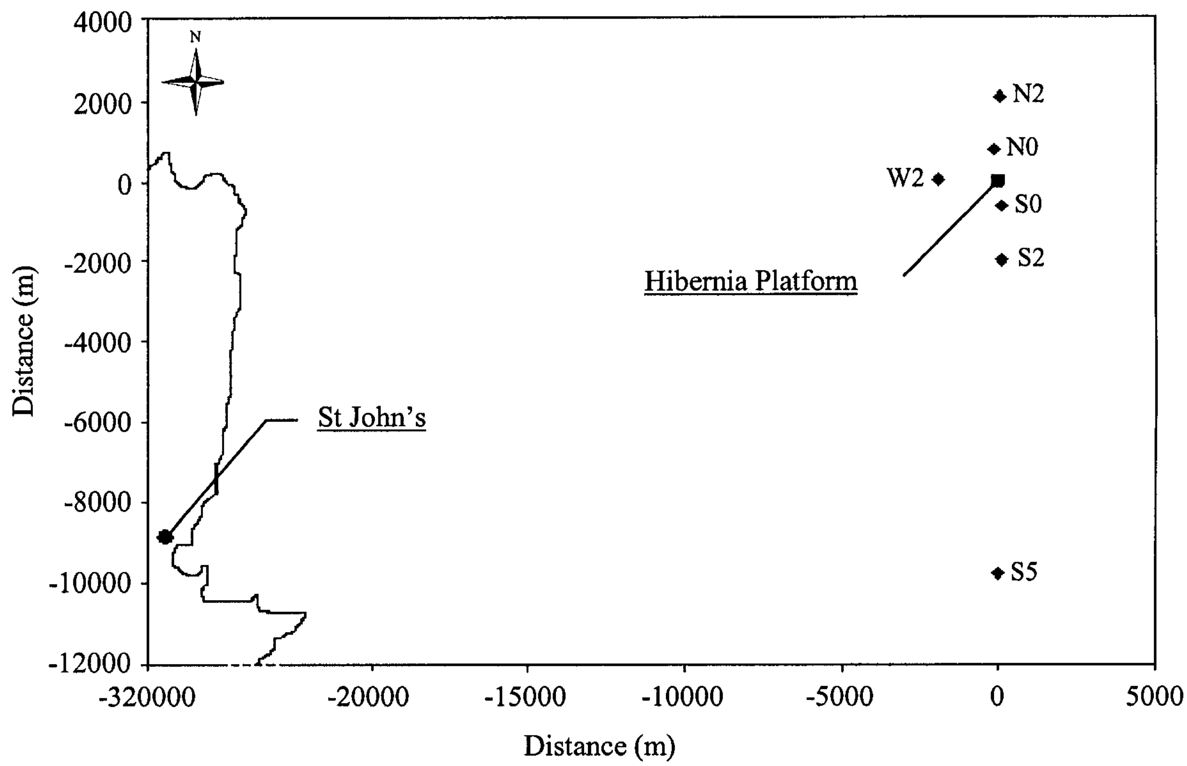

Figure 4-3 Sampling Stations in 2005

4.4.3 Sample Categories

After samples were collected from each location, the samples were labeled and put into different bottles for different analyses. They were then sent to the lab for sub-sample and to be preserved. The sample categories include:

- Produced water samples
- Organic samples
- Nutrient samples

- Salinity samples
- Micro biological samples
- Fluorometry samples
- DNA samples
- Sediment samples
- Inorganic samples (metals)

4.5 Sample Analysis

Samples of produced water were collected directly from the process lab on the Hibernia Gravity Base Structure in 2005. These samples were collected immediately prior to discharge and are representative of the production water that is discharged into the ocean. All sample containers were filled to overflowing to eliminate a headspace in the container.

Samples were processed according to analyses, and sent to the laboratory RPC (Research & Productivity Council, Fredericton, New Brunswick) and BIO for the measurements, analysis and experiments. The metals/inorganic analyses of *seawater* were conducted at RPC. The inorganic analysis (heavy metals) of *produced water* was conducted at TAF (Trace Analysis Facility) at the University of Regina. The organic chemistry analyses were conducted at BIO. All samples were treated in the Lab according to the standard procedures.

In the present thesis study, the dissolved concentration of Pb in the produced water in 2005 has been used to conduct the simulation and analysis. Based on the sample analysis results, the Pb dissolved concentration in the *produced water* is 456.7 ug L^{-1} in

2005. Table 4-2 shows the concentration of Lead at a different depth in *seawater* for each station shown in Figure 4-3.

Table 4-2 Lead concentration in seawater for each station in 2005

Station	Latitude	Longitude	Depth (m)	Pb Concentration (ug L^{-1})
			10	0.0104
S5	46.66095	48.78305	35	0.0073
			60	0.0116
			10	0.0062
S2	46.73252	48.78182	35	0.0127
			60	0.0175
			10	0.0119
S0	46.74425	48.78232	35	0.0253
			60	0.0247
			10	0.0072
N2	46.76882	48.78253	35	0.0070
			60	0.0081
			10	0.0127
N0	46.75721	48.78497	35	0.0151
			60	0.0099
			10	0.0182
W2	46.75001	48.80915	35	0.0045
			60	0.0077

4.6 Data Set for the Model Validation and Simulation

The discharge volume and concentration of produced water and concentration of sea water have been prepared as mentioned above for the model input and validation. Except for production information, other data such as topography and climatic information are required for the model simulations. The observed ocean current data are prepared for model validation. Table 4-3 lists all the information and the sources needed for simulation and validation. The detailed data sets are described as follows:

- **Topography**: topography data are collected from the Fisheries and Oceans Canada Oceanographic database, which includes the depths in 45950 locations from (78W, 35N) to (40W, 60N). The locations with zero depth are along the shorelines of Nova Scotia and Newfoundland. The deepest location is about 5000 m under the water. Appendix A lists the parts of topography data.

- **Temperature and Salinity**: temperature and salinity data are monthly averaged data, which are also from the Fisheries and Oceans Canada Oceanographic database. The data are collected from about 530 locations at 39 different depths. Appendix B lists the parts of temperature and salinity data at different locations and at different depths.

- **Wind**: wind data are hourly averaged data, which are from different sources as shown in Table 4-3. The wind data are collected from 28 locations, including the Hibernia platform. Most of the locations are distributed along the west and south boundaries of the large scale area (Figure 4-1). The wind data in several locations are presented in Appendix C.

- **Current**: the observed current data include near bottom average current data at different locations and the velocity vector data at the Hibernia site. The observed current information is used for model validation in Chapters 5 and 6.

Table 4-3 Model input and validation data preparation

Data Category	Source
Topography	• Fisheries and Oceans Canada Oceanographic database • Data are modified to .csv file
Temperature	• Fisheries and Oceans Canada Oceanographic database • Data are modified to .csv file
Salinity	• Fisheries and Oceans Canada Oceanographic database • Data are modified to .csv file
Wind	• Environment Canada Climatic database • National Data Buoy Centre database • Hibernia Annual Environmental Data Summary (2005) supplied by COOGER • Data are modified to .csv file
Current	• Near bottom current in Web 2. • Hibernia Platform Annual Current Measurement Report (2005) supplied by COOGER • Data are presented in Chapter 5
Discharge volume of produced water	• COOGER (Centre for Offshore Oil and Gas Environmental Research) • Data are described in Section 4.6
Pb concentration in produced water	• COOGER (Centre for Offshore Oil and Gas Environmental Research) • TAF (Trace Analysis Facility) at the University of Regina • Data are described in Section 4.5 and 4.6
Pb concentration in seawater	• COOGER (Centre for Offshore Oil and Gas Environmental Research) • Data are described in Section 4.5 and 4.6

- **Discharge Volume of Produced Water**: the discharge volume of produced water is collected by COOGER on the Hudson research cruise of 2005, which is 882 m^3/hr.

- **Pb Concentration in Produced Water**: samples of produced water were collected by COOGER on the Hudson research cruise of 2005. The Pb concentration in produced water was analyzed by TAF (Trace Analysis Facility) at the University of Regina in 2006, which is 456.7 ug L^{-1}.

- **Pb Concentration in Sea Water**: samples of sea water were also collected by COOGER on the Hudson research cruise of 2005 at different locations (Section 4.4.2) and at different depths (10 m, 35 m, and 60 m). The analysis was conducted by COOGER, and the analysis results have been shown in Table 4-2.

4.7 Summary

In this chapter, the information about the study site and the field investigation results has been described. All the data and information required for the present study are found and modified for modeling uses. The modeling and risk assessment for the Hibernia site can now go forward.

Chapter 5

3D Modeling of the Ocean Current in the Hibernia Region

The information for the study area and the model setting data required for the modeling simulations and assessment are described in Chapter 4. The modeling process and risk assessment results associated with the produced water discharges from the Hibernia platform into the ocean are presented in the following chapters. The present chapter focuses mainly on the simulations of ocean current fields.

5.1 Setup of the Modeling Area and Computational Grid for the Hibernia Site

The ocean current hydrodynamic condition is the major factor affecting the dispersion of the contaminants of produced water discharges in the coastal area. Therefore, the results from the current model directly affect the simulations of the fate and transport of contaminants in produced water discharges. The major issue involved in the ocean current simulation in the present research is that the Hibernia platform is located in an open sea; four lateral boundaries are completely unbounded in the study area (see Figure 4-1). There are no existing current monitoring stations (or existing field observation data) for each lateral boundary. Thus, the situation leaves no choice but to use numerical open boundary conditions (OBCs) for each lateral boundary based on Equation 3.13 and Table 3-1. However, no matter which kinds of OBCs have been chosen, numerical errors will exist and may create an unrealistic flow across the boundary, consequently affecting the simulation results. In order to eliminate the numerical errors for the study area, simulating ocean current on a larger scale covering the study area at the centre is proposed. When the area is large enough, the boundary conditions can hardly influence the inside study area; thus the numerical errors resulting from the OBCs in four lateral boundaries could be minimized to the level that one can ignore. Therefore, in the present research, a large scale area that covers the study area at the middle for ocean current simulation has been conducted. Detailed information is presented as follows:

5.1.1 Selecting Ocean Modeling Area for the Hibernia Region

A large scale area is chosen from (60W, 44N) to (45W, 45N) as shown in Figure 4-1. The left boundary is along the shore of Canada's east coast. A portion of the current modeling results related to the study area is used for pollutant dispersion simulation, which is from (49.135W, 46.54N) to (48.475W, 47.02N), about 50 km × 50 km with the Hibernia site as the centre. The large scale area is almost 200 times the study area, which is located in the center of the large scale area. Therefore, this solution should be enough to achieve our purpose of minimizing the influences of numerical boundary condition on the simulation of velocity components for the study area.

5.1.2 Model Grid Configuration and Bottom Topography

The model grid and bottom topography are shown in Figures 5-1 and 5-2. The solution of the horizontal grid is modified into Cartesian coordinate grids, which have 90×93 nodes for the large scale area. The size of the model grids is generated as about $\Delta x \approx \Delta y \approx 2$ km in the study area. Outside the study area, the size of the model grids is designed to be larger than the inside study area, where the grids vary between $\Delta x \approx 8$ km to $\Delta x \approx 50$ km, $\Delta y \approx 12$ km as shown in Figure 5-1.

The sigma coordinate has 21 vertical layers, σ = (0.0, -0.0263, -0.0526, -0.1053, -0.1579, -0.2105, -0.2632, -0.3158, -0.3684, -0.4211, -0.4737, -0.5263, -0.5789, -0.6316, -0.6842, -0.7368, -0.7895, -0.8421, -0.8947, -0.9474, -1.0) and $\sigma = (z-\eta)/(H+\eta)$ as discussed in Chapter 3. The vertical resolution is a little higher near the surface. For example, for a grid point where the water depth is 80 m, Δz is about 2 m at the surface and 4 m in the other layers.

As shown in Figure 5-2, the water depth in the whole large-scale area extends from the deep ocean of about 3000 m to 10 m on the continental shelf. The study area is in the shallow water, which has depth of between 60 m to 120 m distributed in the area with about 80 meters at the Hibernia site as shown in Figure 5-3. The depth is smaller in the southwest and then becomes greater towards the northeast. The greatest depth is in the corner of the northeast, where the depth is about 113 m.

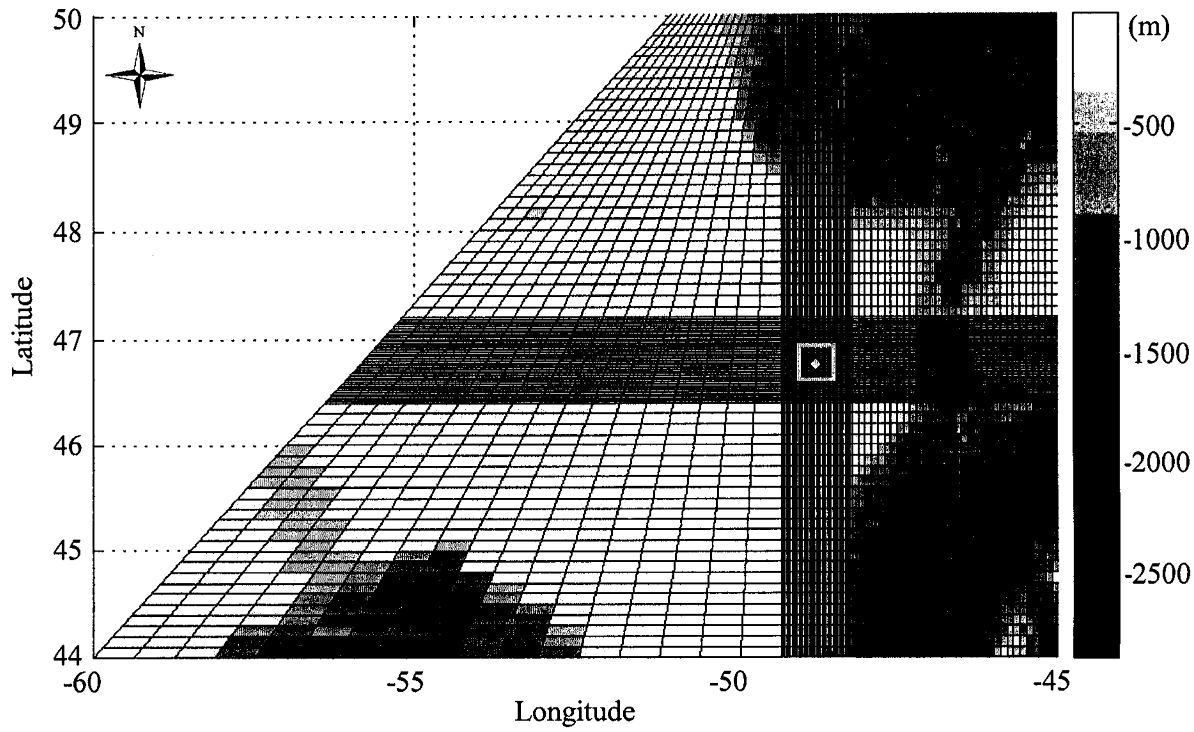

Figure 5-1 Model grid and bottom topography contour map (The diamond point is the location of Hibernia, the square around the Hibernia platform is the study area)

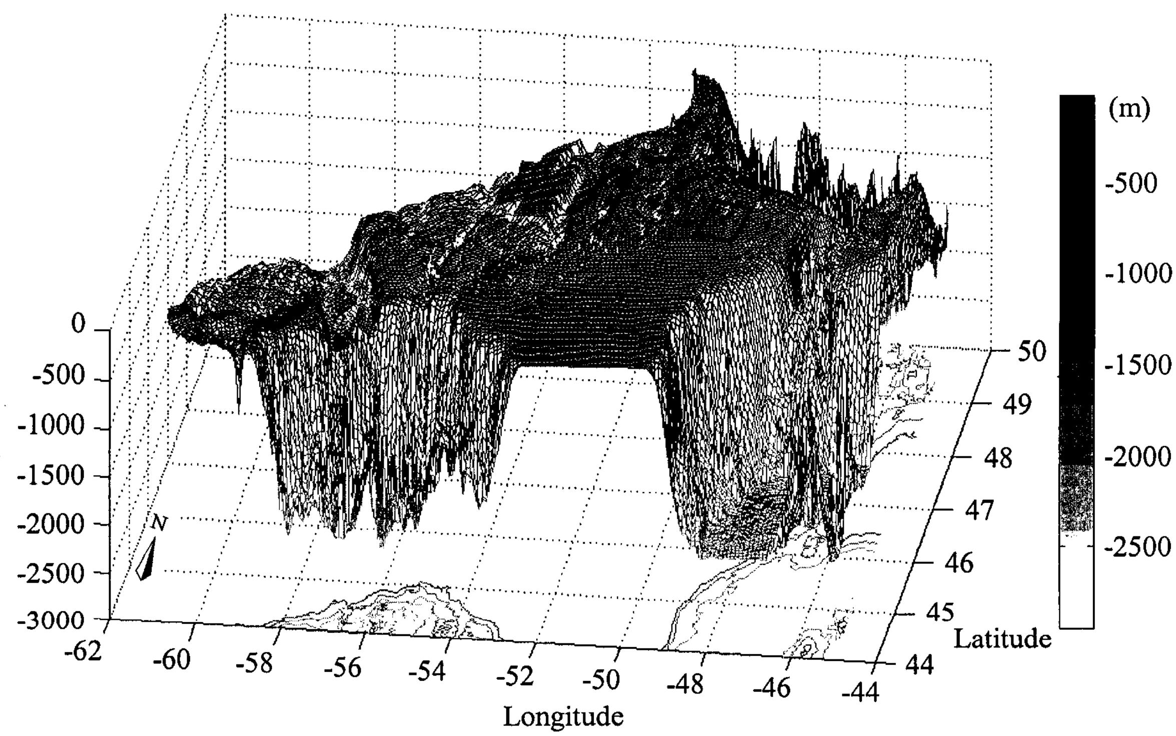

Figure 5-2 3D bottom topography (The diamond point is the location of Hibernia, the square around the Hibernia platform is the study area)

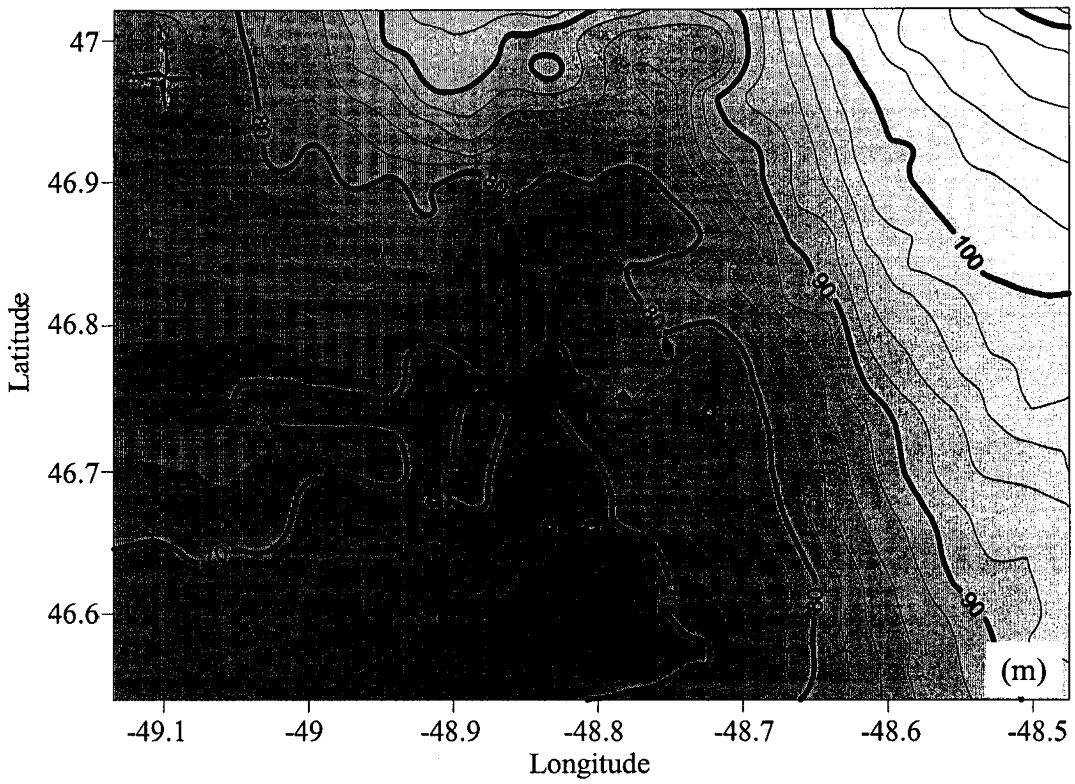

Figure 5-3 Bottom topography in study area (The diamond point is the location of Hibernia. The contour interval is 2 m with a bold line indicating every 10 m interval)

5.2 Model Configuration for Simulating the Ocean Current Field in the Hibernia Region

The initial conditions for the current model are set to zero, that is, when time is zero, the components of the velocity are zero. The horizontal time differencing is explicit, whereas the vertical differencing is implicit. The latter eliminates the time constraints for the vertical grid and permits the use of fine vertical resolution near the surface and in shallow regions. The model has a split time step: a two-dimensional external mode that uses a short time step of 6 s and a three-dimensional internal mode time step of 180 s. At stable thermocline depths, the turbulence closure submodel yields vanishingly small values of vertical viscosity and diffusivity to which is added, however, a constant background value of 2×10^{-5} m^2 s^{-1} (Ezer and Mellor, 1997). A Smagorinsky-type horizontal diffusion is used here such that the diffusion coefficient is calculated (Smagorinsky et al., 1965):

$$A_M = C\Delta x\Delta y\left[\left(\frac{\partial u}{\partial x}\right)^2 + \frac{1}{2}\left(\frac{\partial v}{\partial x}+\frac{\partial u}{\partial y}\right)^2 + \left(\frac{\partial v}{\partial y}\right)^2\right]^{1/2} \tag{5.1}$$

where u and v are the horizontal velocity components and C is a coefficient taken here as 0.2 (Ezer and Mellor, 1997; Ezer, 2001). Table 5-1 lists the major parameters considered in the model.

Table 5-1 Main parameters data used in current modeling for the Hibernia region

Parameter	**Value**
External mode (2-D) time step (dte)	6 s
Internal (3-D) time step / External (2-D) time step (dti/dte)	30 (dimensionless)
Reference density for seawater (rhoref)	1025 kg/m^3
Von Karman's constant (kappa)	0.4
Bottom roughness (z0b)	0.01 meter
Minimum bottom friction coefficient (cbcmin)	0.0025
Maximum bottom friction coefficient (cbcmax)	1.0
Smagorinsky diffusivity coefficient (horcon)	0.2
Background vertical viscosity and diffusivity (umol)	2×10^{-5} m^2 s^{-1}

At the four lateral open boundaries (the locations where the water depths are lower than 10 m are considered as closed boundaries in the model), Sommerfeld-type radiation conditions are used (see Equation 3.13 and Table 3-1). The monthly climatologic data of temperature and salinity (see Appendix B) from the Fisheries and

Oceans Canada Oceanographic database are prescribed on the open boundaries. Upwind advection boundary conditions allow the advection of the climatological temperatures and salinities into the model domain under inflow conditions. This type of boundary condition has been used successfully in the applications of POM (Ezer and Mellor, 1992, 1994; Ezer et al., 1995).

The current model is initialized by using mainly the climatological data of June 2005 and is run for 30 days. Surface forcing includes sea surface temperature (see Appendix B) obtained from the Fisheries and Oceans Canada Oceanographic database and includes the hourly wind speed and directions of June 2005 (see Appendix C) from the Environment Canada climatic database, the National Data Buoy Centre database and Hibernia Annual Environmental Data Summary (2005). The topography, temperature, salinity, and hourly wind data for the larger domain containing the study site are interpolated into Cartesian horizontal grids and vertical sigma coordinate layers.

5.3 Validation with Field Data for the Modeling of the Ocean Current in the Hibernia Area

After the POM model was set up with the created grid and input conditions, the model was run to simulate the 3D ocean current field for June of 2005 on the East Coast of Canada as shown in Figure 4-1. The results have been compared with the field observation data for the testing and the validation of the developed POM for the Hibernia site. Comparisons are described as follows:

5.3.1 Current Velocity Vector Comparison

Comparisons between the modeled and observed velocity fields are conducted at different depths: the surface, 10 meters in the water and 40 meters in the water, respectively, for this 3D modeling study.

Figures 5-4 (a) (b) (c) are the surface current comparisons at a model run of 5 days, 10 days and 15 days, respectively. Corresponding to each day, the field observations are real-time velocities, which are measured by a MIROS Directional Wave and Current Radar installed on the Hibernia Platform. The observation data are collected from the Hibernia Platform Annual Current Measurement Report (2005). As shown, the modeled velocity speed appears slightly smaller than the observations within 10 days, whereas it has a good agreement with the observed data in 15 days. The directions are generally the same.

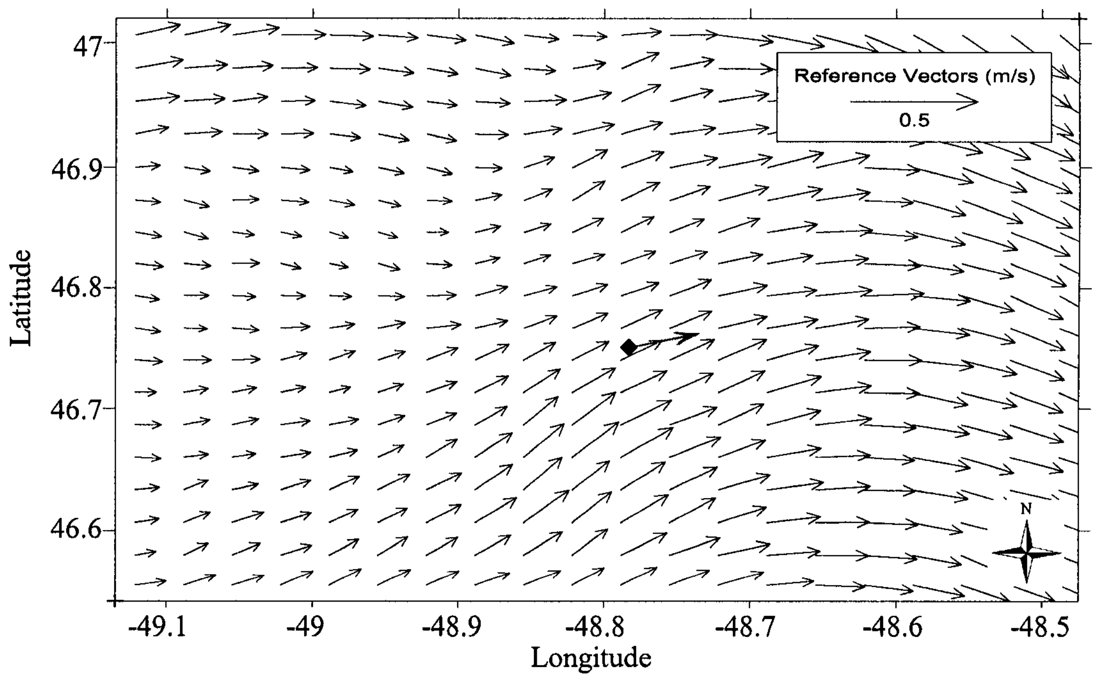

Figure 5-4 (a) Surface current velocity field after a model run of 5 days (the point is the location of Hibernia, and the bolded red vector is the observed velocity of June 5, 2005 at the Hibernia site. The observed velocity is from Hibernia Platform Annual Current Measurement Report (2005))

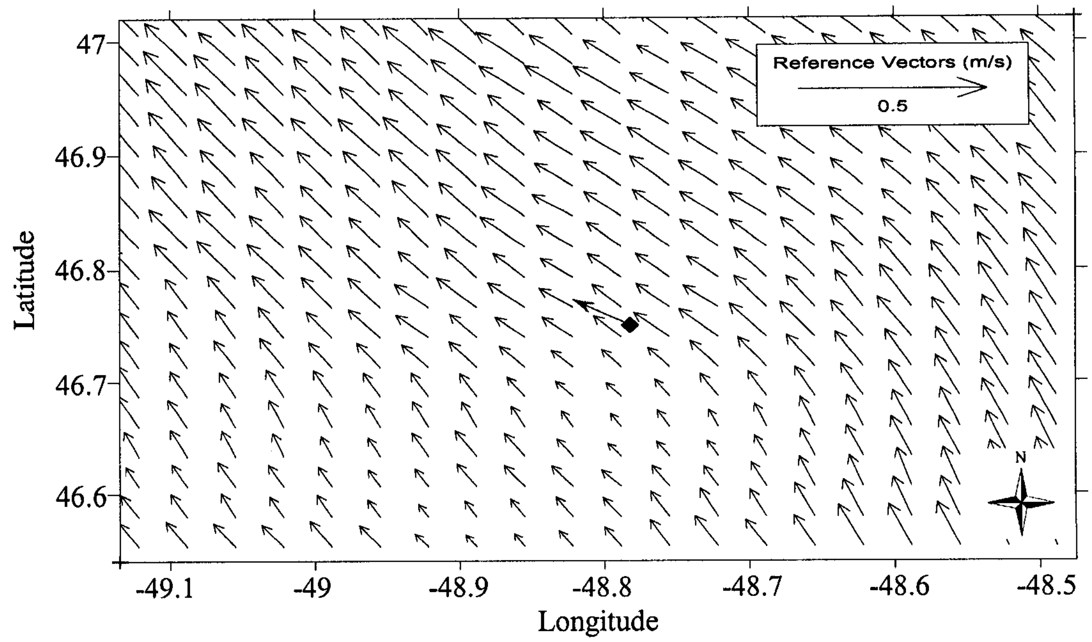

Figure 5-4 (b) Surface current velocity field after a model run of 10 days (the point is the location of Hibernia, and the bolded red vector is the observed velocity of June 10, 2005 at the Hibernia site. The observed velocity is from Hibernia Platform Annual Current Measurement Report (2005))

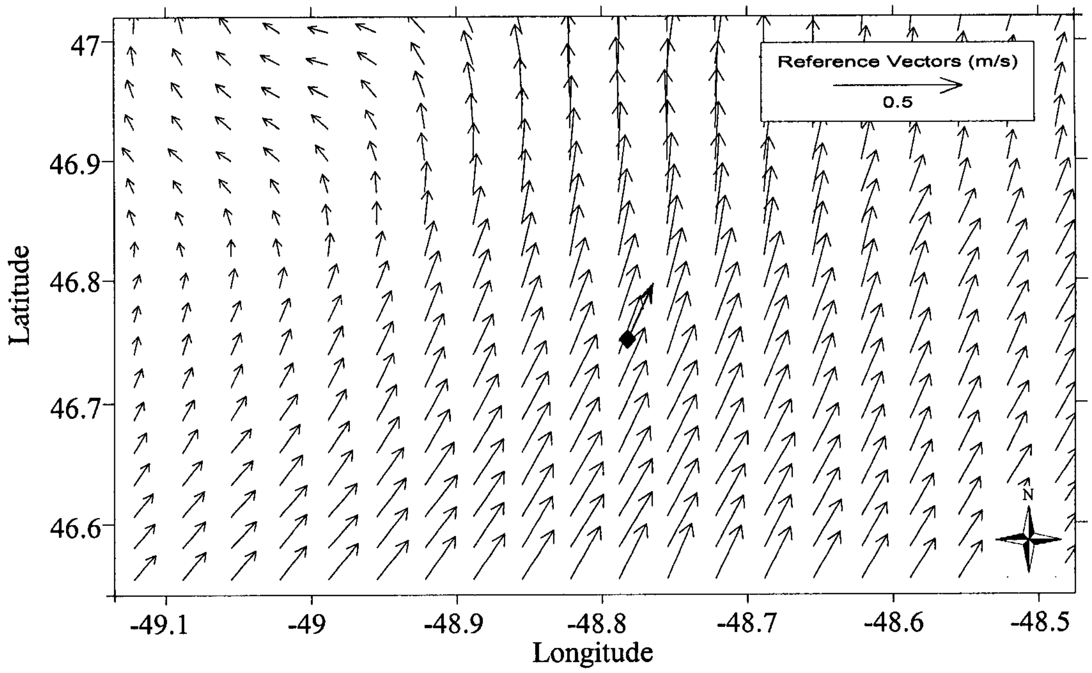

Figure 5-4 (c) Surface current velocity field after a model run of 15 days (the point is the location of Hibernia, and the bolded red vector is the observed velocity of June 15, 2005 at the Hibernia site. The observed velocity is from Hibernia Platform Annual Current Measurement Report (2005))

Figures 5-5 (a) (b) are the current velocity vector comparisons at 10 m of depth in the water after a model run of 16 days and of 23 days, corresponding to the field current velocity data that occurred during the period from June 16, 2005 to June 24, 2005. Figures 5-5 (c) (d) are the current velocity vector comparisons at 10 m of depth in the water after a model run of 25 days and of 28 days, corresponding to the field current velocity data that occurred during the period from June 24, 2005 to June 28, 2005. Figures 5-6 (a) (b) are the current velocity vector comparisons at 40 m of depth in the water after a model run of 16 days and of 23 days, corresponding to the field current velocity data that occurred during the period from June 16, 2005 to June 24, 2005. All field vectors are from the observation data in the Hibernia Platform Annual Current Measurement Report (2005). As the modeling results are not exactly at the same time and on the same day as the observations, there are slight differences between them. Based on the comparisons, most of the modeled velocity fields match with the observations in both speed and direction as shown in Figures 5 and 6.

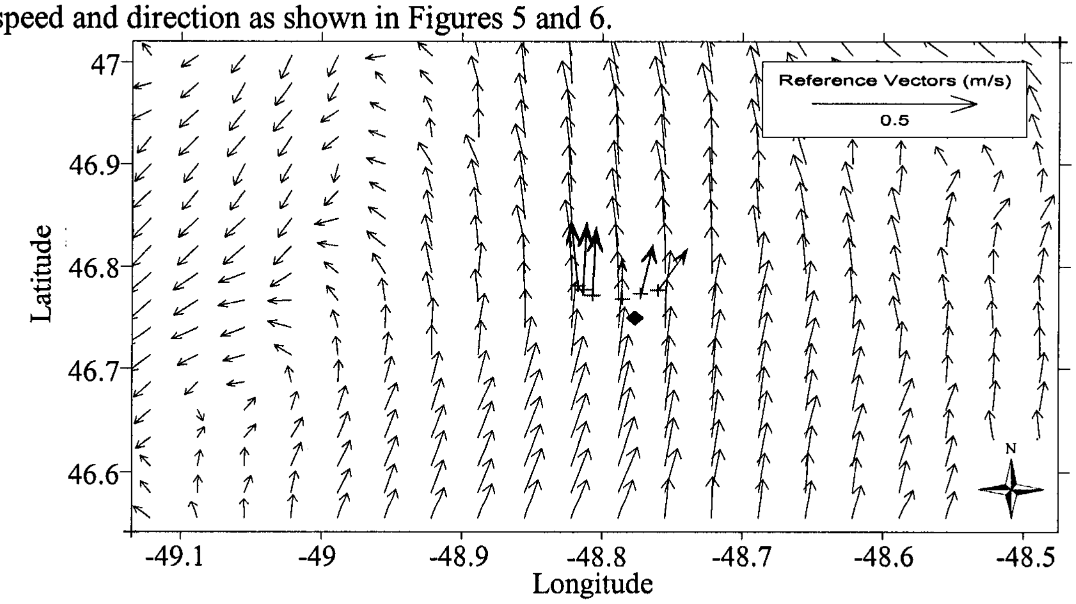

Figure 5-5 (a) Current vectors at 10m of depth in the water after a model run of 16 days (the point is the location of Hibernia, and the bolded red vectors are the observed velocity that occurred during the period from June 16, 2005 to June 24, 2005. The observed velocities are from Hibernia Platform Annual Current Measurement Report (2005))

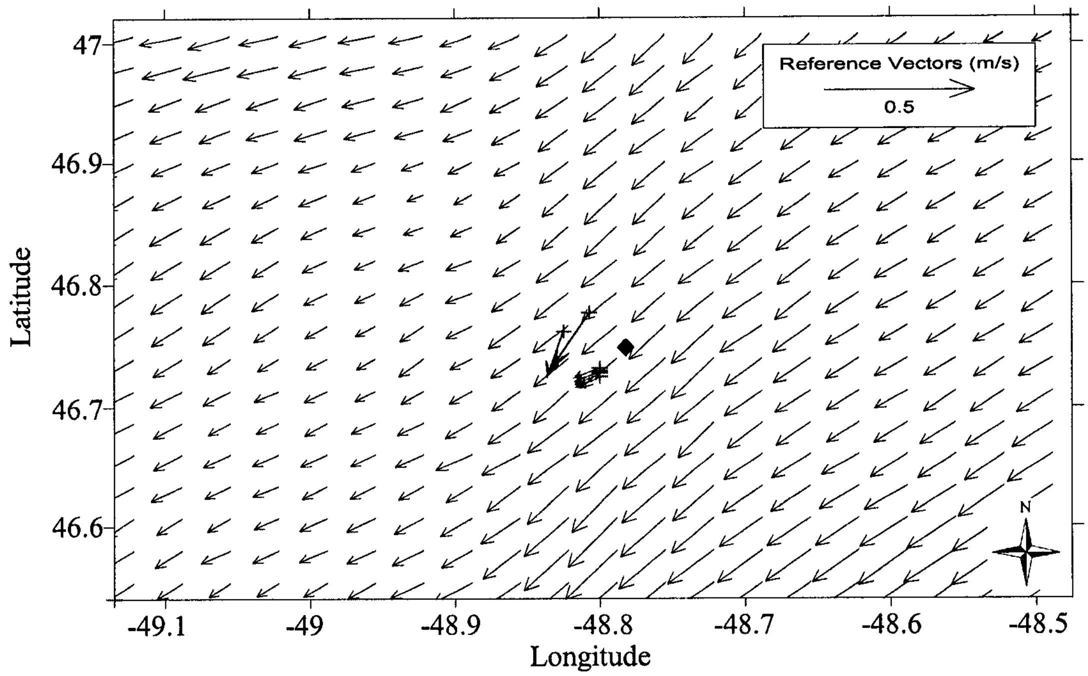

Figure 5-5 (b) Current vectors at 10m of depth in the water after a model run of 23 days (the point is the location of Hibernia, and the bolded red vectors are the observed velocity that occurred during the period from June 16, 2005 to June 24, 2005. The observed velocities are from the Hibernia Platform Annual Current Measurement Report (2005))

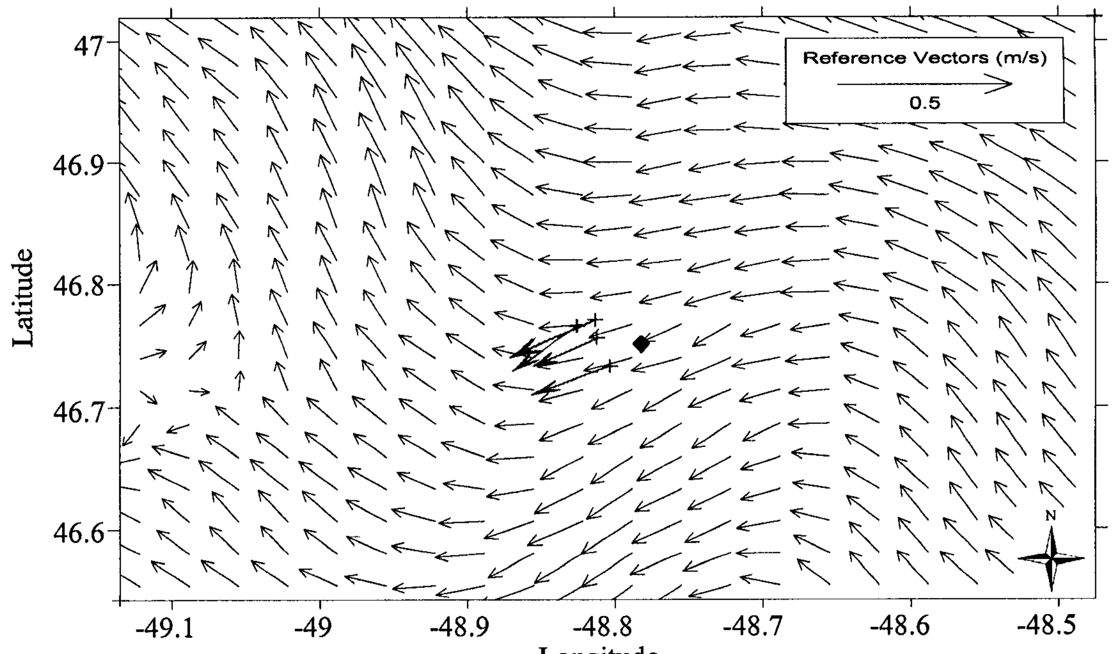

Figure 5-5 (c) Current vectors at 10m of depth in the water after a model run of 25 days (the point is the location of Hibernia, and the bolded red vectors are the observed velocity that occurred during the period from June 24, 2005 to June 28, 2005. The observed velocities are from the Hibernia Platform Annual Current Measurement Report (2005))

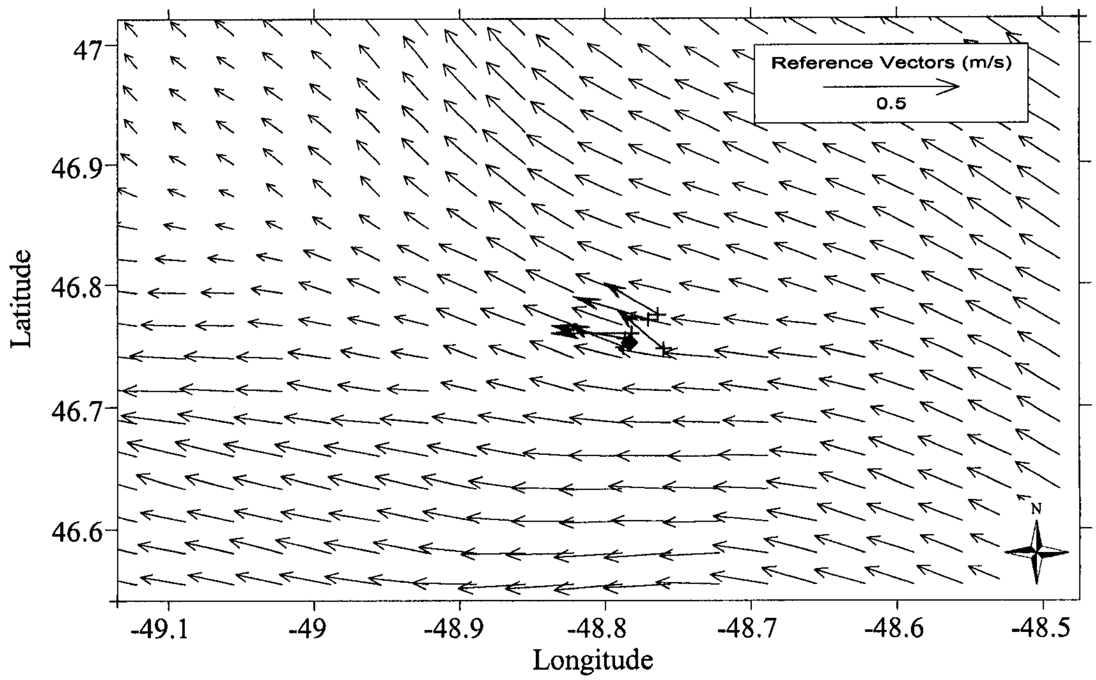

Figure 5-5 (d) Current vectors at 10m of depth in the water after a model run of 28 days (the point is the location of Hibernia, and the bolded red vectors are the observed velocity that occurred during the period from June 24, 2005 to June 28, 2005. The observed velocities are from the Hibernia Platform Annual Current Measurement Report (2005))

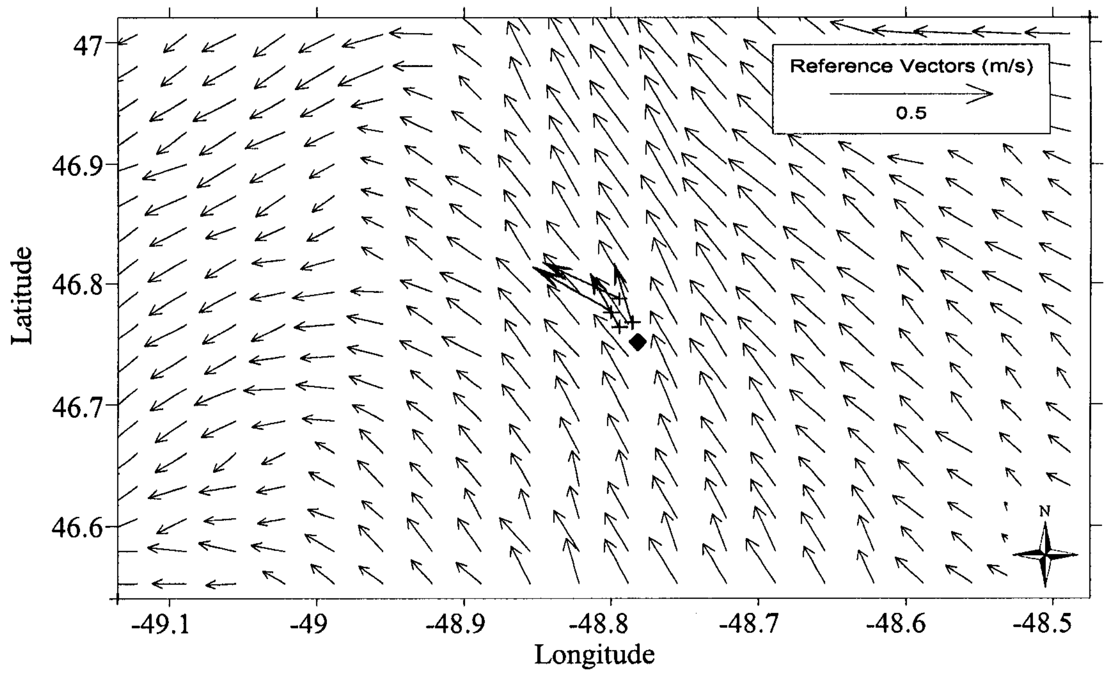

Figure 5-6 (a) Current vectors at 40m of depth in the water after a model run of 16 days (the point is the location of Hibernia, and the bolded red vectors are the observed velocity that occurred during the period from June 16, 2005 to June 24, 2005. The observed velocities are from the Hibernia Platform Annual Current Measurement Report (2005))

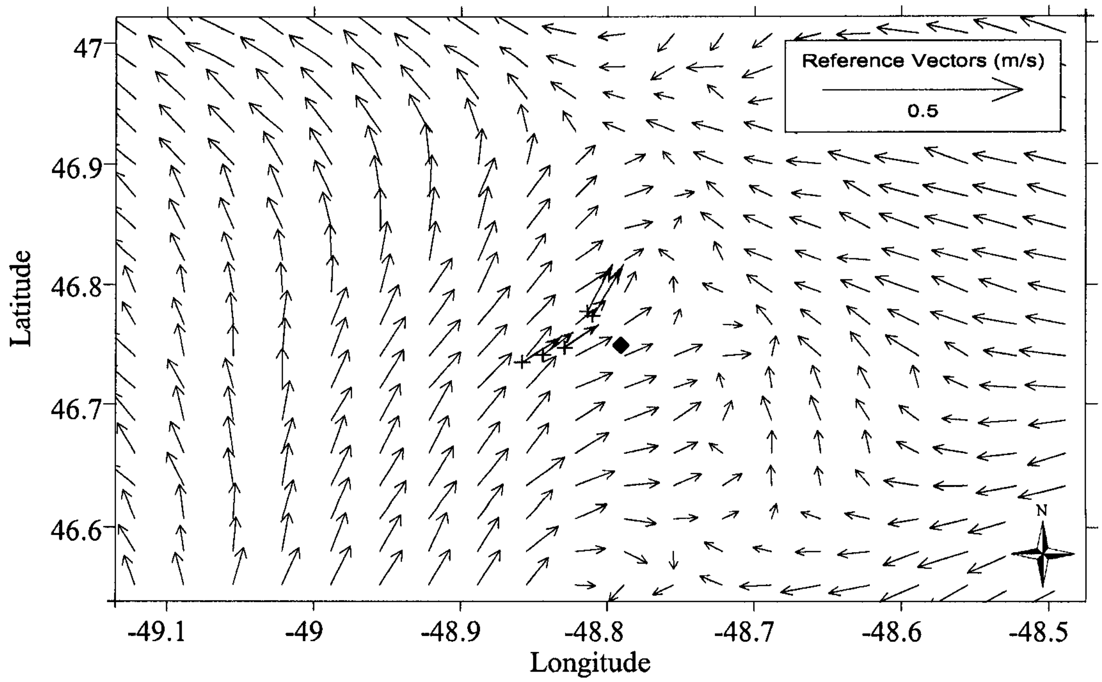

Figure 5-6 (b) Current vectors at 40m of depth in the water after a model run of 23 days (the point is the location of Hibernia, and the bolded red vectors are the observed velocity that occurred during the period from June 16, 2005 to June 24, 2005. The observed velocities are from the Hibernia Platform Annual Current Measurement Report (2005))

5.3.2 Comparison Based on Average Current Data

Table 5-2 shows the comparison of the average velocity speeds and directions between the modeled and observed current data in different locations. The Hibernia surface current measurements are from the Hibernia Platform Annual Current Measurement Report (2005). The observations of 1992 and 1996 are from the near bottom field observation current data available in Web 2 (see Table 4-3). As described in Section 5.1.2, the model grids inside the study area are 1 km × 1 km, whereas the model grids outside the study area are from 8 km to 50 km. Therefore, it is difficult to find exactly the same location and depth with the observation location based on the modeling results. Consequently, differences between the modeling results and field observations occur in the comparison. The differences for the mean velocities at most of the sampling locations are lower than 20%. The minimum difference between the model results and the observed data is 1.6% in point 6 since they have the closest location and depth between the model grid and the observed point. The maximum difference is 30.8% at point 9. As noticed, the modeling location for point 9 is almost 17 km from the observed point. Subsequently, there are some discrepancies between the modeled directions and the observed data.

Table 5-2 Comparison average velocities between model results and measurement data

No.	Date		Latitude	Longitude	Depth (m)	Days	Mean Speed (m/sec)	Mean Directions (True)	Difference in Speed (%)	Difference in Dir (%)
1	June 2005	O	46.75	48.78	0	30	0.220	182	22.7	42
		M	46.81	48.75	0	30	0.170	259		
2	June 1996	O	44.84	55.83	150	6	0.139	272	17.3	49
		M	44.758	55.83	183.6	30	0.115	140		
3	June 1996	O	44.84	55.83	400	6	0.041	263	4.9	53
		M	44.758	55.83	367.1	30	0.043	123		
4	May 1992	O	47.29	48.43	22.5	21	0.050	126	16.0	53
		M	47.31	48.45	23.7	30	0.042	193		
5	May 1992	O	47.57	48.46	46	11	0.041	121	9.8	42
		M	47.58	48.44	31.4	30	0.045	172		
6	May 1992	O	47.67	48.55	135	9	0.064	116	1.6	153
		M	47.67	48.54	130.9	30	0.065	293		
7	May 1992	O	49.75	49.74	900	25	0.071	172	14.1	84
		M	49.75	49.73	684.3	30	0.081	316		
8	June 1992	O	48.27	52.43	40	29	0.069	267	2.9	25
		M	48.245	52.422	80.1	30	0.067	335		
9	June 1992	O	48.91	51.47	30	21	0.052	67	30.8	110
		M	48.874	51.264	48.3	30	0.036	141		
10	June 1992	O	49.27	50.89	300	22	0.043	119	14.0	138
		M	49.262	50.875	217.6	30	0.049	283		

* O represents observed data; M represents modeling results.

Some discrepancies as indicated in Table 5-2 may be due to the fact that 1) the modeling grid locations are not exactly the same as the sampling locations. Some of them may be more than 10 km from each other, which can be improved by using a super-computer in the near future; 2) the input wind data only distribute around the large scale area, while there is a lack of fine wind data inside the study area; 3) synoptic atmospheric forcing and tidal data are not considered as inputs in the model; 4) numerical errors may occur during the computation of the horizontal gradients using the sigma transformation (Huang and Spaulding, 2002).

5.4 3D Current Simulation Results for the Study Area

Figures 5-7 to 5-9 present the modeling results of the 30-day-average velocity fields at 20 m, 40 m, and 60 m, respectively. The vertical velocity, *w(x,y,z)*, in Figures 5-7 (b), 5-8 (b) and 5-9 (b) can be calculated from $\omega(x,y,\sigma)$, the vertical component perpendicular to sigma layers, by using the transformation (Ezer and Mellor, 1997)

$$w = \omega + u\left(\sigma\frac{\partial D}{\partial x} + \frac{\partial \eta}{\partial x}\right) + v\left(\sigma\frac{\partial D}{\partial y} + \frac{\partial \eta}{\partial y}\right) + \sigma\frac{\partial D}{\partial t} + \frac{\partial \eta}{\partial t} \tag{5-2}$$

where $D = H + \eta$ and $\omega = 0$ when $\sigma = 0$ or -1. Trajectories, based on Eulerian velocities in Figures 5-7 (a), 5-8 (a) and 5-9 (a), are launched from every second grid point.

The flow directions in June 2005 are generally from south to north. The velocity at 20 m of depth (Figure 5-7 a) is a little larger than that at 40 m of depth (Figure 5-8 a), whereas it is smaller at 60 m of depth (Figure 5-9 a) since it is near the bottom. The near-bottom flows generally follow the bottom topography contours (see Figure 5-3). As seen in Figure 5-9 (a), the velocity suddenly changes directions in the northeast corner because of the change of the hydraulic gradient in the continental slope, which is well represented by the sigma coordinate model. The flows generally follow a downward flow upslope and an upward flow downslope. The near-bottom vertical velocity contour in Figure 5-9 (b) indicates areas of possible deep locations in the study site.

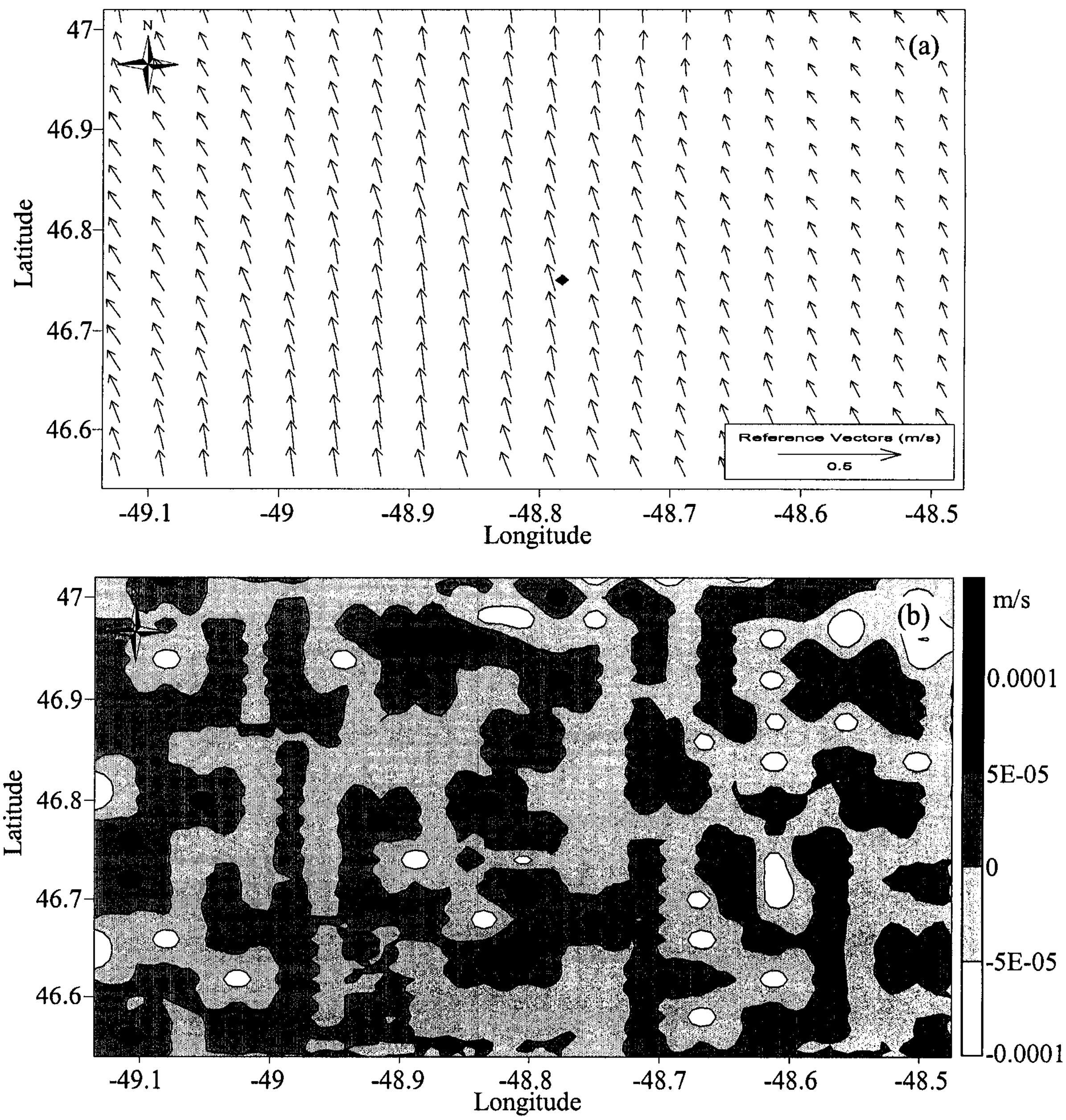

Figure 5-7 30-day-average velocity field at 20 m of depth. (a) Horizontal velocity field and (b) vertical velocity contour; contour interval is 0.5×10^{-5} m s^{-1}

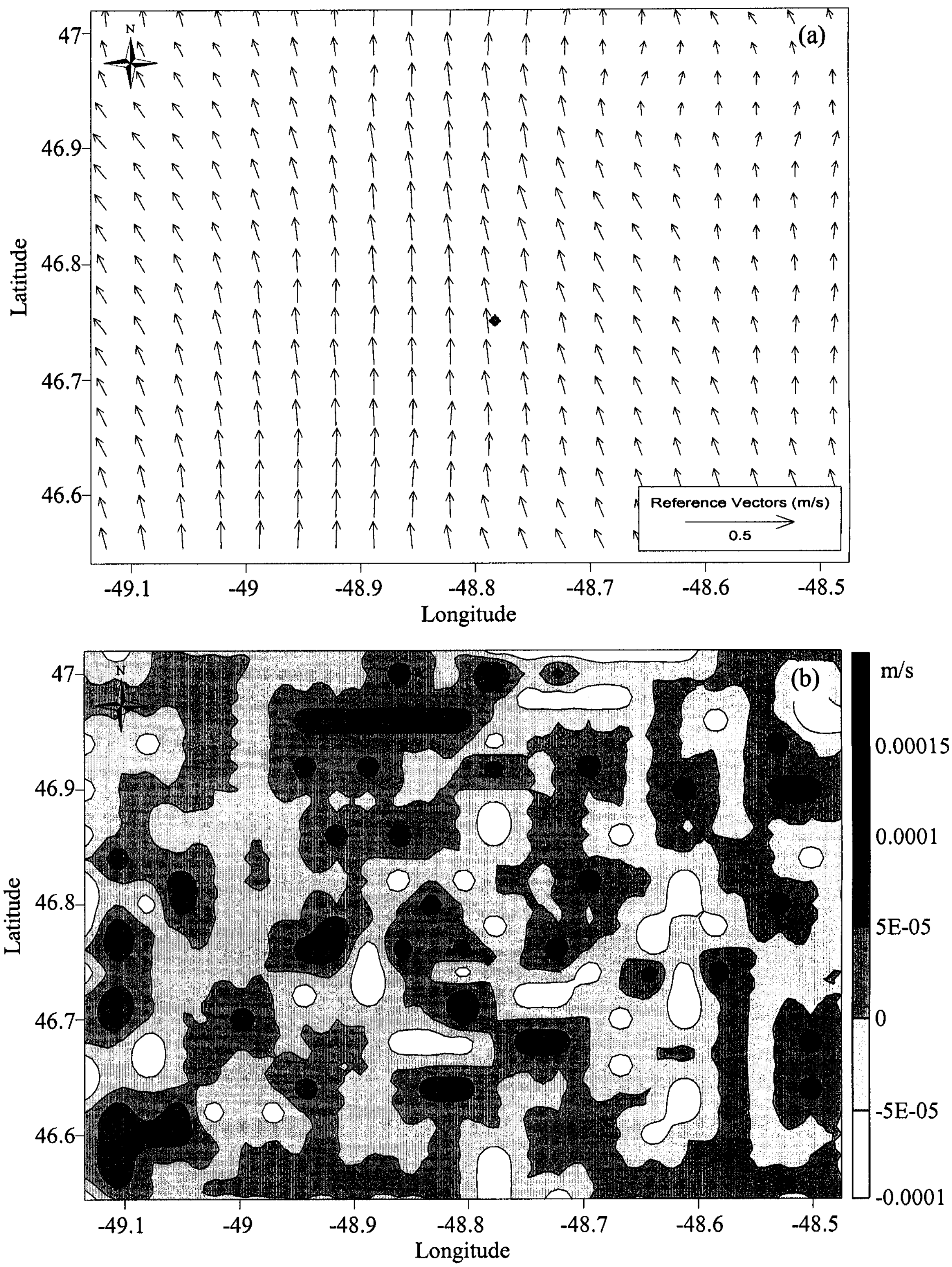

Figure 5-8 30-day-average velocity field at 40 m of depth. (a) Horizontal velocity field and (b) vertical velocity contour; contour interval is 0.5×10^{-5} m s^{-1}.

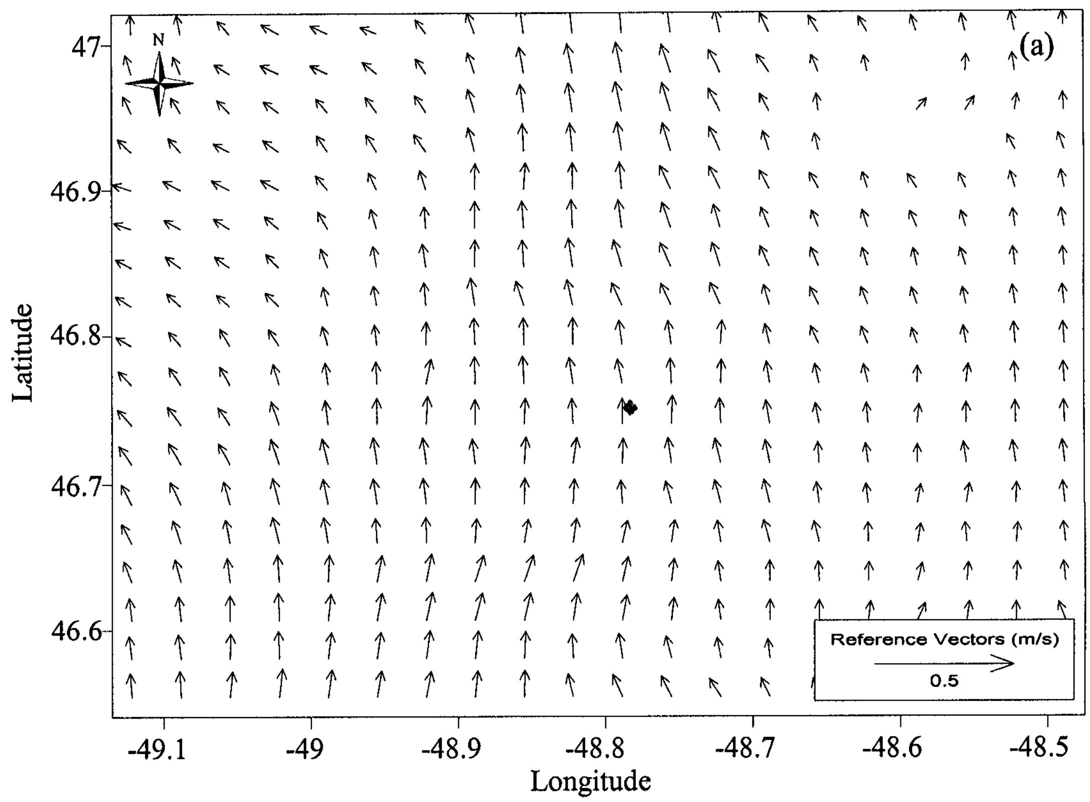

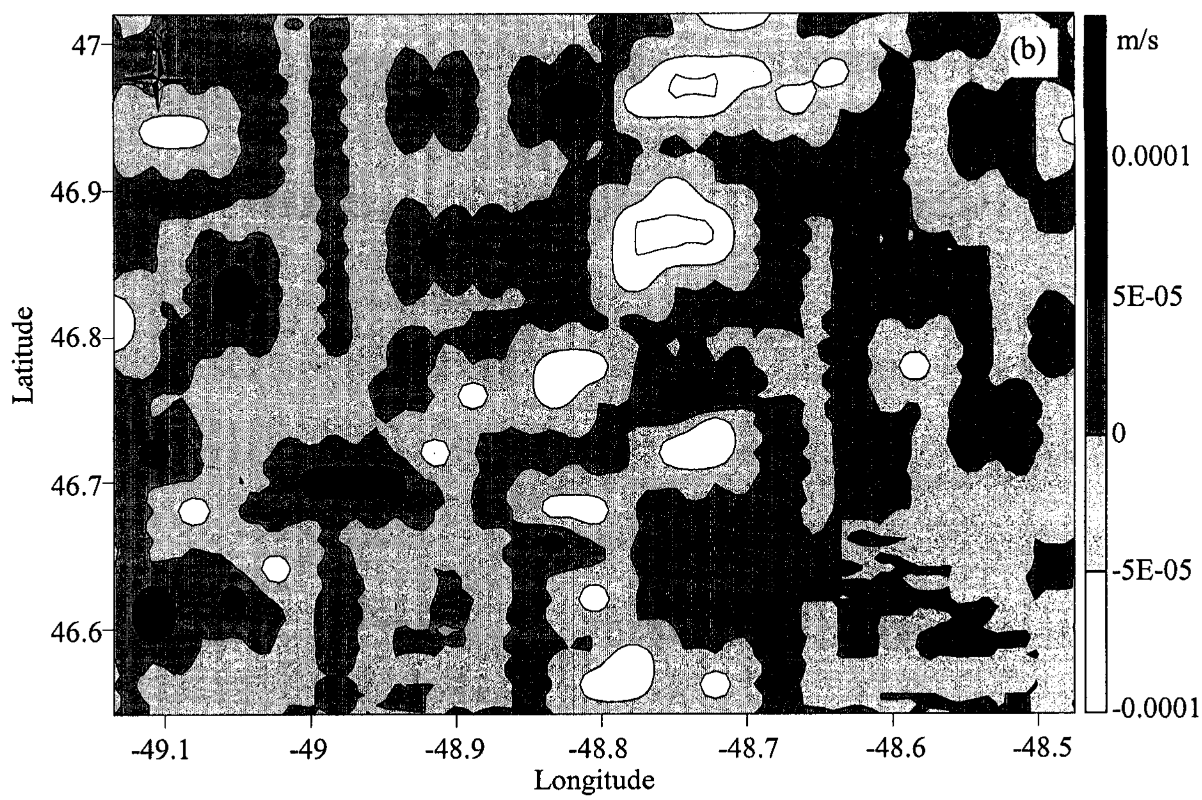

Figure 5-9 30-day-average velocity field at 60 m of depth. (a) Horizontal velocity field and (b) vertical velocity contour; contour interval is 0.5×10^{-5} m s^{-1}.

5.5 Summary

A POM modeling has been developed and validated by the use of field data and investigation to simulate 3D current conditions of the Hibernia area. In order to minimize the influences of numerical open boundary conditions existing in the study area, a large scale area over 200 times the covered study area has been chosen to simulate the regional ocean current field. The validation of the 3D current velocity field modeling indicates that POM can, for the Hibernia region, provide satisfactory current simulations, which will serve as hydrodynamic inputs to the dispersion model. In conjunction with the ocean current velocities described in this chapter, the pollutant dispersion of produced water discharges and potential risk assessment are investigated by using POM-RW in the following chapter.

Chapter 6

Modeling of the Dispersion of Produced Water and the Risk Assessment for the Hibernia Site

In conjunction with the ocean current results simulated in Chapter 5, the present chapter describes the dispersion of produced water and the risk assessment results for the Hibernia site, using the developed POM-RW model and the integrated risk assessment approach described in Chapter 3.

6.1 Modeling of the Dispersion of Produced Water Discharges at the Hibernia Site

The fate and transport of chemicals in produced water discharges at the Hibernia platform can be simulated by the developed POM-RW approach as discussed in Chapter 3. The random walk method is a Lagrangian modeling technique, which characterizes the dispersion of a pollutant based on a particle tracking approach. Coupling the velocity components from POM and random walk dispersion, the POM-RW is formulated to simulate the dispersion of dissolved Lead (Pb) in the produced water effluent in the present case study. The ocean current results from the POM were presented in Chapter 5. They provide the critical ocean hydrodynamic input for the simulation of mass transport, producing the realistic concentration distribution of contaminants in the study area. The developed POM-RW method with the dispersion modeling results is validated with the field data. The details are presented in the following sections.

6.1.1 Modeling Area and Grid Configuration for the Dispersion Model

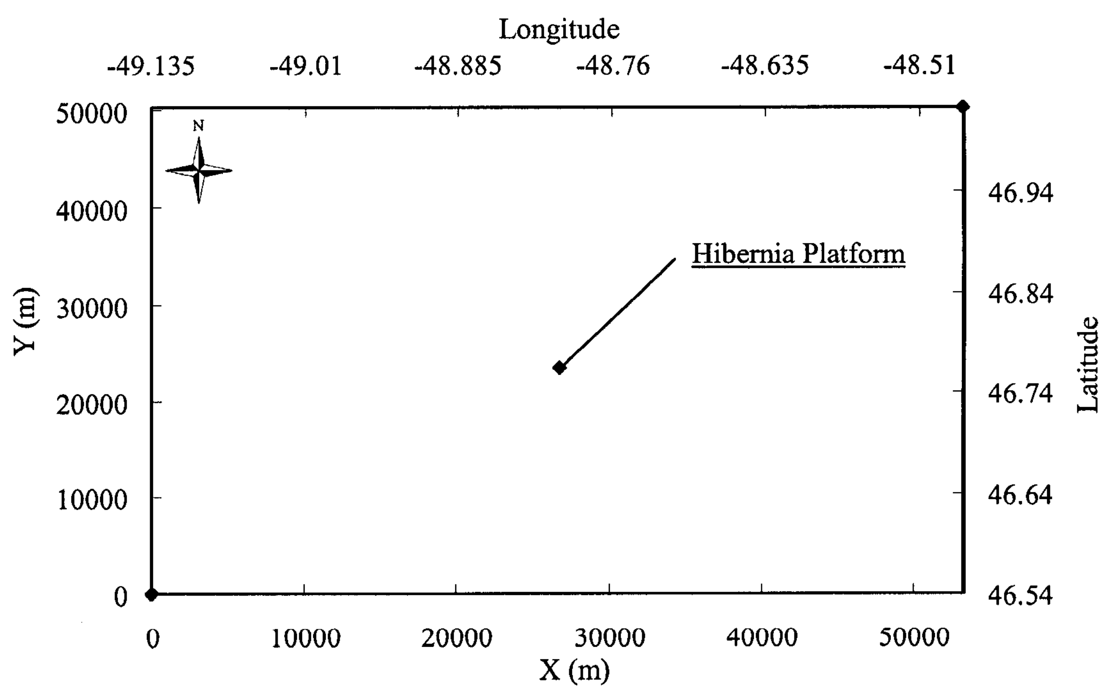

Figure 6-1 Comparison of the coordinate systems

As mentioned before, the study area for the dispersion of pollutants is from (49.135W, 46.54N) to (48.475W, 47.02N), 50 km × 50 km with the Hibernia site as the centre. In the following sections, the results will be presented as the distances in the west-east and south-north directions. Figure 6-1 shows the comparison between the distance coordinate system and the longitude-latitude coordinate system. The (0, 0) point in the distance coordinate system is (49.135W, 46.54N). The location of the Hibernia platform is x = 26824 m and y = 23400 m under the distance coordinate. In order to simulate a more detailed distribution of contaminants of produced water, the model grid for the pollutant dispersion has a higher resolution than the current model, which is 50 m × 50 m for each cell, totaling 1000 × 1000 nodes for the study area. The current results will be interpolated to the dispersion modeling grids.

6.1.2 Chosen Species for Dispersion Simulation

Among those contaminants in the produced water, the dispersion of Pb is studied in the present research for the assessment of its potential impacts on the regional aquatic environment. Lead and its compounds have been known to man for about 7000 years. Eisler (2000) have indicated that all credible evidence shows that Lead is neither essential nor beneficial to living organisms and that all the measured effects are adverse – including those on survival, growth, reproduction, development, behavior, learning, and metabolism. Various living resources are at increased risk from Lead. He also mentioned that the adverse effects on aquatic biota reported at the waterborne Lead concentration of 1.0 to 5.1 ug L^{-1} include reduced survival, impaired reproduction, reduced growth, and high bioconcentration from the medium. Dojlido and Best (1993) also reports that the toxic effects on shellfish can occur even with a very low concentration of Pb present. The body functions of phytoplankton can be disturbed by the interference of Lead.

6.1.3 Configuration of Dispersion Model

Assuming that the background dissolved Lead concentration in seawater is zero, a continuous point discharge of produced water at a depth of 40 m below the surface at the Hibernia platform is identified and considered for dispersion modeling. The emission rate of the produced water is 882 m^3/hr at 456.7 ug L^{-1} of Pb, assuming that Pb is conservative. Based on the comparison with the field observation data, the horizontal mixing coefficient of 80 m^2 s^{-1} and the vertical coefficient of 0.007 m^2 s^{-1} are adopted in this study (validation results shown in Section 6.1.4). The model runs for 30 days with a timestep of 60 s and a release of 200 particles per timestep. Samples of the produced water and the ambient sea water at three depths (10 m, 35 m, 60 m) from the surface to the ocean bottom were collected by the research cruise in June 2005. The analyses of the samples were conducted by COOGER (Centre for Offshore Oil and Gas Environmental Research) and TAF (Trace Analysis Facility) at the University of Regina. These sample results are used to validate the modeling simulations.

6.1.4 Validation of Dispersion Model Based on POM-RW

Based on the initial setup described in Section 6.1.3, using a constant discharge and flow simulations as input, the Lead dispersion results compared with field data at 10 m, 35 m, 60 m are shown in Figures 6-2 (a) (b) (c), respectively. The modeling results are the distribution of average concentration for the model run from 21 days to 30 days. It shows that the model results have a very good agreement with the field observations at the 35 m depth where the model grid is closest to the emission source point. Figure 6-2 (b) also clearly shows the emission source location with the highest concentration in the resulting plume at that layer. The flow modeling results for the layer at the depths of 10 m and 60 m confirm that the general direction of flow current is from south to north. This explains why the dispersed pollutants move a little bit to the north of the Hibernia site as indicated in Figures 6-2 (a) and (c).

The predicted concentrations for field locations far from the emission source are generally lower than the sample concentrations as shown in Figure 6-2 (a) and (c). This could be explained with the following analyses: 1) the model ran for only 30 days; most of the particles could still accumulate in the near field and possibly only a small number of particles reached the surface and the bottom; 2) there are the uncertainties associated with the natural marine condition as well as the possible operational changes of produced water discharges from the source; 3) the mixing coefficients are assumed to be constant in the present study; the different values of the coefficients will affect the dispersion pattern; and 4) the instantaneous changes of current in the study area, due to aquatic life activities, sailing ships, and oil and gas production and transportation activities, would also change the pattern of dispersion; The possible solutions for improving the simulation results are discussed in Chapter 7.

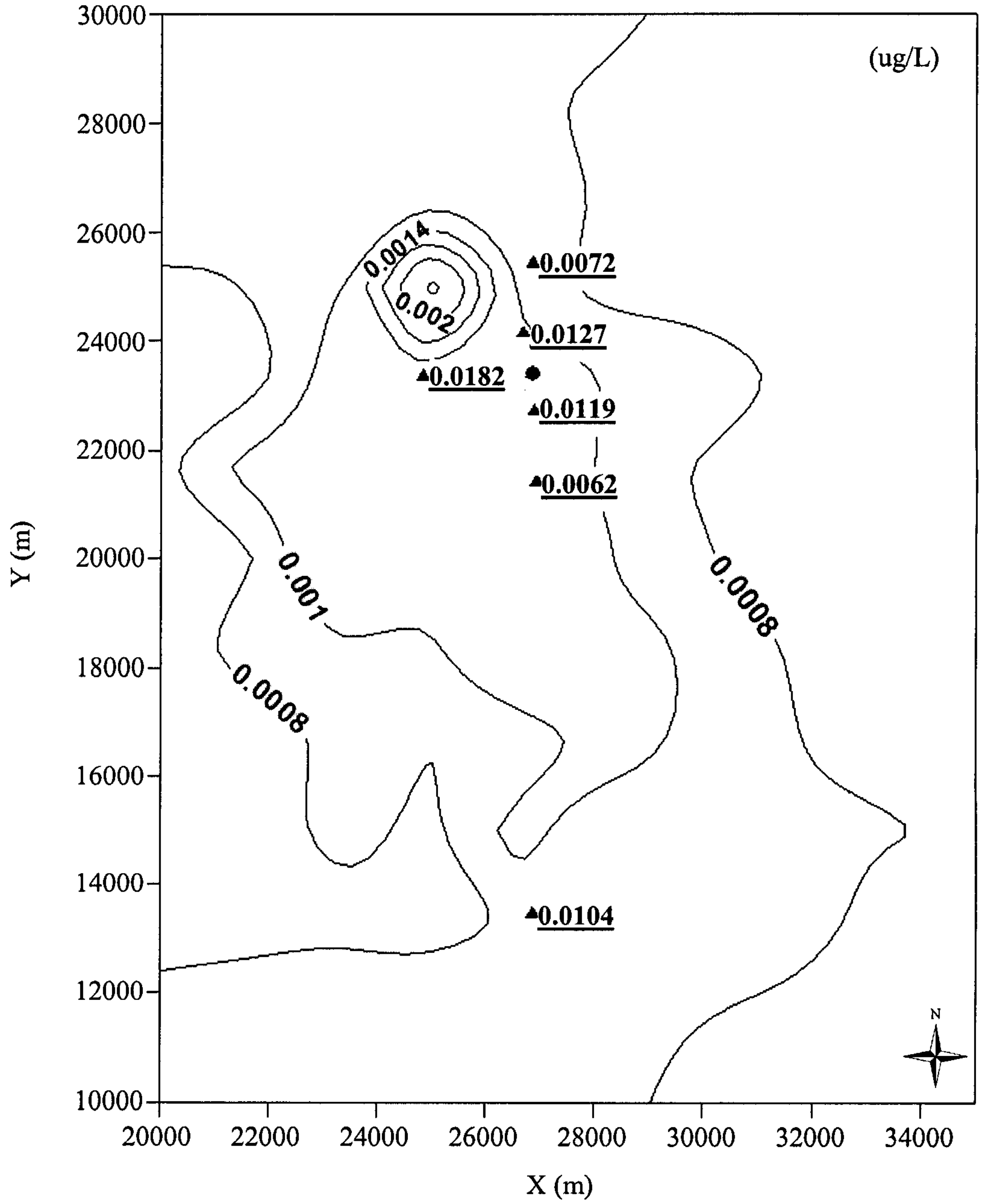

Figure 6-2 (a) Pb dispersion modeling results with field observations at 10 m depth of water (the black filled circle is the location of Hibernia platform)

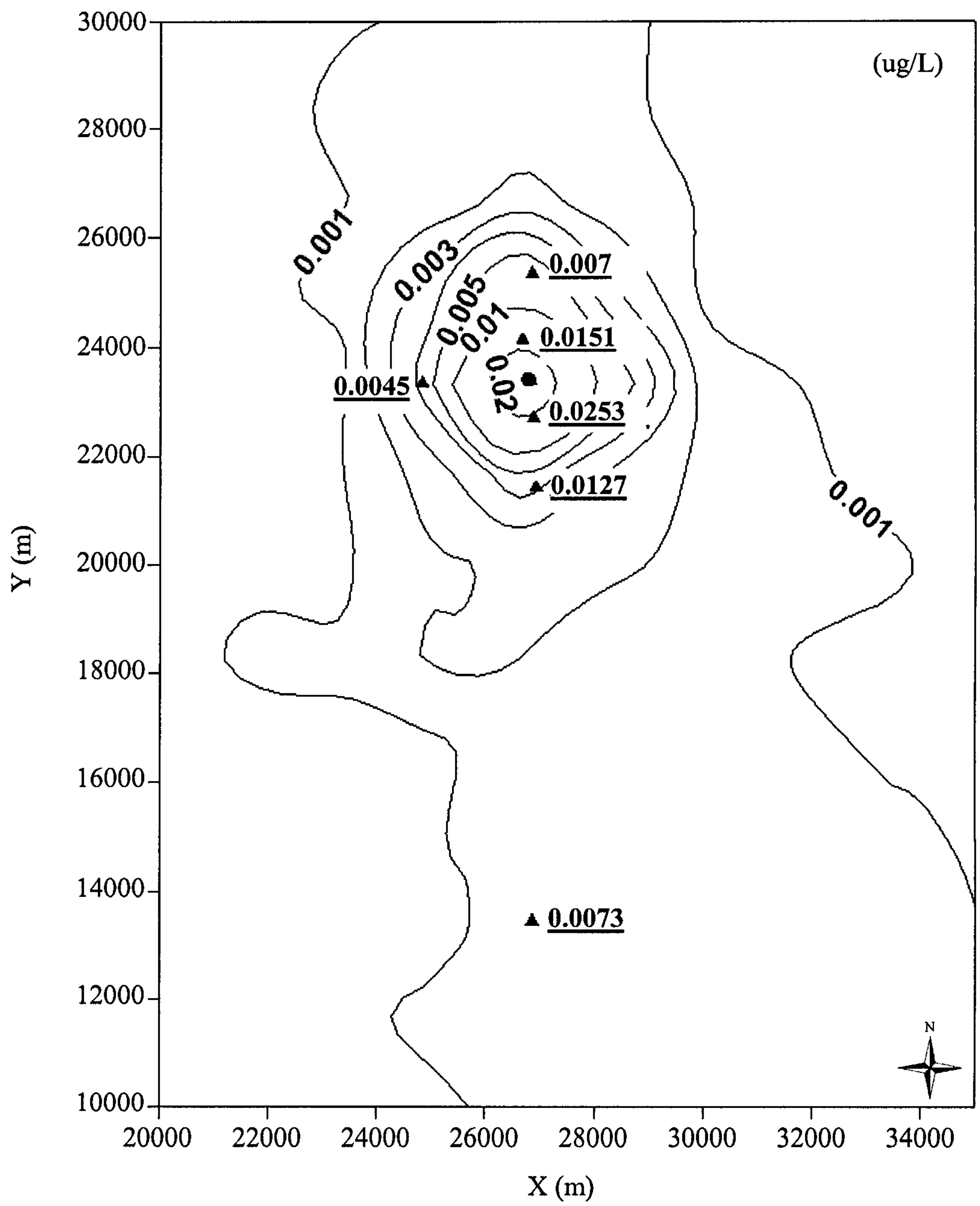

Figure 6-2 (b) Pb dispersion modeling results with field observations at 35 m depth of water (the black filled circle is the location of Hibernia platform)

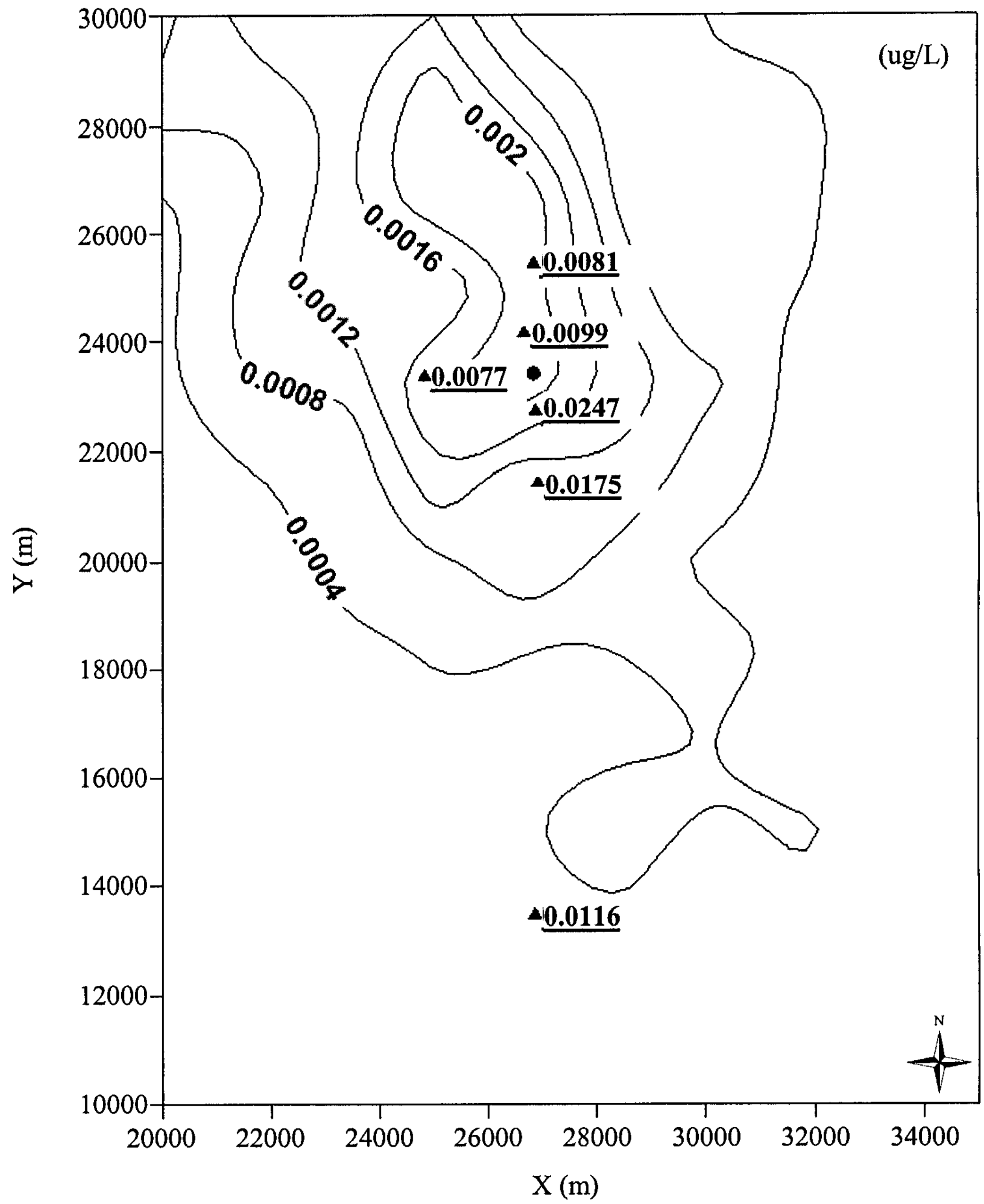

Figure 6-2 (c) Pb dispersion modeling results with field observations at 60 m depth of water (the black filled circle is the location of Hibernia platform)

6.1.5 3D Pollutant Dispersion Simulation Results

Figures 6-3 (a) (b) (c) show the transport of the dissolved Lead after a model run of 10 days, 20 days and 30days at depths of 20 m, 30 m, 40 m, 50 m, and 60 m. The dispersion of Pb is generally towards the north due to the effects of the ocean flow, but a higher concentration accumulates around the Hibernia platform (the point in 40 m depth) due to continuous emissions.

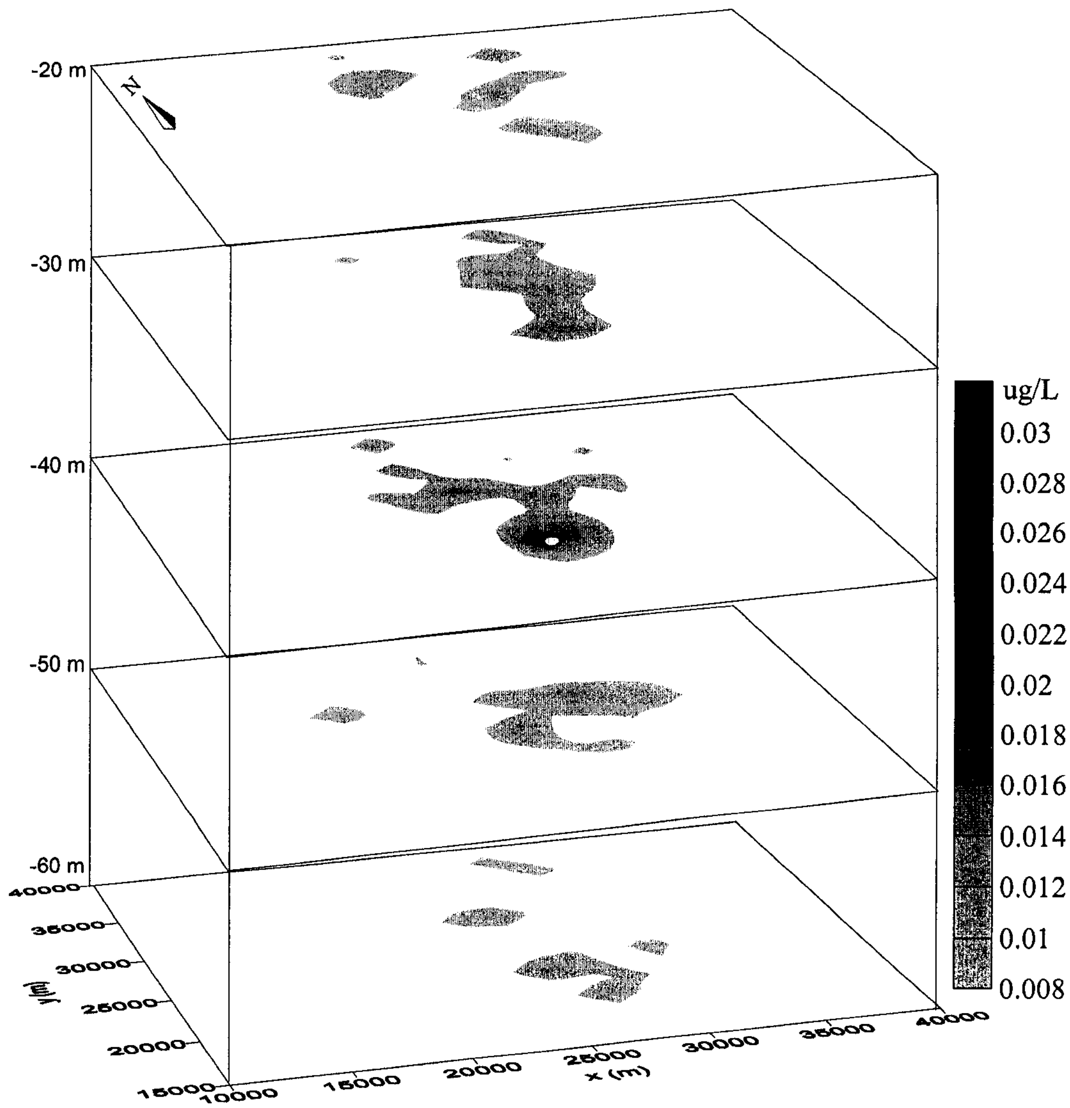

Figure 6-3 (a) Visualization of the 3D dispersion modeling results for 10-day dispersion

Modeling results for the 10-day period are presented in Figure 6-3 (a) for 5 layers, which indicate that the plume reaches to the north boundary in the horizontal, and vertically up to a 20 m depth and down to a 60 m depth, respectively. The Lead concentration within 2000 m around the source is between 0.018 ug L^{-1} to 0.03 ug L^{-1}. In the other layers, the concentration falls to less than 0.014 ug L^{-1}. As noticed, at a 30 m depth, the plume appears in a southwards direction due to the higher velocity in the upper layer (especially near the surface) as discussed in Section 5.1, whereas at 50 m of depth, the pattern is more random, being mainly due to the lower velocity near the bottom and complex sea bed friction effects.

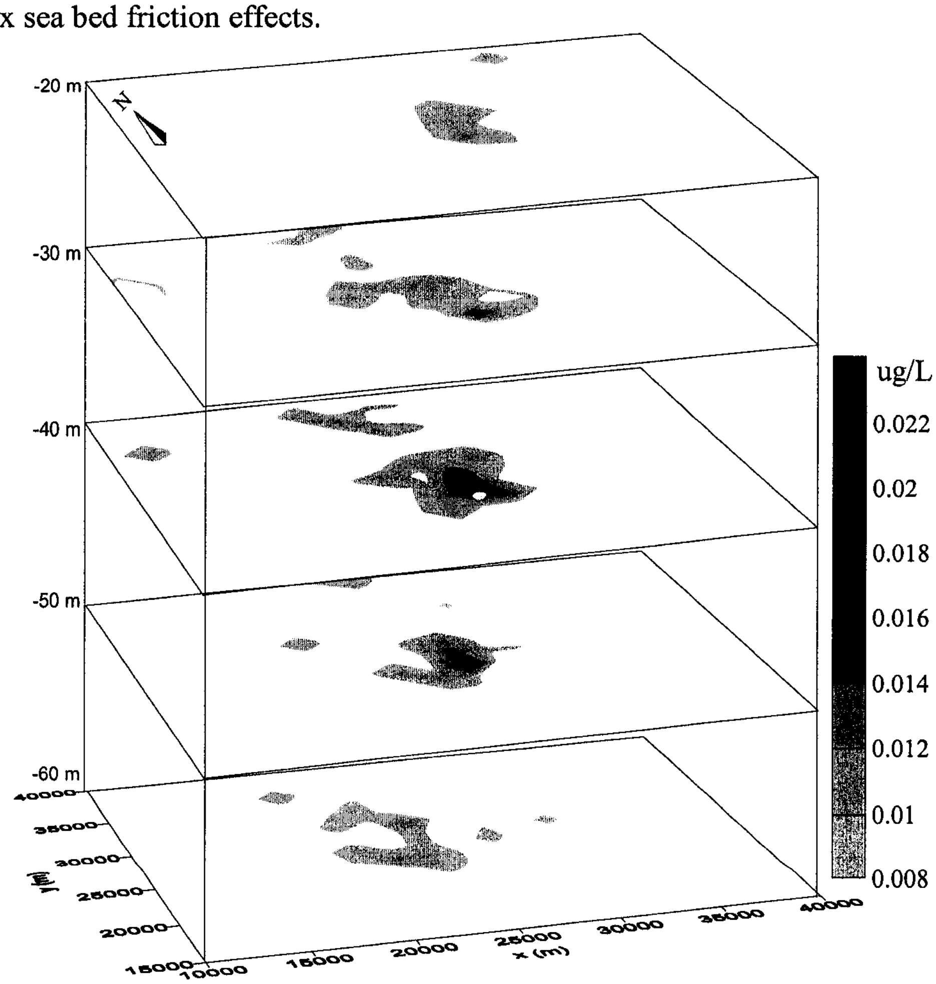

Figure 6-3 (b) Visualization of the 3D dispersion modeling results for 20-day dispersion

Figure 6-3 (b) shows the model results for a 20-day period. Compared with Figure 6-3 (a), the plume is now enlarged horizontally and vertically. The concentration above 0.018 ug L^{-1} expands to about 5000 m away from the source along the plume layer (40 m depth). At 30 m and 50 m depths, the concentration is much higher than is shown in the 10-day results. The concentration at the 50 m depth is even higher than the plume layer. When the model is run for 20 days, the pollutant travels throughout the entire study area from bottom to surface and has a trend to form another pollutant patch.

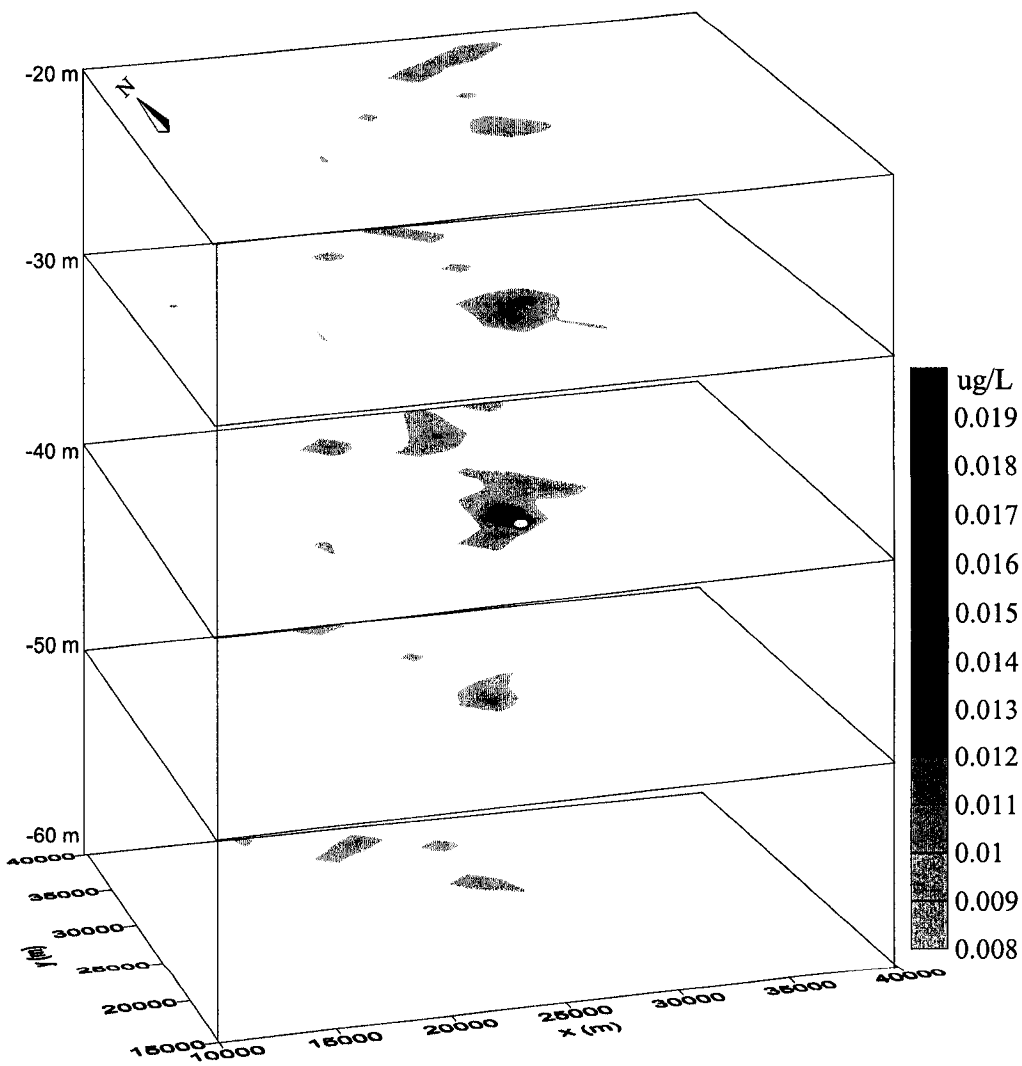

Figure 6-3 (c) Visualization of the 3D dispersion modeling results for 30-day dispersion

Modeling results for 30-day dispersion are given in Figure 6-3 (c), the concentration distribution is scattered in each layer, and the concentration is smaller than the 10-day and the 20-day dispersion results at the same layer. The reason may lie in that another pollutant patch is separated from the main plume after 20 days. It travels past the study area and has been diluted to the background level by the seawater.

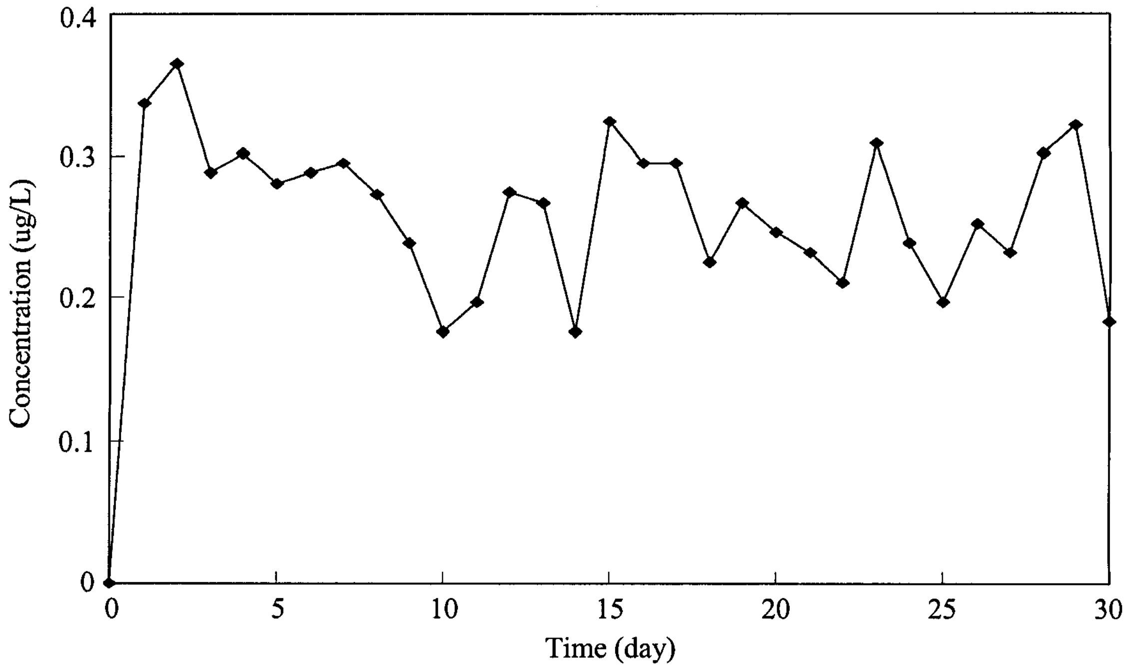

Figure 6-4 Change of concentration with time in the location of (26775m, 23450m) within 60 m radius around the emitting source in 2005 (Hibernia is (26824m, 23400m)

As noticed in Figure 6-3 (c), the concentration after a 30-day run is lower than the other two simulation results. The fact is that not only the pollutant plume pattern will change over time, but the concentration of a chemical at a certain point within a plume of produced water discharges can be very variable. The variation in concentration is caused by factors such as wind and currents that may in turn cause complicated turbulence patterns in the water column (Karman and Reerink, 1998). Figure 6-4 shows the concentration over time at (26775m, 23450m) (Hibernia is (26824m, 23400m)), which is about 60 m away from the source of the produced water discharges. It shows a cycle of about 5 days in the concentration changes. In this location, the lowest concentration appears on 10^{th}, 14^{th} and 30^{th} days. The average concentration is 0.26 ug L^{-1}, which appears on the 5^{th} – 8^{th}, 13^{th}, and 19^{th} days.

6.2 Integrated Risk Assessment for the Hibernia Site

The developed POM-RW model is extended to quantify the risks of the produced water discharges in the Hibernia area as described in Section 3.4. The volumes of produced water discharges are time dependent and usually increase during the production process (Utvik, 1999; Neff, 2002). Therefore, two future emission rates are examined for the risk assessment of the Hibernia area in the years of 2015 and 2025. The year 2015 represents the middle age of the Hibernia oil well, and 2025 represents the end stage, both of which are predicted using the trend of known production from 1997 to 2006. Uncertainties in the system are examined by means of the Monte Carlo method. The probabilistic risk and the risk quotient (RQ) factors combined with the present and future rates of produced water productions will provide the spatial and temporal assessment of the risk from the produced water discharges at the Hibernia site.

6.2.1 Projection of the Produced Water Discharges at the Hibernia Site

As mentioned in Chapter 4, over the life of an oil well, the volume and composition of produced water may change significantly. According to the theory of Stephenson (1992) and Shaw et al. (1999), about 98% of the extraction in nearly depleted fields is produced water and only 2% is the fossil fuel. Therefore, it could be estimated that there will be 5 × 10^8 m^3 yr^{-1} at its end stage based on the oil production of 2006 at the Hibernia oil well (see Table 4-1). The Hibernia site still has 20 to 25 years left for exploration (Petro-Canada, 2005). Based on the published emission rate at the Hibernia platform from 1997 to 2006 (Table 4-1), the trend of the produced water generation at Hibernia is evaluated as shown in Figure 6-5. As shown, the possible emission volume of produced water is 2.8 × 10^7 m^3 in 2015 and 5.1 × 10^7 m^3 in 2025.

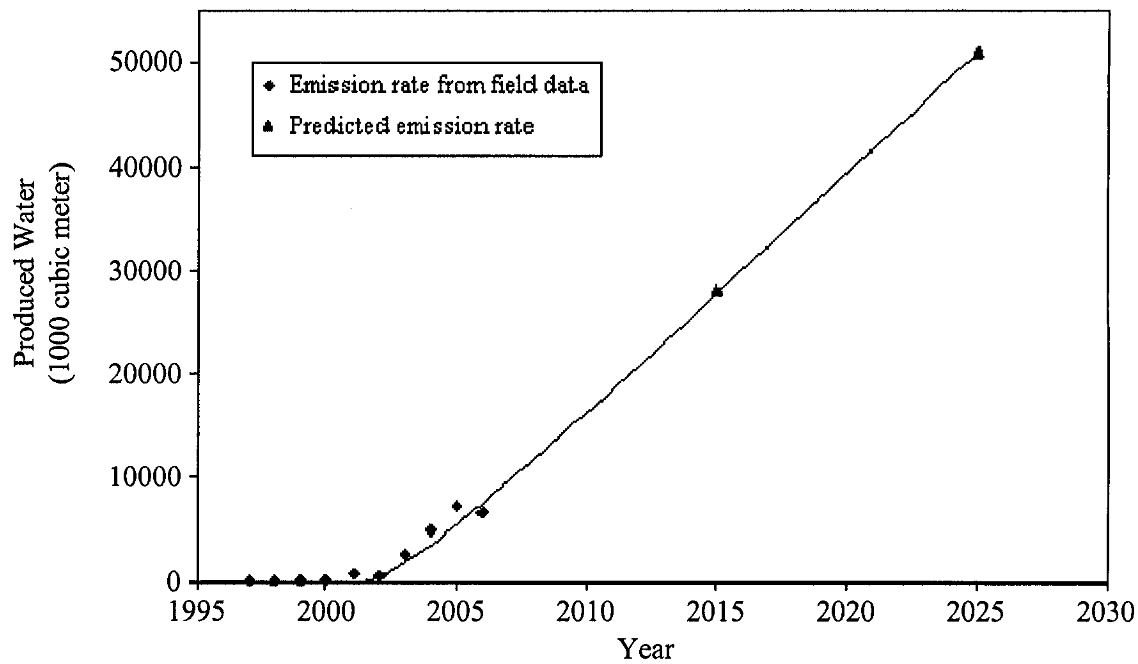

Figure 6-5 Predicted produced water discharges in Hibernia field (existing field emission rates are from BASIN (2007))

6.2.2 Monte Carlo Simulation for Uncertainty Analysis and Risk Assessment

The values of the horizontal mixing coefficient K_h and the vertical mixing coefficient K_z are selected to be normally distributed based on Equation 3.26 (Riddle et al., 2001). The horizontal mixing coefficient is specified from a uniform distribution from 50 to 120 m^2 s^{-1} spanning the range of values, and the vertical mixing from a normal distribution with a mean 0.007 and a standard deviation of 0.003 m^2 s^{-1}. The consideration of these parameter distributions is discussed later in Chapter 7. The sample size of 200 sets has been calculated based on Equation 3.25 with 95% confidence and 5% error with respect to the mean. More details of the computational process have been depicted in Chapter 3 (Figure 3-1).

In the Monte Carlo simulation, in order to reduce the computational time, the model runs only for 5 days for each set of data sample inputs (total sample size is 200 sets). The 5^{th}-day concentration can possibly represent the average concentration as discussed (i.e., Figure 6-4) in the near field. The most concerned area in this analysis is 2000m in diameter surrounding the source, which is 26 km to 28 km in X and 23 km to 25 km in Y in the present study. Other settings are the same with the simulation for the year of 2005 presented in Section 6.1. The Monte Carlo results consist of a concentration distribution for each spatial position, which allows the uncertainty in the concentration predictions and risks to be mapped.

After the application to each of the grid squares, 95^{th} and 5^{th} percentile concentration contour maps are prepared as shown in Figure 6-6. It should be noted that the plots in Figure 6-6 (a) (95^{th} percentile concentration) do not necessarily represent an instantaneous concentration distribution that could occur. Since the 95^{th} percentile concentration for one position might be caused by a different combination of parameters than the 95^{th} percentile concentration for another position, the 95^{th} percentile concentration distribution may represent a "worst case" prediction (Riddle et al., 2001).

The 5th percentile concentrations are generally much lower except for those adjacent to the major discharges. The predicted 95th percentile concentrations are of the order of 0.02 – 0.36 ug L^{-1}, and the corresponding 5th percentile concentrations are of the order of 0.005 – 0.125 ug L^{-1}.

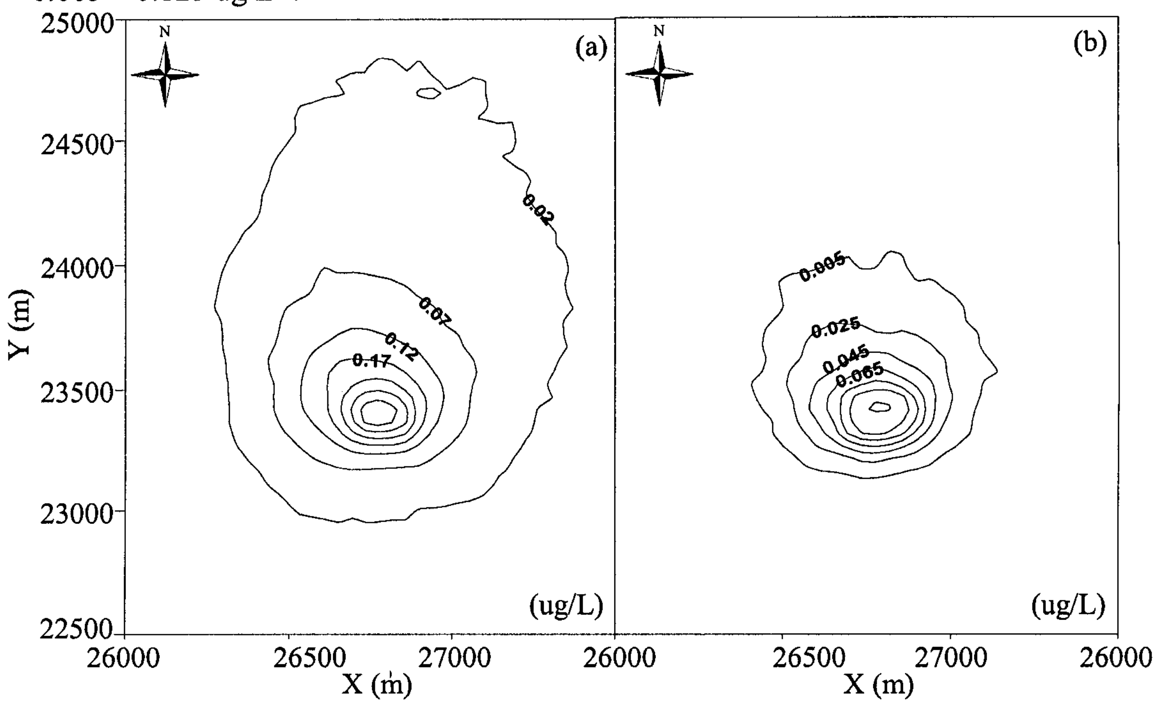

Figure 6-6 Uncertainty predictions showing (a) 95th percentile concentrations and (b) 5th percentile concentrations of produced water dispersion

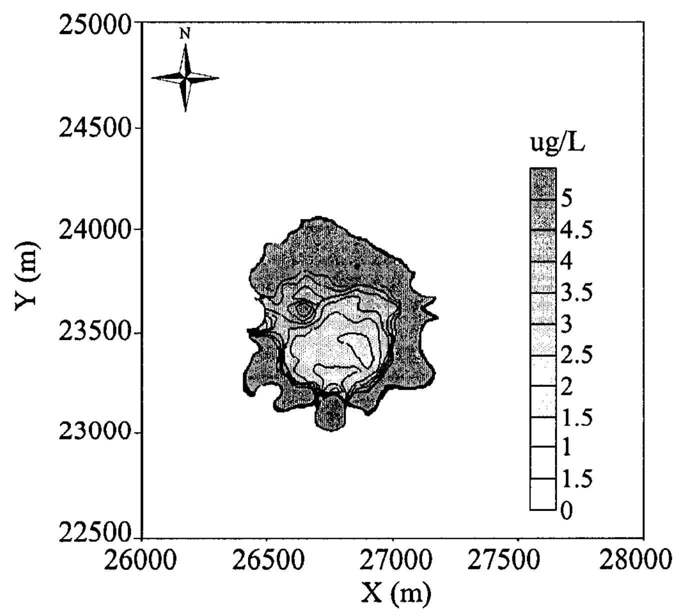

Figure 6-7 Uncertainty factor contour map

The uncertainty factor is calculated as the ratio of the 95 and 5 percentile concentrations as presented in Chapter 3 (Riddle et al., 2001). Figure 6-7 shows the uncertainty factor distribution based on the results from Figure 6-6. The predicted uncertainty factor is of the order of 2 - 5 along the plume. Basically, the uncertainty factor is larger in the low concentration area, and smaller near the discharge source, which indicates that the mixing processes may work well in the near field, whereas may contain more uncertain factors in the far field. This phenomenon demonstrates that the influences of mixing processes will decrease with distances and eventually other concentration reduction mechanisms will dominate after traveling to certain distances (CAPP, 2001).

6.2.3 Risk Assessment for the Hibernia Site

World-wide regulations for protection of aquatic life are highly variable due to population, development, industrialization, and socio-political conditions in different countries, even in different provinces. In the Canadian Water Quality Guidelines for the Protection of Aquatic Life (2006), Environment Canada has issued a range of Lead criterion (1 – 7 ug L^{-1}) for the protection of aquatic life in *freshwater*. The Canadian regulatory values for dissolved Pb considered water hardness a factor. At hardness of 0-60, 60-120, 120-180, and >180 mg L^{-1}, as $CaCO_3$, the 4-d average concentrations of Lead are 1, 2, 4, and 7 ug L^{-1}, respectively. While a Canadian guideline for acceptable Pb emissions in *seawater* does not exist, a value for the protection of aquatic life in seawater of 5.6 ug L^{-1} (over a 4-d running average) has been established by the U.S. Environmental Protection Agency (Eisler, 2000). Taking a precautionary approach, the regulatory standard value of 2 ug L^{-1} for a 6 month median established by the State of California was used (COP, 2001).

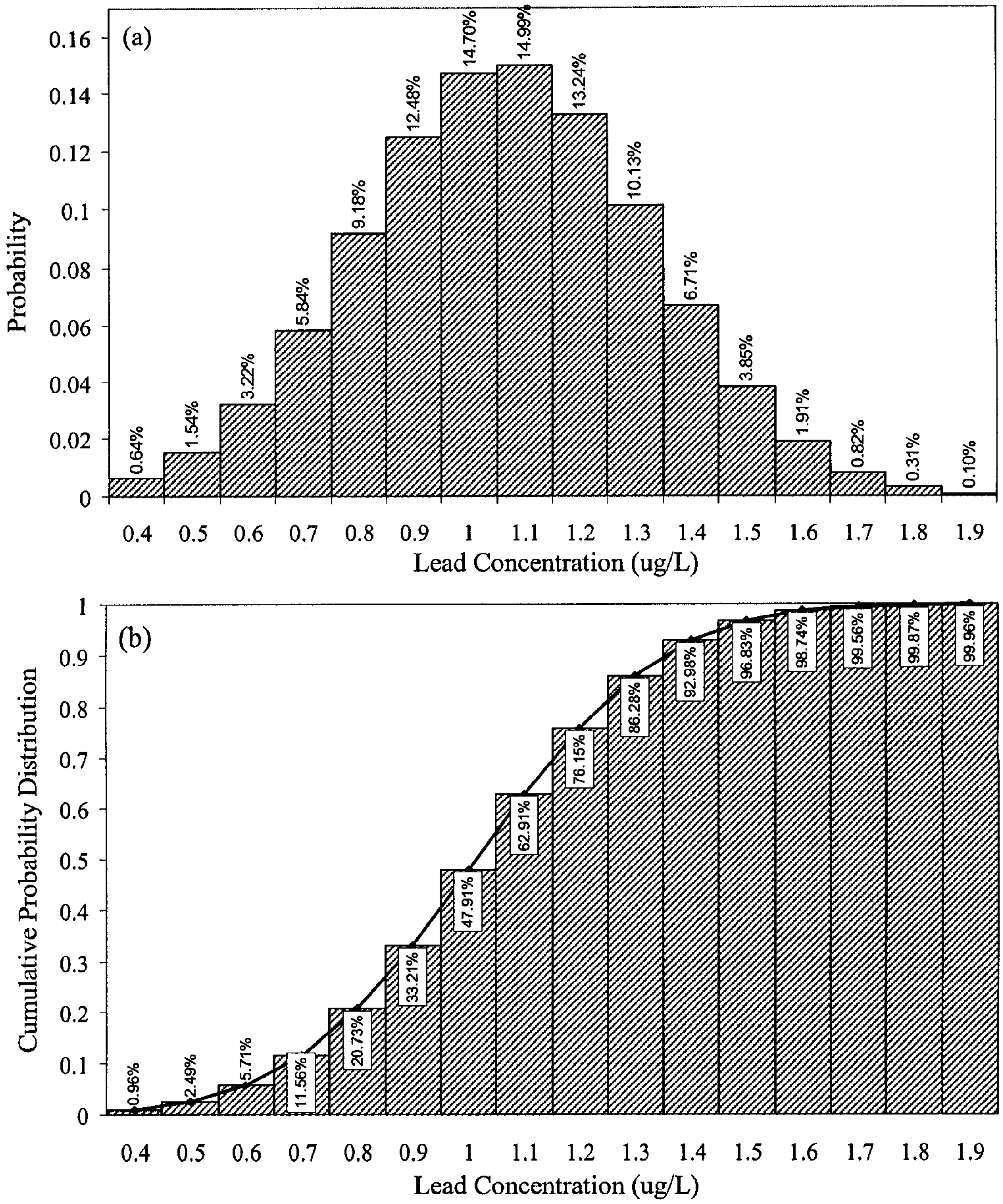

Figure 6-8 Lead concentrations at (26775m, 23450m) about 60 m away from Hibernia site (26824m, 23400m) in 2015: (a) probability distribution and (b) cumulative probability distribution

Figure 6-8 shows the probabilistic analysis results for the year 2015 at the location of (26775m, 23450m) about 60 m away from the Hibernia site (26824m, 23400m) (Point 1 in Figures 6-11 and 6-12) based on the distance coordinate system (see Figure 6-1). As shown in the figures, 90% predicted concentrations occur in the range of 0.7 to 1.4 ug L^{-1}. The probability for Lead concentration larger than 1 ug L^{-1} to occur at this location is 52.1% and the probability for greater than 1.5 ug L^{-1} is 3%. The 5^{th} and 95^{th} percentile Lead concentration are 0.58 ug L^{-1} and 1.44 ug L^{-1} respectively (Table 6-1). Comparing these results with the regulated value (2 ug L^{-1}), all predicted concentrations in 2015 will not exceed the criterion. The risk quotient (RQ) factor is 0.72 under 95^{th} percentile concentration. However, this point's concentration represents the average concentration of a 50 m × 50 m cell; a location very near the source could have a much higher concentration than this point. Moreover, as noticed, the possible maximum concentration in this location is 1.81 ug L^{-1}; the plume concentration near the source may exceed the standards in some extreme situations.

Figure 6-9 shows the probability distribution function for the year 2025 at the point of (26775m, 23450m) about 60 m away from the Hibernia site (26824m, 23400m) (Point 1 in Figure 6-11 and 6-12). In 2025, about 70% of the predicted concentrations fall in the range of 1.3 to 2.2 ug L^{-1}. The maximum concentration is 3.1 ug L^{-1}, and the minimum concentration is 0.75 ug L^{-1}. The 5^{th} and 95^{th} percentile Lead concentration are 0.96 ug L^{-1} and 2.44 ug L^{-1}, respectively (Table 6-1). The probability of Lead concentration exceeding the risk assessment criterion issued by the State of California (2 ug L^{-1}) is 25.2%, demonstrating a potential risk level of 0.25. The risk quotient (RQ) factor is 1.22 for the 95^{th} percentile concentration. Thus, towards its end stage, there is about 25% possibility that the Lead concentration within 60m of the Hibernia platform range may exceed the State of California guidelines for the protection of aquatic life (2 ug L^{-1}).

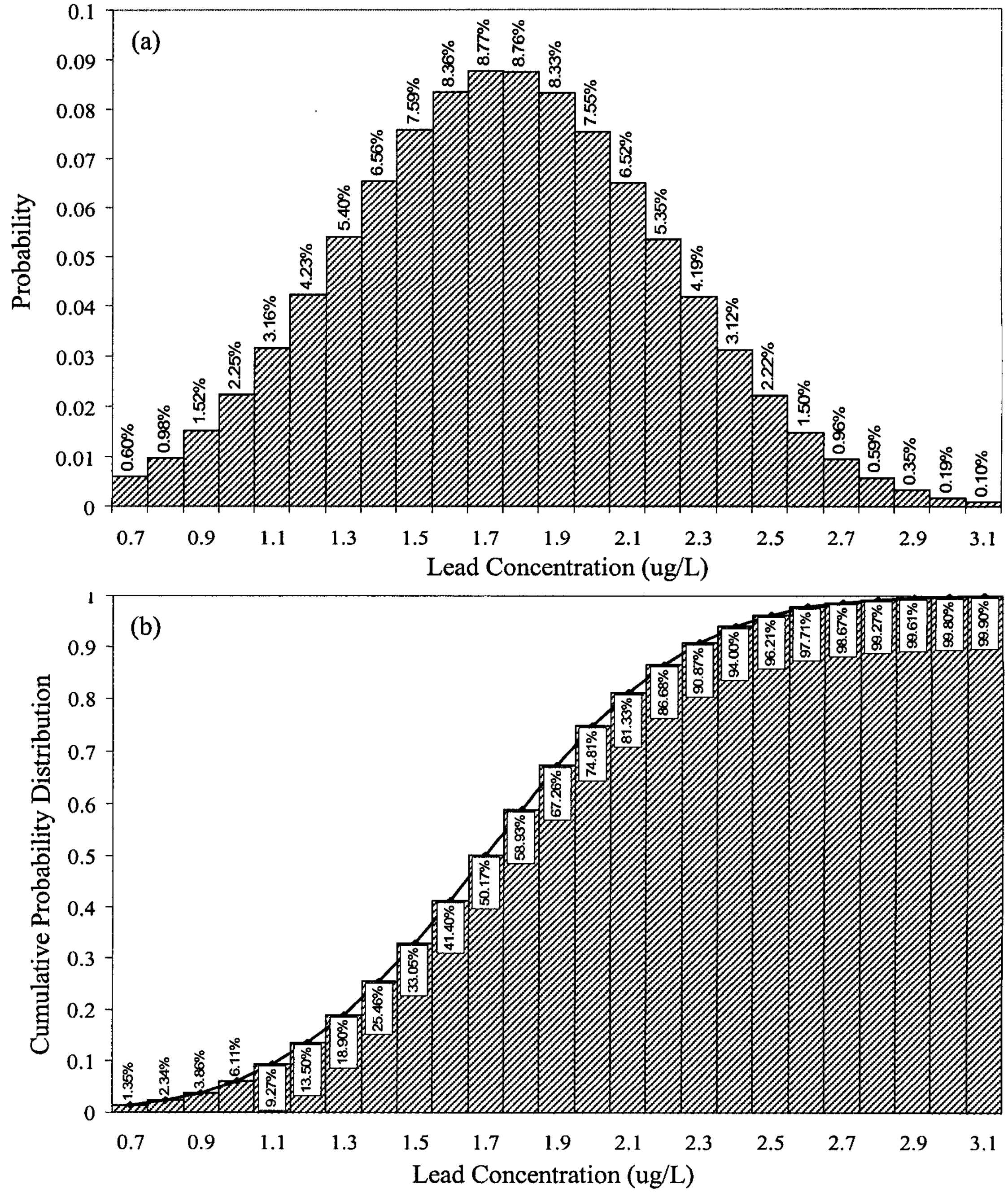

Figure 6-9 Lead concentrations at (26775m, 23450m) about 60 m away from Hibernia site (26824m, 23400m) in 2025: (a) probability distribution and (b) cumulative probability distribution

Figures 6-10 (a) and (b) show the probability distribution in the point of (26775m, 23200m), which is 250 m away from the Hibernia site (26824m, 23400m) (Point 6 in Figure 6-11 and 6-12) in 2025. About 70% of the predicted concentrations fall in the range of 0.2 to 0.45 ug L^{-1}. The maximum concentration is only 0.79 ug L^{-1}. The 5^{th} and 95^{th} percentile Lead concentration are 0.12 ug L^{-1} and 0.59 ug L^{-1} respectively. The RQ factor is only 0.3 for the 95^{th} percentile concentration. Compared with the results from Figure 6-9, the concentration is far less than the concentration at the point of (26775m, 23450m) (Point 1 in Figure 6-11 and 6-12), decreasing at a rate of 4 times over 150 m distance, demonstrating the rapid dilution after releasing from the source due to hydrodynamic effects.

Overall risk to the marine environment from Pb within the produced water discharge stream is considered low due to natural dilution processes. Figure 6-11 clearly illustrates the influence of rapid dilution on risk criteria due to hydrodynamic effects. In point 1 and 2 (about 90 m away from the source), the mean concentration changes very slowly, generally remaining in the range of 1.61 to 1.70 ug L^{-1}. The possibility of exceeding the environmental endpoint (2 ug L^{-1}) is over 19%, and the risk quotient (RQ) is of the order of 1.18 – 1.22. After that, the concentration drops rapidly within 30 m distances (from 90 m to 125 m away from the source as seen in points 3 and 4). The mean concentration will drop from 1.6 to 1.2 ug L^{-1}; the probabilistic risk will drop to 0.37, and the RQ will be lower than 1. Over 125 m away from the source (points 5 and 6), the decrease slows down, and the concentration will be diluted to very small values. The point at which RQ equals 1 under 95^{th} percentile concentration is about 110 m from the source with 5% probability of exceeding the criteria (2 ug L^{-1})

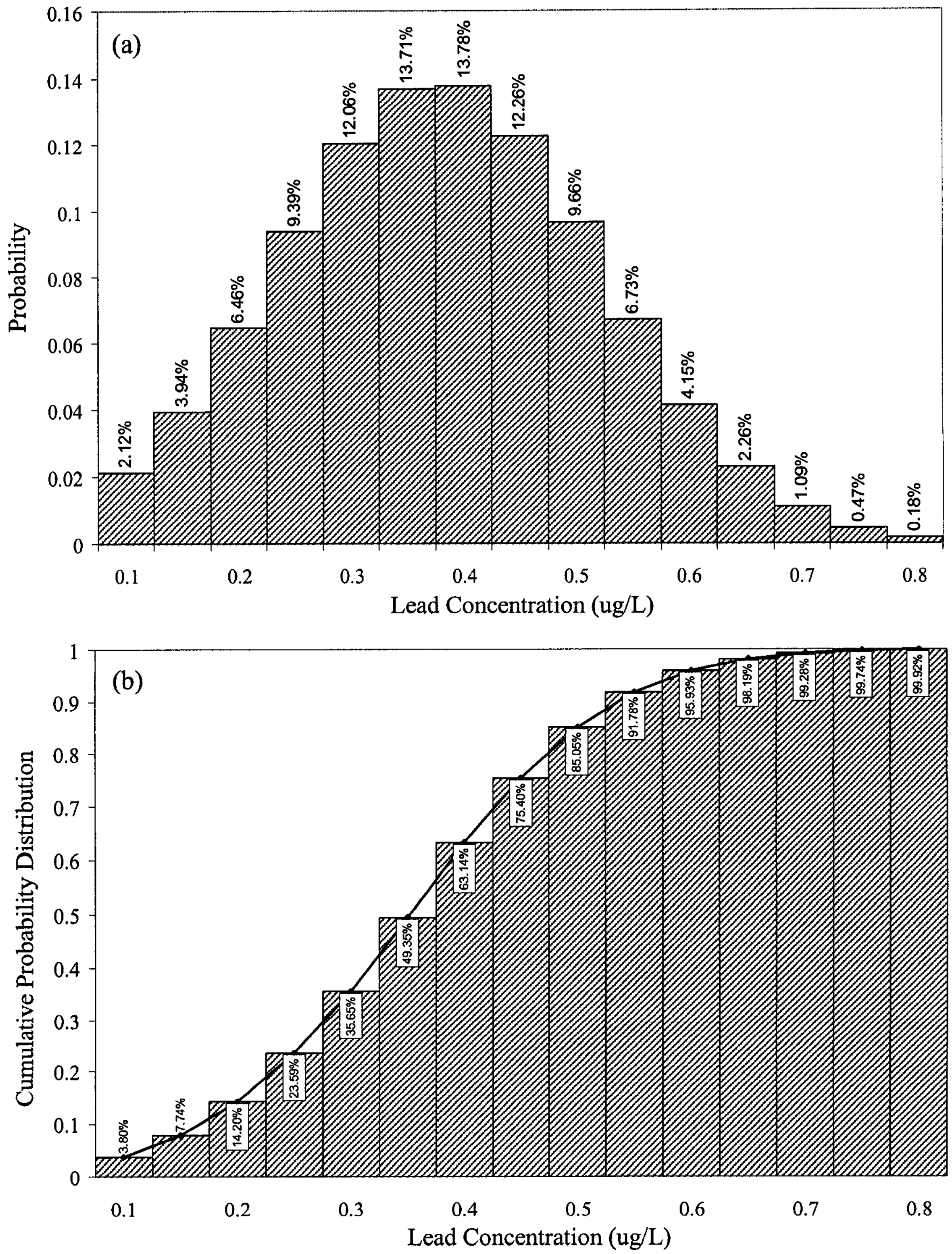

Figure 6-10 Lead concentrations at (26775m, 23200m) 250 m away from Hibernia site (26824m, 23400m) in 2025: (a) probability distribution and (b) cumulative probability distribution

Table 6-1 Summary of risk assessment results

Years	Point[1]	X (m)	Y (m)	Distance from source (m)	Mean (ug/L)	Standard deviation (ug/L)	Percentiles		Risk Level	
							5%	95%	Probabilistic Risk (%)	Risk Quotient[2] (RQ)
2005	1	26775	23450	56	0.24	0.08	0.37	0.11	0	0.06
2015	1	26775	23450	56	1.01	0.26	0.58	1.44	0	0.72
2025	1	26775	23450	56	1.70	0.45	0.96	2.44	25.19	1.22
	2	26725	23400	90	1.61	0.45	0.86	2.35	19.32	1.17
	3	26775	23350	103	1.42	0.39	0.78	2.07	7.17	1.04
	4	26725	23500	125	1.20	0.30	0.71	1.69	0.37	0.85
	5	26675	23300	195	0.91	0.21	0.56	1.25	7e-6	0.62
	6	26775	23200	250	0.35	0.14	0.12	0.58	0	0.29

1 The points correspond to Figures 6-11 and 6-12. Hibernia is at the location of (26824m, 23400m)

2 The value of the Risk Quotient factor is under 95th percentile concentration

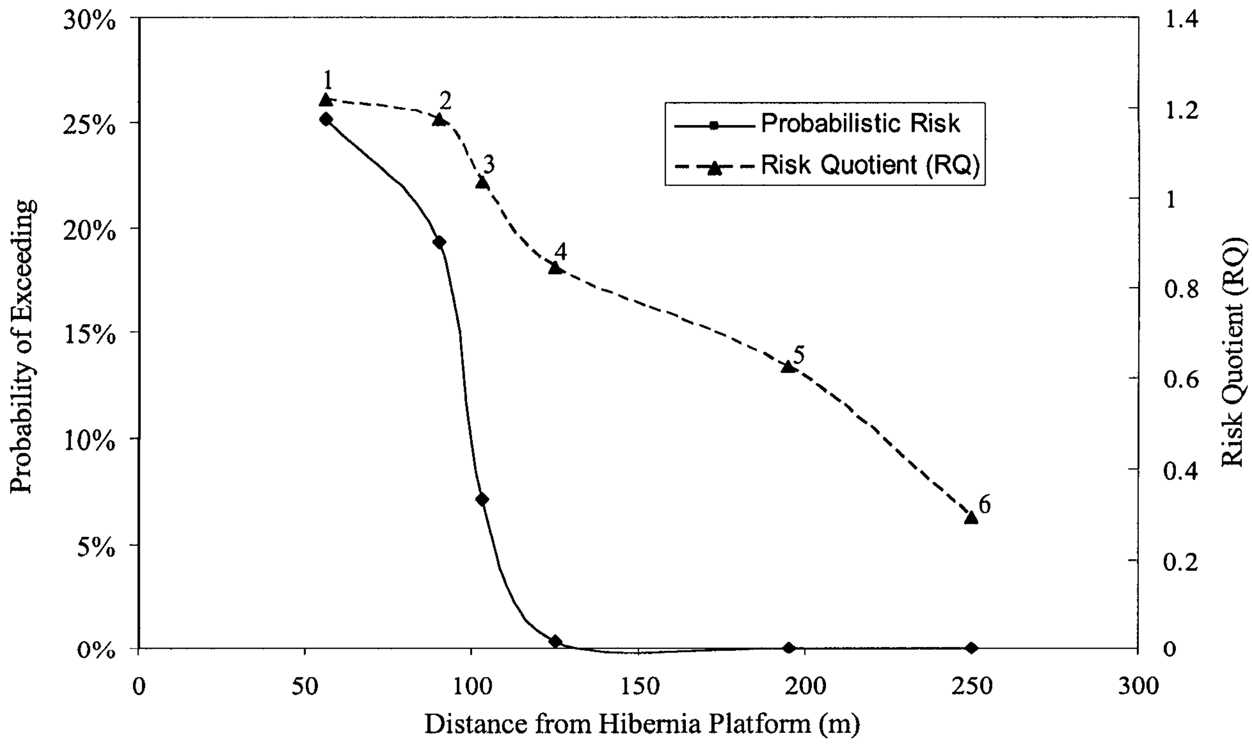

Figure 6-11 Risk distributions along the distance from the source (the left axis is the probability of exceeding the endpoint (2 ug L^{-1}); the right axis is the 95th percentile RQ factor)

Table 6-1 shows the overall risk assessment results for each production stage of the Hibernia Platform. Based on the criterion issued by the State of California (2 ug L^{-1}), the RQ is of the order of 0.06 – 0.72 in 2005 and 2015; the probabilistic risk levels in 2005 and 2015 are zero, indicating that negligible risk is associated with the present discharging of produced water in the Hibernia field within 10 years for typical locations indicated in Table 6-1. However, with the field production towards its end, the concentration will exceed the criterion. In 2025, the probabilistic risk level within 100 m of the source is from 0.7 to 0.25; the RQ factor is of the order of 1.04 – 1.22 for typical locations indicated in Table 6-1.

For decision making process, it is advantageous to transform the modeled values to a scale that indicates the risk severity of impacts on the local environment. The decisionmaker must subjectively assess what ranges of attribute magnitude correspond to the values of the severity scale (Haimes, 1998). This assessment process can be simplified through the use of a graph that maps severity as a function of the attribute over the range of possible attribute values. In the present study, an example of severity scale is constructed as high risk level ($P(L>C_0) > 20\%$), medium risk level ($10\% > P(L>C_0) > 20\%$), and low risk level (($P(L>C_0) < 10\%$)). Figure 6-12 shows the severity scale map associated with the probabilities of exceeding the standard (2 ug L^{-1}) at 40 m depth in 2025. As shown in the figure, the high risk zone (mean concentration >1.6 ug L^{-1}) is approximately 25000 m^2, bounded within a 90 m radius around the Hibernia GBS platform. The majority of the study area had a zero probability to violate the effects threshold value selected. This geo-reference method is a simple and effective way to visually illustrate the level of risks associated with production discharges around an offshore production platform. In a similar illustrative manner the 95th percentile RQ values can be plotted as a map to illustrate environmental risk (Figure 6-13). As noted previously, an RQ larger than 1 generally corresponds to over 5% probability of exceeding the regulatory value.

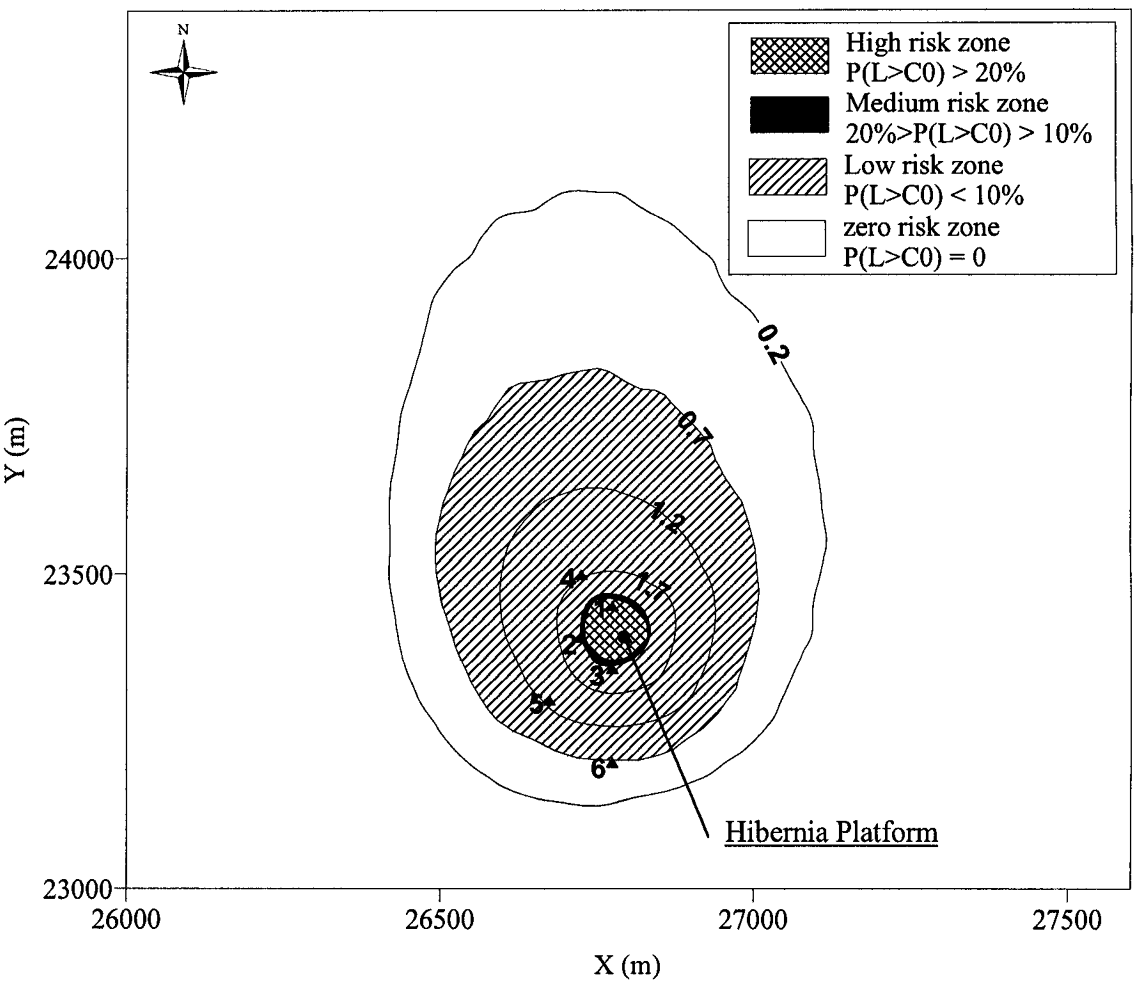

Figure 6-12 Mean concentration distribution and severity scale map for risk of exceeding the criterion issued by the State of California (2 ug/L) at 40 m depth in 2025

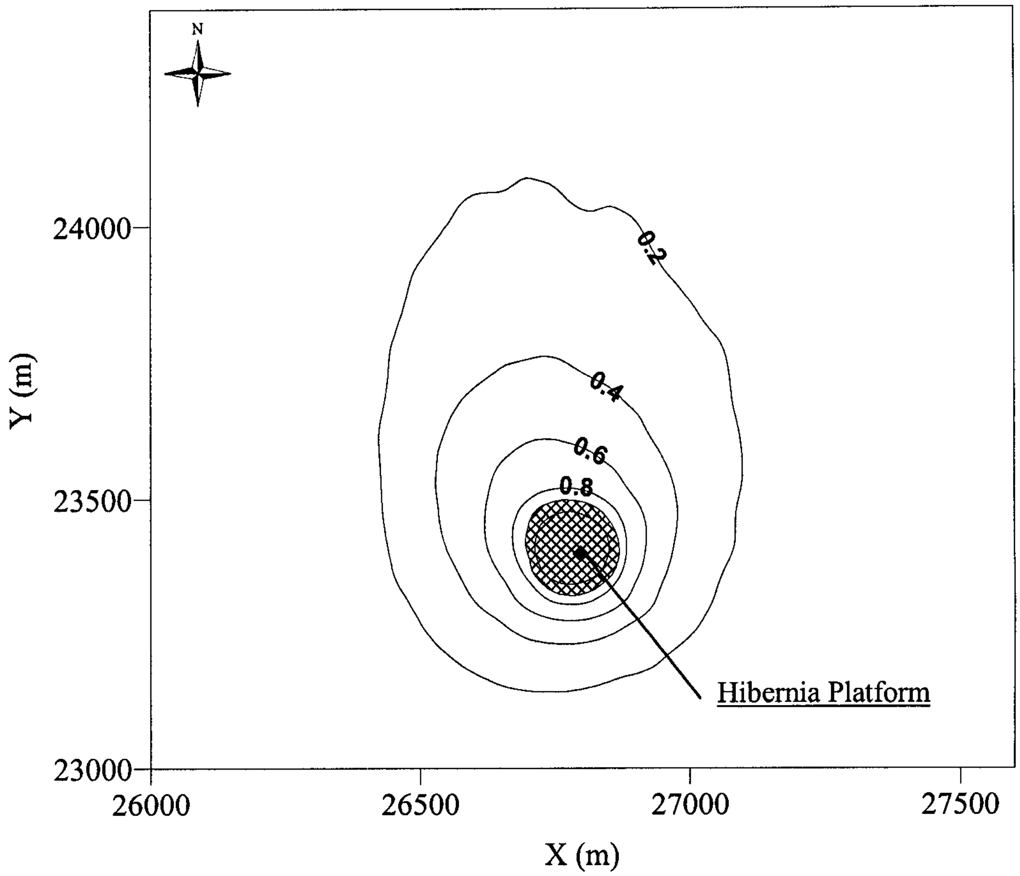

Figure 6-13 The 95th percentile Risk Quotient associated with the criterion issued by the State of California (2 ug/L) at 40 m depth in 2025, the shaded area is RQ $\geq$ 1

6.3 Summary

In the present study, the POM-RW model produces two sets of results: the basic velocity results, which are obtained from 3D flow field simulations, and the metal dispersion results, which are given at different layers and times. The metal dispersion simulation results using a random walk modeling approach in conjunction with well-simulated ocean current fields are reasonable. However, it also reveals that there are limitations in the modeling approach. Based on the simulation results presented in this chapter, the Random Walk model can achieve good simulation in near field, but reveal errors in the far field. Furthermore, the computational requirement for a CPU is also very high when using the Random Walk model.

The integrated risk assessment results have been presented in this Chapter. The results indicate that towards its depleted stage as an oil platform, adverse effects on the aquatic life associated with Pb concentration would be revealed, and the potential risk zone may cover an approximate 38000 m^2 (about 110 m in radius) area with Hibernia in the center. More discussions about the modeling approach and risk assessment results are presented in Chapter 7.

Chapter 7

Discussion

This chapter presents more discussions about the developed modeling system, model validation and application, and risk assessment. The Discussions mainly deal with the methodologies described in Chapter 3 and the results analysis presented in Chapters 5 and 6.

7.1 Ocean Current Model – POM

The determination of boundary conditions is critical for the successful simulation of a costal current field using POM, especially for small domains. Enlarging the boundaries away from the area of interest as a solution to open boundary problems has been used before. It has been confirmed that as the nesting ratio of a small domain to the large scale increases, the resolution increases. In this study, a much larger and wider area, which is approximately 200 times the study area (Figure 4-1), is used to minimize the influence of the boundary conditions on the modeling current field for the study region. Modeling and verification results in this study confirm that the use of this method is appropriate for modeling the current fields in the Hibernia area. In addition, Sommerfeld-type radiation conditions are used to compute the baroclinic velocities based on previous successful applications of POM (Ezer and Mellor, 1992, 1994; Ezer et al., 1995).

The surface boundary condition results mainly from the well-collected climatological wind stress and hourly wind observation data that are input into the circulation model for the entire month of June, 2005. These data have proved to produce a realistic current velocity field for the study area (Figure 5-4 to 5-6).

7.2 Dispersion Model – POM-RW

Field validation indicates that the developed POM-RM approach can provide satisfactory prediction of the pollutant concentration close to the emission source (Figure 6-2 (b)), but the modeling outputs for locations near to the surface and the ocean bottom do not match with the monitoring data very well (Figure 6-2 (b) and (c)). The possible solutions to improve the modeling results are as follows: 1) The model could be run long enough for the particles to be carried the full length of the domain (50 km). This solution would in turn increase the computational effort. 2) Suh (2006) has reported that a random walk particle tracking approach is highly recommendable in the near-field region, but it might result in erroneous particle distributions in the far-field locations. Suh has also recommended combining particle tracking and the Eulerian-Lagrangian method. The random walk model is exploited in the near field region around a source point. In addition, the ELM is applied in the far field for efficient and accurate modeling. Banton (1997) has also coupled the random walk model and the finite element method to conduct the solute transport simulation. This solution will be considered in future work; 3) the tide data are not considered in this study, possibly contributing to more dilution and to carrying the pollutants to a slightly different spatial location from the predicted results; and 4) the emission of produced water is continuous and the emission rate and concentration are assumed constant in this thesis; accurate information regarding the emission pattern from the Hibernia site will help to improve the developed modeling approach and results. Nevertheless, this study shows that the developed POM-RW approach is capable of examining both current and pollutant dispersion processes for the Hibernia site.

The random walk method is used to generate particle locations rather than concentration data. Numerical errors will arise during the conversion from the particle to the concentration representation as the final step of the model in a fixed computational grid system. The smaller the number of particles in each cell, the higher the errors in the concentration. One of the solutions for solving the limitation of the random walk model is to increase the number of particles and to run the model for a long period of time. Then, accordingly, there are enough particles in each cell covering the whole model area. The number of particles used in the simulations depends on the speed of the computation and/or the accuracy required (Perianez, 2002). Proctor et al. (1994b) have used 4000 particles to simulate an oil spill during real-time forecasting of an incident in the Arabian Gulf. Korotenko et al. (2004) have developed a model that can use the number of particles within 10^6. However, this can give rise to another drawback of the model, which is that, even using high performance computers, the particle number must be restricted because saving and tracking the history of every particle requires large amounts of memory and computing time. Table 7-1 and Figure 7-1 compare the simulation results in 2005 under different inputs of particle numbers. The results indicate a small difference between releasing 200 particles and 500 particles in each time step. Therefore, using a release of 200 particles per time step is appropriate in the model simulations.

Table 7-1 Comparisons of releasing different numbers of particles (40 m depth in the water)

	X (km)	Y (km)	50	200	500	Differences between 200 and 50	Differences between 200 and 500
1 day run	25	25	0.0688	0.0743	0.0782	7.40%	5.25%
	25.4	24.6	0.1321	0.1052	0.0974	25.57%	7.41%
	26	23.4	0.1682	0.1544	0.1412	8.94%	8.55%
	26.6	23.2	0.4337	0.4462	0.4521	2.80%	1.32%
	26.6	23.4	0.5284	0.4646	0.4918	13.73%	5.85%
	26.6	23.6	0.368	0.3516	0.3467	4.66%	1.39%
5 day run	24.4	25	0.0358	0.0372	0.0322	3.76%	13.44%
	25	25	0.0716	0.0799	0.0868	10.39%	8.64%
	26	24.2	0.1447	0.1703	0.1738	15.03%	2.06%
	26.6	23.2	0.1578	0.1663	0.1573	5.11%	5.41%
	26.6	23.4	0.2709	0.2979	0.3067	9.06%	2.95%
	26.6	23.6	0.2288	0.2479	0.2512	7.70%	1.33%

Lastly, the determination of key dispersion model parameters is a difficult task during the model application study. Especially, the horizontal and vertical mixing coefficients K_h, and K_z are among the most important factors to determine the concentration of pollutants in the environment. A thorough analysis of the model and the site uncertainties regarding the model parameters is conducted in the isk assessment of Chapter 6.

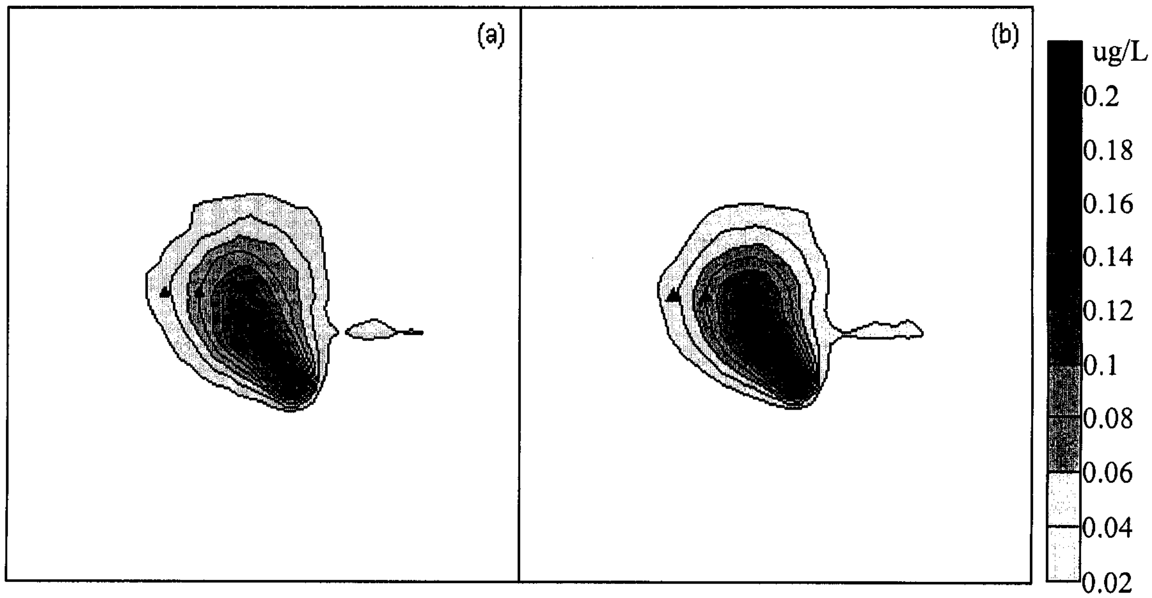

Figure 7-1 Comparison of different numbers of particles releasing (a) Lead distribution in 40 m depth after a 5 day run for particles = 200; (b) Lead distribution in 40 m depth after a 5 day run for particles = 500. The points correspond to the points presented in Table 7-1

7.3 Integrated Risk Assessment

The risk assessment considers parameters that are generally prone to uncertainty because of simplification and the imprecise nature of the available information (Ferson, 1996). Uncertainty can be divided into two categories: (1) uncertainty induced from natural variability, which cannot be reduced; (2) uncertainty resulting from a lack of proper knowledge or partial ignorance of information (Roucher et al., 2002). In the present study, the uncertainties caused by the mixing coefficients result from the first category. A Fickian mixing approach is used to describe the mixing associated with the chemical transport due to dispersion and turbulent diffusion in the present research. The greater the spatial variability in water velocity and the greater the turbulence, the greater the mixing (Hemond and Fechner-Levy, 2000). Mixing in the ocean is due primarily to turbulence. Eddies carry chemicals away from regions of relatively high concentration toward regions of lower concentration. The larger area extent of the sea leads to a scale issue in conducting tracer experiments. A dispersion coefficient that is determined for a small plume of a spreading chemical may not be appropriate to accurately model chemical dispersion at a later time when the plume has spread and larger eddies are contributing to its mixing. Therefore, estimating the mixing coefficients K_h and K_z in the ocean is difficult and complicated and may lead to errors when adopting imprecise distributions of such coefficients.

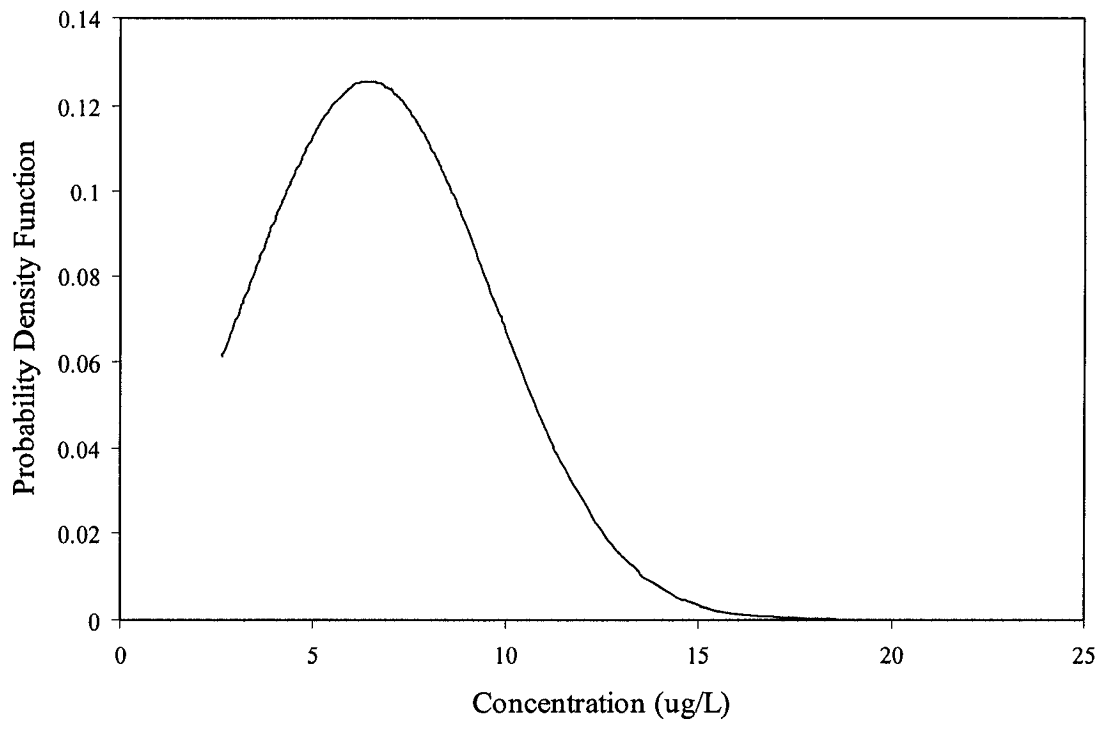

Figure 7-2 Simulation of probability density function of 2025 in Hibernia site using the value of mixing coefficient ranges adapted from Riddle et al. (2001)

Many techniques, including the probabilistic approach and mathematical and numerical modelings, are available to characterize the uncertainties in the natural processes. The most widely used approach to characterize uncertainty in risk assessment studies is the Monte Carlo simulation (USEPA, 1996). Based on the parameters that are naturally variable and difficult to characterize, conducting risk assessment by means of the Monte Carlo approach is appropriate and provides more details of potential risks that may occur in the natural environment.

One of the basic problems with the Monte Carlo method pertains to the difficulty of developing and justifying input distributions (Haimes et al., 1994; Finley et al., 1994). In situations where data are severely limited, selecting input distributions requires assumptions that may not be justified by an appeal to evidence in the absence of a complete empirical base. These unsubstantiated assumptions can make a difference in the results. Bukowski et al. (1995) have indicated that the choice about distribution shape can have a sizeable effect on the risk analysis, especially at the tails. In the published literature, Riddle et al. (2001) have adopted the horizontal mixing coefficient with a distribution from 10 to 50 $m^2\ s^{-1}$ and the vertical mixing coefficient with a mean of 0.05 and standard deviation of 0.004 $m^2\ s^{-1}$ with a minimum value of $1 \times 10^{-4}\ m^2\ s^{-1}$ in the North Sea. As mentioned before, the physical characteristics are completely different between the North Sea and Atlantic Canada. The differences between them lead to different mixing coefficient distributions. Figure 7-2 shows the probabilistic results at the Hibernia site in 2025 when adapting the spanning range of mixing coefficient from Riddle et al. (2001). As noticed, a large tail in the distribution of the probability density function and a much higher concentration appears in the results, indicating that a low mixing process and a high concentration accumulation occur under this distribution of the parameters. In order to avoid such an influence on the risk analysis caused by low mixing coefficients, we have examined the local conditions at the Hibernia area and have conducted a calibration study. The results of both are supporting the use of a uniform distribution from 50 to 120 $m^2 s^{-1}$ for the horizontal mixing coefficient, and of a normal distribution with a mean of 0.007 and a standard deviation of 0.003 $m^2 s^{-1}$ for the vertical mixing coefficient in the present study for the Hibernia area.

The Lead criteria found for the protection of natural resources and human health differ greatly from one another. For example, the criteria for aquatic life protection in Canada range from 1 to 7 ug total waterborne Pb/L in freshwater (Canadian Water Quality Guidelines, 2006). Within this range, high accumulations and adverse effects on growth and reproduction were recorded among sensitive species (Eisler, 2000). Moreover, certain organolead compounds were lethal to some species of aquatic biota within this range, but no criteria have been formulated yet for this highly toxic group of chemicals, especially for seawater. In the present study, the possible risk recommendation zone (see Figure 6-12 and 6-13) depends on the chosen criterion issued by the State of California (2 ug L^{-1}) Figure 7-3 shows the possible risk mapping zone under the endpoint of 1 ug L^{-1}. With a regulated value of 1 ug/L, the high and medium risk zone will expand to an area of approximately 126000 m^2 (about 200 m in radius) around the Hibernia platform (see Figure 7-3 (a)), the same as the area of RQ larger than 1 (see Figure 7-3 (b)), with the maximum RQ over 2.4. It is 5 or more times the area than it is under the criteria of 2 ug L^{-1} (see Figures 6-12 and 6-13).

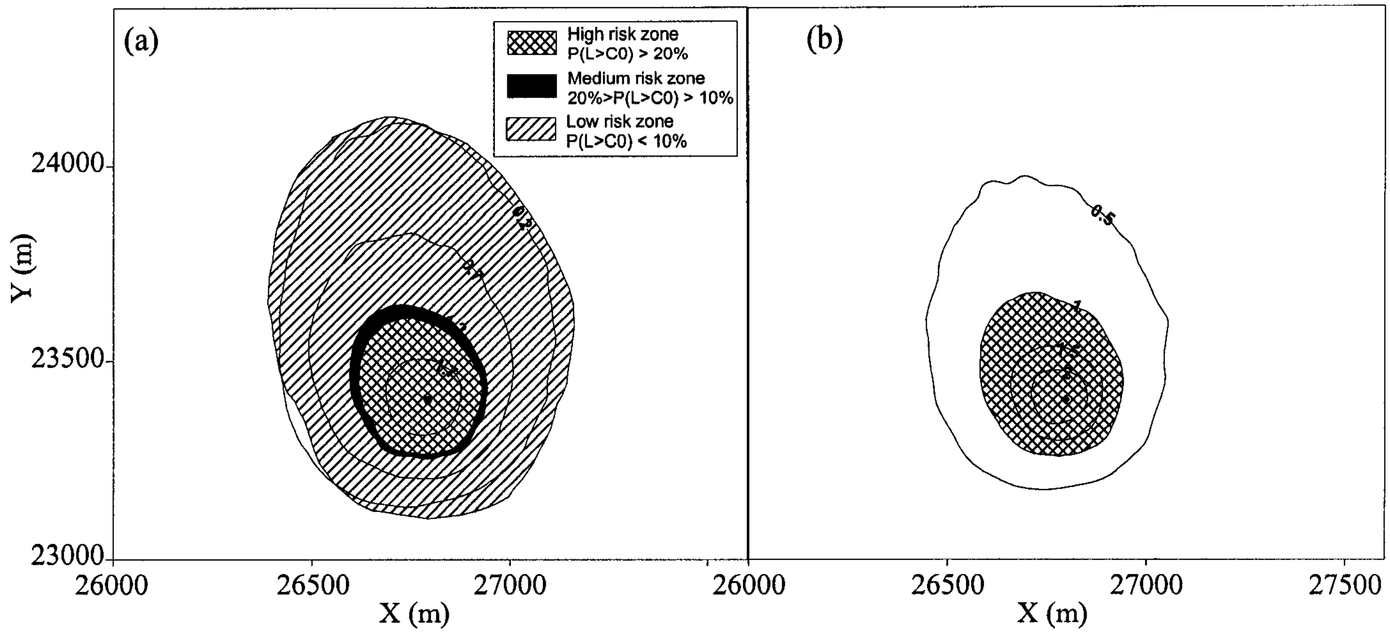

Figure 7-3 Possible risk severity map under the environmental endpoint of 1 ug/L (a) mean concentration and probability of exceeding; (b) the 95th percentile Risk Quotient (RQ)

The long term risk analysis in the present study is based on the predicted increasing volume of produced water discharges in 2015 and 2025 for the month of June. Owing to the CPU requirements of the PC, it is not feasible to run the model for the whole 20 years when using the Monte Carlo approach. Therefore, the risk analysis results might be presenting the risks only near the platform (about 1000 m in radius around the platform). Since the produced water is continuously discharged from the platform over a period of 20 years, the plume would be theoretically spread over a much larger area. The risk assessment over a long period will be studied in the next stage.

Except the volume of produced water could change over time, the composition of produced water may also change over the production life-time of the reservoir as different sectors of the formation become exploited during production. The composition of produced water may also vary from platform to platform (CAPP, 2001). For example, the concentration of Pb at Copan (a Canadian offshore field located on the Cotian Shelf off Nova Scotia) is in the range of 8 – 45 ug L^{-1}, whereas produced water Pb concentration for Gulf of Mexico Oil Platforms range from 0.08 ug L^{-1} to 5700 ug L^{-1} (Table 1-1). The sample analysis of produced water at the Hibernia platform shows current dissolved Pb concentrations in the range of 0.02 ug L-1 (2004) to 500 ug L^{-1} (2005). Anticipated time-series changes in contaminant concentrations over the life-span of offshore production platforms would require updates in risk analysis.

Chapter 8

Conclusion and Recommendation

8.1 Conclusions

In the present study, a numerical model, POM-RW, based on POM and the random walk method has been developed to simulate the dispersion of contaminants from offshore platforms.

The random walk transport model is developed in conjunction with the use of the Princeton Ocean Model (POM) to fully consider the hydrodynamic conditions of the marine environment including the current, tide, salinity, density, and wave. Therefore, their impacts on the fate and transport of pollutants can be included in the pollutant fate and transport modeling.

Based on the consideration of boundary conditions, the results of the flow field obtained from POM show good agreement with the field observations. Using the discharge and the well-simulated flow field as the input conditions, the fate and transport of metal concentration at different depths are simulated to examine the metal dispersion in three dimensions with quantified concentrations. Comparison of monitoring and ambient water quality data from a regional environmental effects monitoring program around an offshore platform confirmed that the POM-RW approach can provide a realistic field assessment of the produced water discharge. The results also indicate that the random walk model can achieve good simulations in the near field, but much smaller concentrations than observations in the far field. In order to solve this problem, future studies and possible solutions are discussed in the following sections.

A Monte Carlo approach is developed to reflect uncertainties and to conduct the long term risk assessment associated with the evaluation criteria for produced water discharges in the ocean. In terms of overall environmental impact to the Grand Banks region, the Pb concentration results from the Monte Carlo simulation suggest a negligible level of risk (110m radius risk zone) associated with the current discharging of produced water in the Hibernia field due to the limited size of the predicted impact zone and additional natural dispersion processes.

This study has demonstrated the utility of linking a three-dimensional hydrodynamic ocean circulation model to provide inputs into a mass transport model. The resultant POM-RW model provided a quantitative means to examine the dispersion of toxic components of produced water effluent on a regional spatial scale. An effective risk assessment protocol for the management of produced water discharges was established by integration of the POM-RW model with the Monte Carlo risk assessment approach.

8.2 Research Contributions

In addition to the conclusions in Section 8.1, the research contributions for this present thesis study are summarized below:

1. A new modeling approach (POM-RW) consisting of coupling the pollutant dispersion model with the 3D ocean current modeling component has been developed. Specifically, the pollutant dispersion model based on the random walk – particle tracking method is developed using FORTRAN language. This model has been integrated with the ocean current model (POM);

2. With a full consideration of boundary conditions, the developed POM-RW has performed to simulate the Lead dispersion resulting from the produced water discharges at an offshore facility located on the Grand Banks of Canada;

3. Validations for both the 3D ocean current and the pollutant dispersion modeling results with the site sampling results at the study area in 2005 have been conducted. The validation results show that the developed POM-RW can provide a realistic field assessment of the produced water discharge activities. It is, furthermore, useful for addressing the long term environmental risks associated with the produced water discharges.

4. An integrated risk assessment approach based on a POM-RW model and the Monte Carlo method has been developed in the present thesis study. Two methods of

quantifying the risk levels have been used to map the possible environmental risk severities in the study area.

5. Long term risks associated with the produced water discharges into Atlantic Canada have been assessed and evaluated on the basis of the integrated risk assessment approach, showing that the developed risk assessment approach can contribute extensively to environmental risk assessment and to effective pollution control decisions.

8.3 Recommendations for Future Work

Future studies that can be recommended are as follows:

1. Reviewing the results presented in the previous chapters, there are still limitations related to the new modeling approach. The validations in the present thesis study were conducted only for 2005. Therefore, future study should include an extended development of the numerical simulation of the dispersion of pollutants to improve the modeling results in the far field area. More tests and validations can be expected based on the site sampling results for other periods of time or on other platforms.

2. Although Lead is studied in the present research, the dispersion and the risks of other contaminants including organic and inorganic chemicals should be examined using the developed modeling approach.

3. In the present thesis, only a single produced water discharge source (Hibernia platform) has been considered. With the development of Canada's offshore oil and gas reserves, new oil and gas fields will be expected in the future. Therefore, the Simulation

of concentration fields of produced water components from multiple discharge sources can be established in the future.

4. In an attempt to map the ecotoxicological effects of discharges of produced water, it is important to examine which parts of the ecosystem are exposed to produced water components. In future study, the modeling results can be used in conjunction with the toxicity experimental results to evaluate the ecological risks from exposure to the toxic effluent for different groups of species in the ocean.

5. In the present uncertainty analysis, the uncertainty parameters have been specified in a relatively higher mixing range. In the ongoing studies, these parameters can be measured through experimental investigation and can be combined with sensitive analysis to understand more about important modeling uncertainties.

6. Other dispersion analyses, such as that of the suspended solids in the produced water and the buoyancy effects near the source point, can also be included in the future study.

REFERENCES

Banton, O., Porel, G., and Delay, F., 1997. Coupling of the time domain random walk method with the finite fragment mentod to simulate flow and transport in 1-D heterogeneous medis. Journal of Hydrology 201, 49-61.

Baptista, A.M., Zhang, Y.-L., Chawla, A., Zulauf, M.A., Seaton, C., Myers, E.P., Kindle, J., Wilkin, M., Burla, M., and Turner, P.J., 2005. A cross-scale model for 3D baroclinic circulation in estuary-plume-shelf systems: II. Application to the Columbia River. Available at: http://www.stccmop.org/corie/modeling_system. Continental Shelf Research 25, 935-972.

BASIN, 2007. Offshore Eastern Canada hydrocarbon database. Available at: Nature Resources Canada Website. http://basin.gsca.nrcan.gc.ca/index_e.php

Batchelder, H.P., 2002. Spatial and temporal distributions of mesozooplankton in idealized models using individual based particle tracking simulations. ICES/GLOBEC workshop on transport of cod larvae, Hillerod, Denmark.

Blumberg, A.F., and Mellor, G.L., 1978. A coastal ocean numerical model. In: Sunderman, J., Holtz, K.-P. (eds.), Mathematical modeling of Estuarine Physics. Proceedings of International Symposium, Hamburg, Springer, Berlin, 203-214.

Blumberg, A.F., and Mellor, G.L., 1987. A description of a three-dimensional coastal ocean circulation model. Geophysical Fluid Dynamics Program, Princeton University, Princeton, New Jersey 08544.

Boesh, D.F., and Rabalais, N.M., 1989. Produced waters in sensitive coastal habitats, an analysis of impacts. Central Coastal Gulf of Mexico, OCS Report/MMS 89-0031, United States Department of the Interior, Minerals Management Service, Guif of Mexico OCS Regional Office, New Orieans, LA.

Bouchard, D.C., Ambrose, R.B., Jr., Barnwell, T.O., Jr., and Disney, D.W., 1995. Environmental modeling software at the U.S. Environmental Protection Agency's Center for exposure assessment modeling. In: Beroggi, G.E.G., Wallace, W.A. (eds.), Computer Supported Risk Management, 321-360, Kluwer Academic Publishers, Dordrecht, The Netherlands.

Boudreau, P.R., Gordon, D.C., Harding, G.C., Loder, J.W., Black, J., Bowen, W.D., Campana, S., Cranford, P.J., Drinkwater, K.F., Van Eeckhaute, L., Gavaris, S., Hannah, C.G., Harrison, G., Hunt, J.J., McMillan, J., Melvin, G.D., Milligan, T.G., Muschenheim, D.K., Neilson, J.D., Page, F.H., Pezzack, D.S., Robert, G., Sameoto, D., and Stone, H., 1999. The possible environmental impacts of petroleum exploration activities on the Georges Bank ecosystem. Can. Tech. Rep. Fish. Aquat. Sci. 2259: iv + 106 p.

Brandsma, M.G., and Sauer, T.C., Jr., 1983a. The OOC model: prediction of short term fate of drilling fluid in the ocean. Part 1: model description. Proceedings of MMS Workshop on An Evaluation of Effluent Dispersion and Fate Models for OCS Platforms, February 7-10, 1983, Santa Barbara, California, Minerals Management Service, Contract No. 14-21-0001-29122, 58-84.

Brandsma, M.G., and Sauer, T.C., Jr., 1983b. The OOC model: prediction of short term fate of drilling fluid in the ocean. Part 2: model results. Proceedings of MMS Workshop on An Evaluation of Effluent Dispersion and Fate Models for OCS

Platforms, February 7-10, 1983, Santa Barbara, California, Minerals Management Service, Contract No. 14-21-0001-29122, 86-106.

Brandsma, M.G., Smith, J.P., O'Reilly, J.E., Ayers, R.C., Jr., and Holmquist, A.L., 1992. Modeling offshore discharges of produced water. In: Ray, J.P., Englehardt, R. (eds.), Produced Water: Technological/Environmental Issues and Solutions, Plenum Press , NY, 59-71.

Bryan, G.W., and Langston, W.J., 1982. Bioavailability, accumulation and effects of heavy metals in sediments with special reference to United Kingdom estuaries: a review. Environ. Pollut. 76, 89-131.

Bukowski, J., Korn, L., and Wartenberg, D., 1995. Correlated inputs in quantitative risk assessment: the effects of distributional shape. Risk Analysis 15, 215-219.

Canadian Water Quality Guidelines for the Protection of Aquatic Life, 2006. Canadian Environmental Quality Guidelines. Canadian Council of Ministers of the Environment. The guidelines were originally published in CCREM 1987, Chapter 3. The guidelines updated 2002 are available at: http://www.ccme.ca/assets/pdf/ e1_06.pdf.

CAPP, 2001. Offshore produced water waste management. Publication by the Canadian Association of Petroleum Producers (CAPP), August.

CCREM (Canadian Council of Resource and Environment Ministers), 1987. Canadian water quality guidelines. Prepared by the Task Force on Water Quality Guidelines.

Chapman, D.C., 1985. Numerical treatment of cross-shelf open boundaries in a barotropic coastal ocean model. J. Phys. Oceanogr. 25, 1060-1075.

Chen, Z., Huang, G.H., Chakma, A., and Tontiwachwuthikul, P., 1998. Environmental risk assessment for aquifer disposal of carbon dioxide. Proc., 4th Int. Conf. on Greenhouse Gas Control Technologies, Interlaken, Switzerland.

Chowdhury, S., Husian, T., Veitch, B., Bose, N., and Sadiq, R., 2004. Human health risk assessment of naturally occurring radioactive materials in produced water – a case study. Human and Ecological Risk Assessment 10, 1155-1171.

COP, 2001. California Ocean Plan. Ocean Quality Control Plan: Ocean Waters of California. State Water Resources Control Board, Resolution No. 2000-108. California Environmental Protection Agency.

Crawford, W., Cretney, W., Cherniawsky, J., and Hannah, C., 2002. Modeling oceanic fates of oil, drilling muds and produced water from the offshore oil and gas industry, with application to the queen charlotte basin. Can. Sci. Advisory Secretariat Res. Doc., 2002/120, 54p.

Delft3D-FLOW User Manual, 2006. Simulation of multi-dimensional hydrodynamic flows and transport phenomena, including sediments. Available at: http://delftsoftware.wldelft.nl/index.php?option=com. November 2006, WL | Delft Hydraulics.

DFO-OES, 2007. Ocean and sea-ice model. Ocean and Ecosystem Science (OES). Fisheries and Oceans Canada. Available at: http://www.mar.dfo-mpo.gc.ca/science/ocean/icemodel/forecast_models.html.

Dimou, K., 1989. Simulation of estuary mixing using a 2-dimensional random walk model. MS theis, MIT.

Dojlido, J.R., and Best, G.A., 1993. Chemistry of water and water pollution. Ellis Horwood Limited.

Doneker, R.L., and Jirka, G.H., 1990. Expert system for hydrodynamic mixing zone analysis of conventional and toxic submerged single port discharges (CORMIX 1), EPA/600/3-90/-12, United States Environmental Protection Agency, Athens, GA.

Eisler, R., 2000. Handbook of chemical risk assessment: health hazards to humans, plants and animals. VI Metals. Lewis Publishers, New York.

Environment Canada Climatic database. Available at: http://www.climate.weatheroffice.ec.gc.ca/climateData/ menu_e.html?Prov=NF.

Ezer, T., 1999. Decadal variabilities of the upper layers of the subtropical North Atlantic: An ocean model study. J. Phys. Oceanogr. 29, 3111-3124.

Ezer, T., 2001. Can long-term variability in the Gulf Stream transport be inferred from sea level? Geophys. Res. Let. 28, 1031-1034.

Ezer, T., Arango, H., and Shchepetkin, A.F., 2002. Developments in terrain-following ocean models: intercomparisons of numerical aspects. Ocean Model 4, 249-267.

Ezer, T., and Mellor, G.L., 1992. A numerical study of the variability and the separation of the Gulf Stream induced by surface atmospheric forcing and lateral boundary flows. J. Phys. Oceanogr. 22, 660-682.

Ezer, T., and Mellor, G.L., 1994. Diagnostic and prognostic calculations of the North Atlantic circulation and sea level using a sigma coordinate ocean model. J. Geophys. Res. 99, 14159-14171.

Ezer, T., and Mellor, G.L., 1997. Simulations of the Atlantic Ocean with a free surface sigma coordinate ocean model. Journal of Geophysical Research 102(C7), 15647-15657.

Ezer, T., and Mellor, G.L., 2004. A generalized coordinate ocean model and a comparison of the bottom boundary layer dynamics in terrain-following and in z-level grids. Ocean Modelling 6, 379-403.

Ezer, T., Mellor, G.L., and Greatbatch, R.J., 1995. On the interpentadal variability of the North Atlantic ocean: Model simulated changes in transport, meridional heat flux and coastal sea level between 1955-1959 an 1970-1974. J. Geophys. Res. 100, 10559-10566.

Ferson, S., 1996. What Monte Carlo methods cannot do. Human and Ecological Risk Assessment 2, 990-1007.

Finley, B., Proctor, D., Scott, P., Harrington, N., Pasutenbach, D., and Price, P., 1994. Recommended distributions for exposure factors frequently used in health risk assessment. Risk Analysis 14, 533-553.

Fisheries and Oceans Canada Oceanographic database. Fisheries and Oceans Canada: Ocean and Ecosystem Science (OES). Available at: http://www.mar.dfo-mpo.gc.ca/science/ocean/sci/sci-e.html.

Foreman, M.G.G., Beauchemin, L., Cherniawsky, J.Y., and Pena, M.A., 2005. A review of models in support of oil and gas exploration off the North Coast of British Columbia. Caniadian Technical Report of Fisheries and Aquatic Sciences 2612. Institute of Ocean Sciences. Fisheries and Oceans Canada.

Foster, P., 1976. Concentrations and concentration factors of heavy metals in brown algae. Environ. Pollut. 10, 45-53.

Gallaway, B.J., Martin, L.R., Howard, R.L., Bowland, G.S., and Dennis, G.S., 1981. Effects on artificial reef and demersal fish and macrocrustacean communities. In: Middieditch, B.S. (eds.), Environmental Effects of Offshore Oil Production, The Buccaneer Gas and Oil Field Study, Plenum Press, New York, 237-299.

Gillibrand, P.A., Stagg, R., and Turrell, W.R., 1995. Furness G. Observations and modelling of the results of low-level hydrocarbon discharges in the North Sea. ICES CM 11, 421–429.

Gordon, D.C., Cranford, P.J., Hannah, C.G., Loder, J.W., Milligan, T.M., Muschenheim, D.K., and Shen, Y., 2000. The potential effects of exploratory hydrocarbon drilling on Georges Bank scallop populations. Canadian Technical Report of Fisheries and Aquatic Sciences, 2317: 116 p.

Gordon, D.C., Griffiths, L.D., Hurley, G.V., Muecke, A.L., Muschenheim, D.K., and Wells, P.G., 2000. Understanding the environmental effects of offshore hydrocarbon development. Canadian Technical Report of Fisheries and Aquatic Sciences, 2311: 82p.

Haimes, Y.Y., 1998. Risk modeling, assessment, and management. Wiley Series in Systems Engineering.

Haimes, Y.Y., Barry, T., and Lambert, J.H., 1994. When and how can you specify a probability distribution when you don't know much? Risk Analysis 14, 661-706.

Hakkinen, S., and Mellor, G.L., 1992. Modeling the seasonal variability of a coupled Arctic ice-ocean system. J. Geophys. Res. 97, 20285-20304.

Hannah, C.G., Loder, J.W., and Shen, Y., 1996. Shear dispersion in the benthic boundary layer. In Estuarine and Coastal Modeling. Proc. 4th Intern. Confer. Edited by M.L. Spaulding and R.T. Cheng. Amer. Soc. Civil Engin., New York, 454-465.

Hannah, C.G., Shen, Y., Loder, J.W., and Muschenheim, D.K., 1995. bblt: Formulation and exploratory applications of a benthic boundary layer transport model. Can. Tech. Rep. Hydrogr. Ocean Sci. 166: vi + 52 p.

Hannah, C.G., Xu, Z., Shen, Y., and Loder, J.W., 1998. A model for suspended sediment transport in the benthic boundary layer. In Estuarine and Coastal Modeling. Proc. 5th Intern. Confer., Amer. Soc. Civil Engin., New York, 708-722.

Hasse, L., and Smith, S.D., 1996. Local sea surface wind, wind stress, and sensible and latent heat fluxes. Journal of Climate 10 (11), 2711–2724.

Hemond, H.F., and Fechner-Levy, E.J., 2000. Chemical Fate and Transport in the Environment. Academic Press. A Harcourt Science and Technology Company, California, USA.

Henderson, S.B., Grigson, S.W., Johnson, P., and Roddie, B.D., 1999. Potential impact of production chemicals on toxicity of produced water discharges in North Sea oil platforms. Marine Pollution Bulletin 38(12), 1141-1151.

Hibernia Annual Environmental Data Summary, 2005. Prepare for Exxon Mobil, Newfoundland. Prepare by PAL Environmental Services. January 01 – December 31, 2005.

Hibernia Platform Annual Current Measurement Report, 2005. Hibernia Management and Development Company Limited (HMDC), St John's, Newfoundland. Submitted by: Oceans Ltd., March 2006.

Hodgins, D.O., 1993. Hibernia effluent fate and effects modeling. Report prepared for Hibernia management and Development Company Ltd. By seaconsult Marine Research Ltd. (revised January 1994).

Karman, C.C., and Reerink, H.G., 1998. Dynamic assessment of the ecological risk assessment of the discharge of produced water from oil and gas producing platforms. J Hazardous Materials 61, 43-51.

Karman, C.C., and Vik, E.A., 1996. TNO Report R96/355.

Kolluru, V.S., Spaulding, M.L., and Anderson, E.L., 1993. Application and verification of Worldwide Oil Spill Model (WOSM) to selected spill events. Proceedings of the 16th Arctic and Marine Oil Spill Program Technical Seminar, Edmonton, Alberta, Canada, June 7-9.

Korotenko, K.A., 2000. Matter transport in meso-scale oceanic fronts of river discharge type. Journal of Marine Systems 24, 85–95.

Korotenko, K.A., Mamedov, R.M., Kontar, A.E., and Korotenko, L.A., 2004. Particle tracking method in the approach for prediction of oil slick transport in the sea: modeling oil pollution resulting from river input. Journal of Marine Systems 48, 159-170.

Korotenko, K.A., Mamedov, R.M., and Mooers, C.N.K., 2000. Prediction of the dispersal of oil transport in the Caspian Sea resulting from a continuous release. Spill Science & Technology Bulletin 6, 323-339.

Lee, H.M., 1996. Applying fuzzy set theory to evaluate the rate of aggregative risk in software development. Fuzzy Sets and Systems 26, 1182-1191.

Lee, K., Azetsu-Scott, K., Cobanli, S.E., Dalziel, J., Niven, S., Wohlgeschaffen, G., and Yeats, P., 2005. Overview of Potential impacts from produced water discharges in Atlantic Canada. In: Armsworthy, S.L., Cranford, P.J., Lee, K. (eds.), Offshore Oil and Gas Environmental Effects Monitoring Approaches and Technologies, Battelle Memorial Institute, 319-342.

Lowrance, W.W., 1976. Of Acceptable Risk, William Kaufmann, Inc., Los Altos, CA.

Madala, R. V., and Piacsek, S. A., 1977. A semi-implicit numerical model for baroclinic oceans. J. Comput. Phys. 23, 167-178.

Manson, J.R., and Wallis, S.G., 1998. Modeling fluvial water quality response to contaminant spills with DISCUS. Proceedings of 3rd International Conference on Hydroscience and Engineering, Cottbus/Berlin, August 31st - September 3rd.

McDaniels, T., and Small, M.J., 2004. Risk Analysis and Society. Cambridge University Press, New York, USA

Meinhold, A.F., Holtzman, S., and DePhillips, M.P., 1996a. Risk assessment for produced water discharges to Open Bays in Louisiana. In: Reed, M., Johnsen, S. (eds.), Produced Water 2: Environmental Issues and Mitigation Technologies, Plenum Press, New York.

Meinhold, A.F., DePhillips, M.P., and Holtzman, S., 1996b. Final report: risk assessment for produced water discharges to Louisana Open Bays. BNL-62975. Brookhaven National Laboratory, New York, NY, USA.

Meinhold, A.F., Holtzman, S., and DePhillips, M.P., 1996c. Produced water discharges to the Gulf of Mexico: background information for ecological risk assessments. BNL-63331. Brookhaven National Laboratory, New York, NY, USA.

Mellor, G.L., 1996. Users guide for a three-dimensional, primitive equation, numerical ocean model. Program in Atmos. and Ocean. Sci. report, Princeton University, Princeton, NJ.

Mellor, G.L., 2004. Users guide for a three-dimensional, primitive equation, numerical ocean model. Princeton University, Princeton, NJ 08544-0710.

Mellor, G.L., and Ezer, T., 1995. Sea level variations induced by heating and cooling: An evaluation of the Boussinesq approximation in ocean model. J. Geophys. Res. 100, 20565-20577.

Mellor, G.L., Ezer, T., and Oey, L.-Y., 1994. The pressure gradient conundrum of sigma coordinate ocean models. J. Atmos. Oceanic. Technol. 11, 1126-1134.

Mellor, G.L., and Kantha, L., 1989. An ice-ocean coupled model. Journal of Geophysical Research 94, 10937-10954.

Mellor, G.L., Oey, L.-Y., and Ezer, T., 1998. Sigma coordinate gradient errors and the seamount problem. J. Atmos. Oceanic. Technol. 12, 1122-1131.

Mendenhall, W., and Sincich, T., 1994. Statistics for engineering and the sciences. Prentice Hall, Inc. Upper Saddle River, NJ 07458.

Meteorological Institute, 2007. Numerical ocean models: MI-POM. Available at: http://www.met.no/english/r_and_d_activities/method/num_mod/ocean_mod/mi_pom.html

Mukhtasor, Husain, T., Veitch, B., and Bose, N., 2004. An ecological risk assessment methodology for screening discharge alternatives of produced water. Human and Ecological Risk Assessment 10, 505-524.

Mukhtasor, Lye, L.M, and Sharp, J., 2002. Methods of compliance evaluation for ocean outfall design and analysis. Environ. Manage. 30(4), 536–46

Murray-Smith, R.J., Gore, D., Flynn, S.A., Vance, I., and Stagg, R., 1997. Development and appraisal of a Particle Tracking model for the dispersion of produced water discharged from an oil production platform in the North Sea. Proc. Int. Produced Water Seminar, 25-28 September, 1995, Trondheim, Norway. Plenum Press, New York.

National Data Buoy Centre database. NOAA National Data Buoy Center. Available at: http://www.ndbc.noaa.gov/station_page.php? station=44138.

National Research Council, 1985. Oil in the sea. National Academy Press, Washington, DC.

Neff, J.M., 2002. Bioaccumulation in marine organisms. Effects of Contaminants from Oil Well Produced Water. Elsevier Science Publishers, Amsterdam, 452.

Neff, J.M., Johnsen, S., Frost, T.K., Utvik, T.I.R., and Durell, G.S., 2006. Oil well produced water discharges to the North Sea. Part II: Comparison of deployed mussels (Mytilus edulis) and the DREAM model to predict ecological risk. Marine Environmental Research 62, 224–246.

Oey, L.-Y., 2005. A wetting and drying scheme for POM. Ocean Modelling 9, 133-150.

Oey, L.-Y., 2006. An OGCM with movable land-sea boundaries. Ocean Modelling 13, 176-195.

Oey, L.-Y., Ezer, T., Forristall, G., Cooper, C., DiMarco, S., and Fan, S., 2005. An exercise in forecasting loop current and eddy frontal positions in the Gulf of Mexico. Geophysical Research Letters 32, L12611.

Oil and Gas, 2006. The Economic Review 2006. Available at: www.economics.gov.nl.ca.

O'Reilly, J.E., Sauer, T.C., Jr., Ayers, R.C., Jr., Brandsma, M.G., and Meek, R.P., 1988. Field verification of the OOC mud discharge model. In Drilling Wastes, Proceedings of the 1988 International Conference on Drilling Wastes. Calgary, Alberta, Canada, April 5-8, 1988. Elsevier Applied Science Publishers Ltd., London, England, 1989.

Orlanski, I., 1976. A simple boundary condition for unbounded hyperbolic flows. J.Comput. Phys. 21, 251-269.

Palma, E.D., and Matano, R.P., 1998. On the implementation of passive open boundary conditions for a general circulation model: The barotropic mode. Journal of Geophysical Research, January, 1319-1341.

Perianez, R., and Elliott, A.J., 2002. A particle tracking method for simulating the dispersion of non conservative radionuclides in coastal waters. Journal of Environmental Radioactivity 58, 39-59.

Petro-Canada, 2005. Available at: http://www.petro-canada.ca/en/about/717.aspx.

Proctor, R., Elliott, A.J., and Flather, R.A., 1994. Forecast and hindcast simulations of the Braer Oil Spill. Marine Pollution Bull, 26(4), 219-229.

Ray, J.P., and Engelhardt, F.R., 1992. Produced water: Technological/ Environmental Issues and Solutions. Plenum Press, New York, 371-386.

Reed, M., Hetland, B., Ditlevsen, M.K., and Ekrol, N., 2001. DREAM Version 2.0. Dose related Risk Effect Assessment Model. Users manual. SINTEF Applied Chemistry, Environmental Engineering, Trondheim, Norway.

Reed, M., and Johnsen, S., 1996. Produced water 2: Environmental Issues and Mitigation Technologies. Plenum Press, New York, NY.

Reed, M., Johnsen, S., Rye, H., and Melbye, A., 1996. PROVANN: A model system for assessing exposure and bioaccumulation of produced water components in marine pelagic fish, eggs, and larvae. In: Reed, M., Johnsen, S. (eds.), Produced Water 2: Environmental Issues and Mitigation Technologies, Plenum Press, New York. Proceedings of the 1995 International Produced Water Seminar, Trondheim, Norway, Plenum Press, NY, 317 – 332.

Riddle, A,M., 1997. Modelling tidal flows in the Forth estuary and over the intertidal mudflats at Grangemouth. Coastal Zone Topics.

Riddle, A.M., 1998. The specification of mixing in random walk models for dispersion in the sea. Continental Shelf Research. 18, 441-456.

Riddle, A.M., Beling, E.M., and Murray-Smidth, R.J., 2001. Modeling the uncertainties in predicting produced water concentrations in the North Sea. Environmetal Modelling & Software 16, 659-668.

Robertson, R., and Beckmann, A., 2001. A Comparison of POM and ROMS for Modeling Internal Tides in Weak Stratification. Second joint biannual Terrain-following modeling communities (POM, ROMS, SCRUM, SPEM) meeting, Boulder, Colorado, USA.

Røe, T.I., and Johnsen, S., 1996. Discharges of produced water to the North Sea. The Norwegian Oil Industry Association (OLF). In: Reed, M., Johnsen, S. (eds.), Produced Water 2: Environmental Issues and Mitigation Technologies, Plenum Press, New York.

Roucher, R.S., Agras, J., Mills, D., Harrod, M., and Chestnut, L., 2002. Quantifying Public Health Risk Reduction Benefits. AWWA Research Foundation and AWWA, Denver, USA. ISBN 1-58321-192-6.

Rye, H., Reed, M., and Ekrol, N., 1998. The PARTRACK model for calculation of the spreading and deposition of drilling mud, chemicals and drill cuttings. Environmental Modelling & Software 13, 431-441.

Rye, H., Reed, M., Melbye, A., and Johnsen, S., 1996. An intercomparison between field measurements and three different calculation models for the estimation of dilution factors. In: Reed, M., Johnsen, S. (eds.), Produced Water 2: Environmental Issues and Mitigation Technologies, Plenum Press, New York.

Sabeur, Z.A., Hockley, M.C., and Barker, R.G., 2002. Use of PROTEUS for advanced environmental impact assessment and management of marine industrial chemicals. Proceedings of IMEMS2002.

Sabeur, Z.A., and Tyler, A.O., 2003. Validation and application of the PROTEUS model for the physical dispersion, geochemistry and biological impacts of produced waters. Environ. Model. Software 19(7-8), 717-726.

Schuhmacher, M., Meneses, M., Xifro, A., and Domingo, J.L., 2001. The use of Monte-Carlo simulation techniques for risk assessment: study of a municipal waste incinerator. Chemosphere 43, 787-799.

Schobben, H.P.M., and Scholten, M.C.Th., 1993. Probabilistic methods for marine ecological risk assessment. ICES Journal of Marine Science 50, 349-358.

Shaw, D.G., Farrington, J.W., Connor, M.S., Trippm, B.W., and Schubel, J.R., 1999. Potential environmental consequences of petroleum exploration and development on grand banks. New England Aquarium Aquatic Forum Series Report 99-3, Boston, 64.

Simons, T. J., 1974. Verification of numerical models of Lake Ontario. Part I, circulation in spring and early summer. J. Phys. Oceanogr. 4, 507-523.

Smagorinsky, J., Manabe, S., and Holloway, J.L., 1965. Numerical results from a nine-level general circulation model of the atmosphere. Mon. Weather Rev. 93, 727-768.

Smith, J.P., Brandsma, M.G., and Nedwed, T.J., 2004. Field verification of the offshore operators committee (OOC) mud and produced water discharge model. Environmental Modelling & Software 19, 739-749.

Song, Y., and Haidvogel, D.B., 1994. A semi-implicit ocean circulation model using a generalized topography-following coordinate system. J. Comp. Physiol. 115, 228-244.

Spagnol, S., et al., 2002. An error frequently made in the evaluation of advective transport in two-dimensional Lagrangian models of advection–diffusion in coral reef waters. Marine Ecology Progress Series 235, 299–302.

Stephenson, M.T., 1992. A Survey of produced water studies. In: Ray, J.P. and Engelhardt, R.F. (Eds), Produced Water: Technological/Environmental Issues and Solutions, pp.46. Plenum Press, New York.

Suh, S.W., 2006. A hybrid approach to particle tracking and Eulerian-Lagrangian models in the simulation of coastal dispersion. Environmental Modelling & Software 21, 234-242.

Tang, Y., and Grimshaw, R., 1996. Radiation boundary conditions in barotropic coastal ocean numerical models. Journal of Computaional Physics 123, 96-110.

Thatcher, M., Robson, M., and Henriquez, L.R., 1999. A CIN revised CHARM III report. A user guide for the evaluation of chemicals used and discharged offshore, version 1.0. Netherlands Ministry of Transportation, The Netherlands.

Thatcher, M., Robson, M., Henriquez, L.R., and Karman, C.L., 2001. An user guide for the evaluation of chemicals used and discharged offshore: version 1.2. CIN revised CHARM III Report, Charm Implementation Network (CIN), Eurpean Oilfield Speciality Chemicals Association (EOSCA).

USEPA (U.S. Environmental Protection Agency), 1996. Summary report for the workshop on Monte Carlo Analysis risk assessment forum. USEPA, Washington, DC. EPA-630-R-96-010.

Utivik, T., 1999. Chemical characteristics of produced water from four offshore oil production platforms in the North Sea. Chemosphere 39, 2593-2606.

Web 1. Princeton Ocean Model website: http://www.aos.princeton.edu/WWWPUBLIC/ htdocs.pom.

Web 2. Hibernia website: http://www.hibernia.ca.

Web 3. DFO Ocean and Ecosystem Science (OES) website. http://www.mar.dfo-mpo.gc. ca/science/ocean/current_statistics/BottomCurrents. html.

Weidemann, H., 1973. The ICES Diffusion Experiment RHENO 1965. Rapportes et Proces-verbaux des Reuions, vol. 163.

Wu, J., 1980. Wind-stress coefficient over sea surface near neutral conditions-a revisit. J. Physical Oceanography 10, 727-740.

Xie, H., and Yapa, P.D., 2002. Simulating the behavior and the environmental effect of sediment plumes from manganese nodule mining. Proceedings of IMEMS2002, 115–136.

Yao, T., Tang, C.L., and Peterson, I., 2000. Modeling the seasonal variation of sea ice in the Labrador Sea with a coupled multi-category ice model and the Princeton Ocean Model. Journal of Geophysical Research 105, 1153-1165.

Zhang, J., and Baptista, A., 2004. SELFE: is there a higher-order alternative? ELCIRC Users Group First Annual Meeting. OGI School of Science & Engineering. Portland, Oregon.

Zhang, Y.-L., Baptista, A.M., and Myers, E.P., 2004. A cross-scale model for 3D baroclinic circulation in estuary-plume-shelf systems: I. Formulation and skill assessment. Available at: http://www.stccmop.org/corie/modeling_system. Continental Shelf Research 24, 2187-2214.

Zhang, A., Parker, B., and Wei, E., 2002. Assimilation of water level data into a coastal hydrodynamic model by an adjoint opticmal technique. Continental Shelf Research 22, 1909-1934.

Zheng, C., Wang, P.P., and Dortch, M.S., 2000. Subsurface contaminant transport modeling: challenges and resolutions. Proceedings of 16th IMACS World Congress.

APPENDIX A

Representative Bottom Topography Data Used in the Modeling Study

The representative bottom topography data used in the modeling simulation

Longitude	Latitude	Depth (m)	Longitude	Latitude	Depth (m)
-59.4	47.59	0	-48.78	46.56	-75
-59.39	50.34	-5	-48.78	46.57	-69
-59.37	48.3	0	-48.78	46.7	-77
-59.33	47.59	-2	-48.77	46.73	-74
-59.24	50.67	0	-48.74	46.75	-67
-59.18	49.23	-2	-48.71	46.48	-73
-59.11	50.02	0	-48.7	46.75	-78
-59.09	48.22	0	-48.69	45.97	-77
-59.02	44.65	-5	-48.69	46.37	-74
-58.92	48.87	-2	-48.68	46.81	-84
-58.9	48.8	-8	-48.65	46.75	-85
-58.82	49.1	-2	-48.64	45.68	-85
-58.81	47.35	0	-48.63	46.55	-82
-58.8	48.69	-9	-48.62	46.61	-83
-58.79	48.69	-6	-48.61	46.38	-84
-58.72	49.45	-2	-48.6	45.76	-80
-49.2	47.11	-83	-48.55	45.64	-92
-49.1	46.95	-74	-48.5	46.38	-89
-49.06	46	-62	-48.47	46.5	-90
-49	45.86	-61	-48.46	46.35	-90
-48.94	46.73	-72	-48.44	46.52	-93
-48.93	45.63	-66	-48.43	46.45	-91
-48.92	45.12	-72	-48.42	46.45	-92
-48.92	45.58	-68	-44.99	48.41	-412
-48.92	46.44	-64	-44.94	48.18	-416
-48.92	46.6	-65	-44.81	48.11	-415
-48.91	46.82	-78	-44.73	48.16	-448
-48.79	46.72	-77	-44.7	48.22	-418

The representative bottom topography data used in the modeling simulation (cont.)

Longitude	Latitude	Depth (m)	Longitude	Latitude	Depth (m)
-44.45	48.02	-457	-45.83	39.08	-990
-44.45	48.25	-441	-43.04	51.17	-984
-44.35	48.06	-416	-42.56	42.73	-984
-44.32	46.61	-449	-41.51	43.04	-984
-44.28	47.84	-412	-40.82	48.03	-965
-44.16	47.72	-428	-59.67	41.18	-1532
-43.98	47.52	-459	-58.6	57.1	-1332
-43.91	47.45	-412	-57.18	44.06	-1064
-43.9	47.06	-417	-57.18	37.87	-1999
-43.9	47.34	-432	-55.95	42.06	-1976
-43.88	47.51	-406	-54.37	58.17	-1999
-59.85	58.52	-649	-53.45	44.2	-1377
-58.17	44.13	-743	-52.52	43.62	-1316
-55.75	44.82	-674	-50.1	50.78	-1122
-50.67	50.73	-632	-48.19	44.64	-1949
-48.06	45.68	-639	-47.99	43.65	-1979
-47.84	45.82	-662	-46.97	46.96	-1192
-46.95	47.72	-753	-44.68	55.29	-1998
-45.52	48.39	-772	-42.23	50.57	-1048
-44.76	59.26	-782	-41.66	40.63	-1999
-43.47	46.37	-738	-41.57	38.63	-1925
-42.51	46.54	-737	-59.63	42.31	-2010
-41.41	47.36	-733	-57.93	43.78	-3000
-58.58	57.88	-878	-57.61	43.42	-3748
-53.97	56.84	-802	-55.86	44.37	-2006
-50.41	58.64	-803	-52.54	55.97	-2002
-48.74	48.25	-865	-50.32	52.96	-2009
-48.55	51.27	-986	-48.61	43.05	-2479
-48.18	51.54	-937	-41.87	45.42	-2004
-47.92	49.63	-936	-41.45	43.07	-2013

APPENDIX B

Representative Monthly Temperature and Salinity Data Used in the Modeling Study

The representative temperature and salinity data used in the modeling simulation at different depths

Depth (m)	Longitude	Latitude	Temperature (°C)	Salinity (ug/L)
0	-59.55	47.43	7.03	31.82
0	-50.15	45.34	6.99	32.67
0	-49.37	48.42	6.43	32.22
0	-48.85	45.57	5.25	32.48
0	-48.81	47.17	5.39	32.42
0	-48.78	45.39	5.2	32.59
0	-48.78	46.07	5.72	32.51
0	-48.78	46.77	6.83	32.26
0	-48.74	45.26	5.31	32.69
0	-48.74	46.75	6.77	32.25
0	-48.72	45.23	5.18	32.64
0	-48.71	47.06	5.24	32.38
0	-48.69	56.65	7.42	34.76
0	-48.64	46.83	5.8	32.44
0	-48.54	46.1	5.33	32.49
0	-48.51	46.75	6.57	32.19
0	-48.5	47.37	6.02	32.32
0	-47.57	46.41	5.57	32.39
0	-46.6	55.13	8.28	34.7
10	-58.96	49.6	7.31	31.46
10	-53.85	48.17	2.1	32.14
10	-49.92	46.17	6.38	32.68
10	-48.97	45.67	5.72	32.53
10	-48.92	44.21	5.37	32.68
10	-48.91	55.83	7.79	34.71
10	-48.86	59.97	6.39	34.67
10	-48.85	45.57	5.03	32.48
10	-48.81	47.17	5.38	32.42

The representative temperature and salinity data used in the modeling simulation at different depths (cont.)

Depth (m)	Longitude	Latitude	Temperature (°C)	Salinity (ug/L)
10	-48.74	45.26	5.21	32.71
10	-48.72	45.23	4.73	32.87
10	-48.71	47.06	5.23	32.37
10	-47.99	56.13	7.96	34.63
10	-46.95	48.02	6.5	33.4
50	-53.94	46.22	0.08	32.34
50	-52.32	53.5	3.16	34.56
50	-49.8	46.48	1.86	32.84
50	-48.78	46.92	0.83	32.54
50	-47.79	45.98	-1.15	32.85
50	-45.93	49.11	4.54	34.31
100	-50.67	47.47	-0.02	33.02
100	-49.43	48.37	-0.86	33.18
100	-47.98	45.8	-0.41	33.17
100	-45.93	49.11	3.36	34.56
200	-53.66	48.16	-0.16	33.16
200	-50.06	49.19	3.12	34.55
200	-49.43	48.37	2.24	34.22
200	-48.92	44.21	3.15	34.47
200	-47.75	48.11	3.51	34.69
200	-45.93	49.11	3.63	34.77
500	-50.06	49.19	3.74	34.82
500	-48.93	44.16	3.93	34.81
500	-47.96	45.72	3.9	34.82
500	-47.48	45.48	4.21	34.9
500	-46.7	55.93	3.65	34.85
500	-45.93	49.11	3.85	34.87
1000	-47.57	49.03	3.5	34.88
1000	-47.48	45.48	3.83	34.92
1000	-45.93	49.11	3.48	34.87

APPENDIX C

Representative Hourly Wind Data Used in the Modeling Study

Location of wind measurement stations

Name	Longitude	Latitude	Name	Longitude	Latitude
44005	-69.16	43.19	44037	-67.88	43.49
41025	-75.4	35.01	44038	-66.55	43.62
44004	-70.43	38.48	44040	-73.58	40.96
44009	-74.7	38.46	cartw	-57.03	53.7
44013	-70.69	42.35	gander	-54.57	48.95
44014	-74.84	36.61	halifax	-63.52	44.87
44017	-72.1	40.7	hopodale	-60.22	55.45
44018	-69.29	41.26	portab	-59.15	47.57
44024	-65.93	42.31	stjohns	-52.73	47.62
44025	-73.17	40.25	sydney	-60.05	46.17
44029	-70.57	42.52	tracadie	-61.67	45.6
44030	-70.43	43.18	hibernia	-48.78	46.75
44033	-69	44.06	rightbot	-40	35
44034	-68.11	44.11	righttop	-40	56

Hourly wind data at station of 44024 in June, 2005

Year	Month	Day	Hour	Wind Direction (N)	Wind Speed (knots)
2005	6	1	0	40	4
2005	6	1	1	60	5
2005	6	1	2	40	3
2005	6	1	3	360	3
2005	6	1	4	10	2
2005	6	1	5	20	3
2005	6	1	6	360	4
2005	6	1	7	20	4
2005	6	1	8	20	5
2005	6	1	9	20	5
2005	6	1	10	50	5

Hibernia hourly wind data in June, 2005

Year	Month	Day	Hour	Wind Direction (N)	Wind Speed (knots)
2005	6	1	0	360	16
2005	6	1	1	360	16
2005	6	1	2	360	16
2005	6	1	3	340	15
2005	6	1	4	340	15
2005	6	1	5	340	15
2005	6	1	6	340	8
2005	6	1	7	340	8
2005	6	1	8	340	8
2005	6	1	9	340	10
2005	6	1	10	350	11
2005	6	1	11	360	9
2005	6	1	12	360	9
2005	6	1	13	360	7
2005	6	1	14	360	8
2005	6	1	15	360	8
2005	6	1	16	360	8
2005	6	1	17	360	8
2005	6	1	18	0	0
2005	6	1	19	0	0
2005	6	1	20	0	0
2005	6	1	21	320	4
2005	6	1	22	320	4
2005	6	1	23	320	4
2005	6	2	0	150	5
2005	6	2	1	150	5
2005	6	2	2	150	5
2005	6	2	3	170	6
2005	6	2	4	170	6
2005	6	2	5	170	6
2005	6	2	6	0	0

St. John's hourly wind data in June, 2005

Year	Month	Day	Hour	Wind Direction (N)	Wind Speed (knots)
2005	6	1	0	70	1.1
2005	6	1	1	65	1.1
2005	6	1	2	30	0.6
2005	6	1	3	0	0
2005	6	1	4	85	0.6
2005	6	1	5	85	0.6
2005	6	1	6	105	0.3
2005	6	1	7	225	1.1
2005	6	1	8	260	1.1
2005	6	1	9	215	1.3
2005	6	1	10	140	1.9
2005	6	1	11	135	1.9
2005	6	1	12	130	3.6
2005	6	1	13	135	4.7
2005	6	1	14	150	4.9
2005	6	1	15	155	5.4
2005	6	1	16	150	4.7
2005	6	1	17	155	4.9
2005	6	1	18	175	5.4
2005	6	1	19	195	4.7
2005	6	1	20	230	4.2
2005	6	1	21	240	4.4
2005	6	1	22	245	5
2005	6	1	23	255	5.7
2005	6	2	0	250	6.4
2005	6	2	1	250	6.7
2005	6	2	2	250	6.7
2005	6	2	3	255	6.4
2005	6	2	4	260	6.7
2005	6	2	5	260	6.9